STATE OF ALASKA

DEPARTMENT OF NATURAL RESOURCES

DIVISION OF GEOLOGICAL & GEOPHYSICAL SURVEYS

Walter J. Hickel, *Governor*

Harold C. Heinze, *Commissioner*

Thomas E. Smith, *Director and State Geologist*

May 1992

This report is a preliminary publication of DGGS. The author is solely responsible for its content and will appreciate candid comments on the accuracy of the data as well as suggestions to improve the report.

Report of Investigations 92-1

GEOLOGY AND GEOCHEMISTRY OF THE GEYSER BIGHT GEOTHERMAL AREA, UMNAK ISLAND, ALEUTIAN ISLANDS, ALAKSA

By

Christopher J. Nye, Roman J. Motyka, Donald L. Turner and Shirley A. Liss

STATE OF ALASKA
Department of Natural Resources
DIVISION OF GEOLOGICAL & GEOPHYSICAL SURVEYS

According to Alaska Statute 41, the Alaska Division of Geological and Geophysical Surveys is charged with conducting "geological and geophysical surveys to determine the potential of Alaskan land for production of metals, minerals, fuels, and geothermal resources; the locations and supplies of ground water and construction materials; the potential geologic hazards to buildings, roads, bridges, and other installations and structures; and shall conduct such other surveys and investigations as will advance knowledge of the geology of Alaska."

In addition, the Division of Geological and Geophysical Surveys shall collect, record, evaluate, and distribute data on the quantity, quality, and location of underground, surface, and coastal water of the state; publish or have published data on the water of the state and require that the results and findings of surveys of water quality, quantity, and location be filed; require that water-well contractors file basic water and aquifer data, including but not limited to well location, estimated elevation, well-driller's logs, pumping tests, flow measurements, and water-quality determinations; accept and spend funds for the purposes of AS 41.08.017 and 41.08.035, and enter into agreements with individuals, public or private agencies, communities, private industry, and state and federal agencies; collect, record, evaluate, archive, and distribute data on seismic events and engineering geology of the state; and identify and inform public officials and industry about potential seismic hazards that might affect development in the state.

Administrative functions are performed under the direction of the State Geologist, who maintains his office in Fairbanks. The locations of DGGS offices are listed below:

▪794 University Avenue
Suite 200
Fairbanks, Alaska 99709-3645
(907) 474-7147

▪400 Willoughby Avenue
(3rd floor)
Juneau, Alaska 99801
(907) 465-2533

▪Geologic Materials Center
18225 Fish Hatchery Road
P.O. Box 772116
Eagle River, Alaska 99577
(907) 696-0070

This report, printed in Fairbanks, Alaska, is for sale by DGGS for $5. DGGS publications may be inspected at the following locations. Address mail order to the Fairbanks office.

Alaska Division of Geological & Geophysical Surveys
794 University Avenue, Suite 200
Fairbanks, Alaska 99709-3645

U.S. Geological Survey Earth Science Information Center
Grace Hall, Alaska Pacific University Campus
4230 University Drive, Room 101
Anchorage, Alaska 99508-4664

CONTENTS

FIGURES

TABLES

SHEETS

[In report envelope]

GEOLOGY AND GEOCHEMISTRY OF THE GEYSER BIGHT GEOTHERMAL AREA, UMNAK ISLAND, ALEUTIAN ISLANDS, ALASKA

By
C.J. Nye,[1] R.J. Motyka,[2] D.L. Turner,[3] and S.A. Liss[1]

ABSTRACT

The Geyser Bight geothermal area is located on Umnak Island in the central Aleutian Islands. It contains one of the hottest and most extensive areas of thermal springs and fumaroles in Alaska and is the only documented geyser site in the state. The zone of hot springs and fumaroles lies at the head of Geyser Creek, 5 km up a broad, flat, alluvial valley from Geyser Bight. At present, central Umnak Island is remote and undeveloped.

This report describes results of a combined program of geologic mapping, K-Ar dating, detailed description of hot springs, petrology and geochemistry of volcanic and plutonic rock units, and chemistry of geothermal fluids. Our mapping shows that plutonic rock is much closer to the area of hotsprings and fumaroles than previously known, which increases the probability that plutonic rock hosts the geothermal system. K-Ar dating of 23 samples provides a time framework for the eruptive history of volcanic rocks and a plutonic cooling age.

Heat for the geothermal system is derived from the Mt. Recheshnoi volcanic system. Mt. Recheshnoi is a large calcalkaline stratocone that has been active over at least the past 500,000 yr. Petrochemical studies indicate that successive passages of magma have probably heated the crust to near its minimum melting point and produced the only high-SiO_2 rhyolites in the oceanic part of the Aleutian arc. There is no indication of a large, shallow magma chamber under Mt. Recheshnoi.

Surface expressions of the geothermal system include six zones of thermal springs and small geysers dispersed over a 4-km^2 area and three zones of fumarolic activity. Thermal-spring water chemistry indicates that at least two intermediate-level hydrothermal reservoirs underlie the geothermal area. Their minimum temperatures are 165° and 200°C, respectively, as estimated by geothermometry. Sulfate-water isotope geothermometers suggest that a deeper reservoir with a minimum temperature of 265°C underlies the shallower reservoirs. The $^3He/^4He$ ratio of 7.4 found in thermal-springs gases provides evidence for a magmatic influence on the hydrothermal system. The 7.4 value is nearly the same as the average value for summit fumaroles in circum-Pacific volcanic arcs.

The thermal-spring waters have low to moderate concentrations of Cl (650 ppm) and total dissolved solids (1760 ppm), but are rich in B (60 ppm) and As (6 ppm) compared to most other geothermal systems. The As/Cl ratios in Geyser Bight thermal spring waters are among the highest reported for geothermal areas. The source of B and As is unknown, but may be in part of magmatic origin. Convective heat discharge by springflow is estimated at 17 MW for 1988. The reservoir system probably contains about 5.4 to 7.3 x 10^{18} J of thermal energy, sufficient to produce 132 MW to 225 MW of electrical power for 30 yr.

INTRODUCTION AND BACKGROUND

DESCRIPTION OF THE GEYSER BIGHT GEOTHERMAL AREA

The Geyser Bight geothermal area,[4] located on Umnak Island in the central Aleutian Islands (fig. 1), contains one of the hottest and most extensive areas of thermal springs and fumaroles in Alaska. It is the only area in

[1]Alaska Division of Geological & Geophysical Surveys, 794 University Avenue, Suite 200, Fairbanks, Alaska 99709-3645
[2]Alaska Division of Geological & Geophysical Surveys, 400 Willoughby Avenue, 3rd Floor, Juneau, Alaska, 99811
[3]Geophysical Institute, University of Alaska Fairbanks, Fairbanks, Alaska, 99775
[4]The Geyser Bight geothermal area is contained within the Geyser Springs Basin Known Geothermal Resource Area. We use the name Geyser Bight geothermal area because it is the most commonly used name in the literature, despite the fact that the springs, geysers, and fumaroles are located on Geyser Creek, rather than in Geyser Bight.

Alaska where geyser activity has been documented. Although Geyser Bight is remote and undeveloped, its accessibility from the sea and its large estimated reserve of geothermal energy should make the area an economically attractive future source of power. Our estimates of minimum temperatures for intermediate level reservoirs are 165 and 200°C; our minimum estimate for an underlying deep reservoir is 265°C. Estimates of convective heat dissipated by spring flow range from about 25 MW in 1947 to 16.7 MW in 1988. Muffler (1979) estimated that 136 MW of electrical energy are available over 30 yr at Geyser Bight, a resource comparable to Beowawe and Brady Hot Springs in Nevada.

The site is located at lat 53°13'N., long 168°28'W., at the approximate center of the north side of Umnak Island (fig. 1). The thermal area consists of five zones of numerous thermal springs and small geysers dispersed over a 4 km_2 area in the upper reaches of a broad glacial valley that has excellent access to the Bering Sea (fig. 1). The hot springs occur mostly along Geyser Creek and its tributaries and emerge in the valley floor and at the base of steep valley walls. Two small fumarole fields are located at elevations of 140 and 300 m in a small tributary valley at the headwaters of Geyser Creek. We discovered a third, superheated fumarole field about 2.5 km south of the previously reported fields.

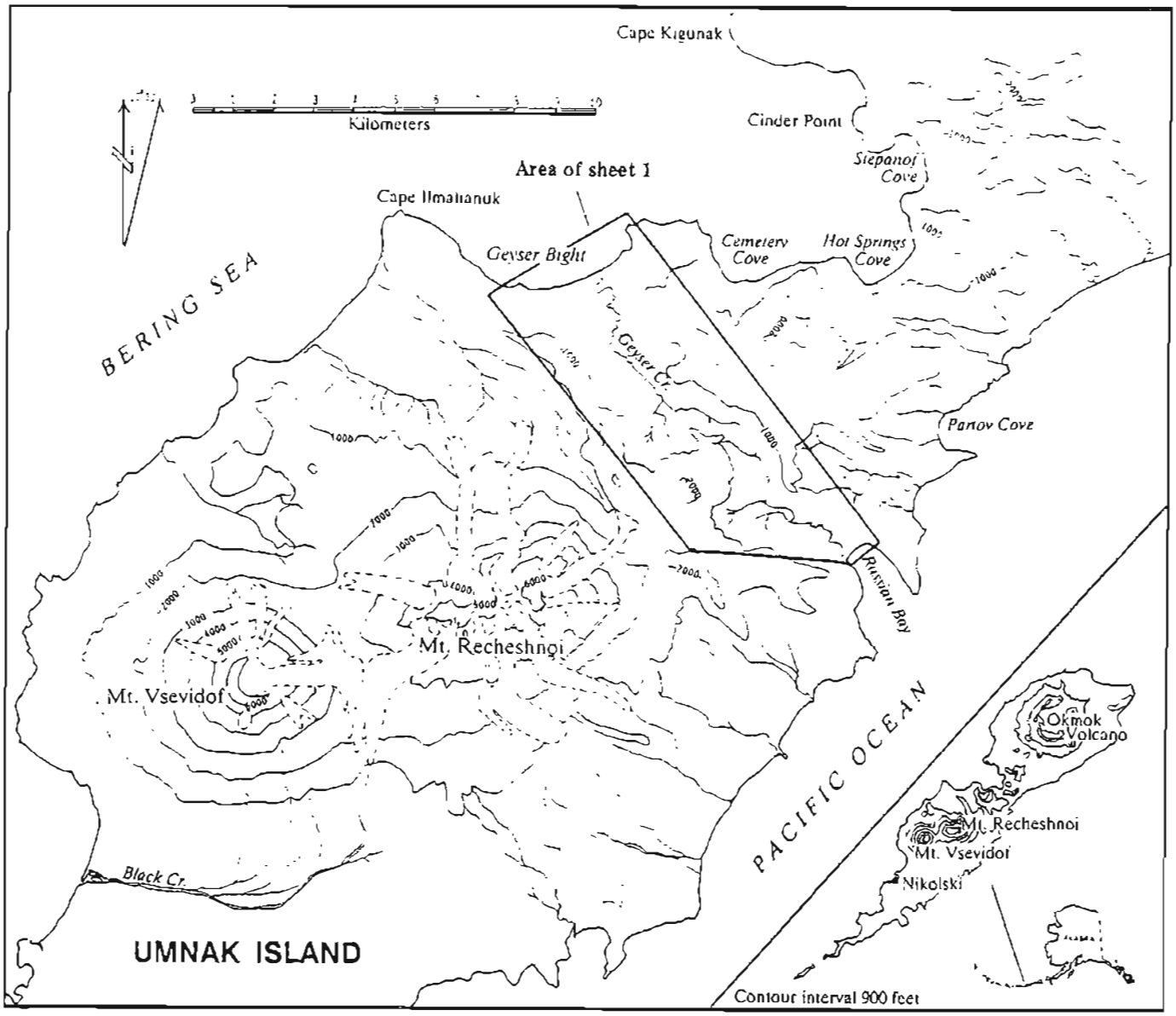

Figure 1. *Generalized map of Umnak Island showing boundaries of geologic map (sheet 1).*

REGIONAL GEOLOGIC SETTING

Recent reviews of the geology and tectonics of the Aleutian arc region are given by Scholl and others (1987) and Stone (1988). These reviews provide a convenient entry into the extensive literature about the Aleutian arc and the Bering Sea, and are summarized here.

The part of the North American plate that underlies the Aleutian arc is oceanic west of 166°W., composed of a broad continental shelf between 166°W., and about 156°W., and continental east of 156°W. The Pacific plate is oceanic throughout, except for a small sliver of continental crust at its easternmost margin. Umnak Island and the Geyser Bight geothermal area are located just west of the oceanic-continental transition. There are no major tectonic anomalies in the arc in the vicinity of Umnak Island.

Formation of the oceanic part of the Aleutian arc began during early Tertiary time (approximately 55 Ma) when the Kula plate buckled and began to subduct beneath itself. A piece of oceanic crust that was trapped between the arc and the edge of the Bering shelf was accreted to the North American plate. That trapped piece of oceanic crust is now the floor of the southwestern half of the Bering Sea.

Since that time, the Kula plate and then the Pacific plate underthrust the margin of the North American plate. The broad geometry of the subduction system did not change during Tertiary and Quaternary time. Subduction under the continental part of the arc occurred at least intermittently during much of Mesozoic and Cenozoic time, although that part of the arc was not yet accreted to North America (see Panuska and Stone, 1985; Coe and others, 1985, for reviews).

The oceanic part of the Aleutian arc formed as an igneous and sedimentary welt on abyssal oceanic crust and grew to sea level by the end of Eocene time. During the Oligocene and Miocene Epochs, arc growth slowed, and erosive processes became relatively more important. The transition from early, rapid growth to waning activity was approximately coincident with the demise of the Kula-Pacific spreading center and the change in subduction angle. Starting in Pliocene time, wave action truncated to a shallow, $\leq$ 100-km-wide platform at the summit of the ridge. The Aleutian Islands are the emergent portions of this platform. Quaternary volcanism is confined to a narrow belt in the northern part of the summit platform.

Rocks deposited during the early phase of rapid growth-the lower series (Scholl and others, 1987)-consist of volcanic rocks, hypabyssal intrusives, stocks and plutons, and locally derived sedimentary rocks. They are pervasively altered and lightly metamorphosed, generally at less than greenschist facies. Lower series rocks are often broadly folded and regionally tilted. Rocks of southwestern Umnak Island belong to the lower series and appear to have accumulated in summit basins adjacent to active volcanic centers (McLean and Hein, 1984). In the Geyser Bight area, the lower series is represented by Tertiary sedimentary and volcanic rocks (Tvs, see p. 12). Although exposures are limited, the unit in Geyser Creek valley appears to have a higher proportion of volcanic rocks than the unit (to the southwest) described by McLean and Hein (1984).

The middle series includes rocks deposited as volcanic activity waned during the Oligocene and Miocene Epochs (Scholl and others, 1987). This series consists mostly of a blanket of slightly deformed, diagenetically altered, marine sedimentary rocks that drape the outer flanks of the arc. These rocks are not exposed on Umnak Island. The plutonic rocks in the Geyser Bight area also belong to the middle series. Plutonic masses comprise much of the middle series along the crest of the arc (see Scholl and others, 1987, for a summary of occurrences).

Large-scale structural features of the arc are described by Geist and others (1988). These features consist of tear-away canyons and summit basins that formed by the rotation of at least five discreet blocks, each 150 to 400 km long and 125 km wide. This block rotation was presumably in response to oblique subduction in the western part of the arc. Within these blocks, deformation is restricted to broad folding and minor faulting (Scholl and others, 1987). Volcanoes are generally located at or continentward of the continentward limit of the blocks. The analysis by Geist and others (1988) does not extend as far east as Umnak Island.

PREVIOUS WORK

Reports of the Geyser Bight hot springs appear in Grewingk (1850), Dall (1870), and Waring (1917), and their existence was probably known to Aleut villagers at Nikolski since ancient times. Byers and Brannock (1949) conducted an extensive survey of the thermal spring areas during their reconnaissance geologic mapping of Umnak Island (1946-48) and reported analyses of water samples from two springs. Samples from four thermal springs were collected and analyzed by Ivan Barnes (written commun., U.S. Geological Survey, 1981) in 1975 as part of a U.S. Geological Survey's reconnaissance investigation of hot-spring sites in the Aleutian arc. In 1980, a party from the Alaska Division of Geological and Geophysical Surveys sampled and analyzed seven Geyser Bight thermal springs and measured spring discharges during a regional assessment of geothermal resources in the Aleutian Islands (Motyka and others, 1981). Their preliminary studies suggested that these hot springs are fed by multiple reservoirs, with temperature ranges from 160° to 190°C. These multiple reservoirs are related to a deeper parent reservoir with temperatures as high as 265°C.

Prior to this study, the most detailed geologic map of the Geyser Bight geothermal area was a 1:96,000-scale map of southwestern Umnak Island produced during a 6-wk reconnaissance in 1947 (Byers, 1959). This map shows the major rock units that we subsequently mapped in more detail during 1988. McLean and Hein (1984) provide additional detail on Tertiary rocks southwest of Umnak's volcanoes. Byers (1959) provides petrographic descriptions and some chemical analyses of many rock units found in the Geyser Bight area, and Byers (1961) provides detailed petrogenetic interpretations of the chemistry and mineralogy of central Umnak volcanic rocks. However, his interpretations focus on petrogenetic processes rather than the temporal and stratigraphic evolution of volcanic systems that are the focus of this study.

PURPOSE AND SCOPE OF THIS STUDY

The purpose of this resource assessment is twofold: (1) to obtain new geologic and geochemical data for one of Alaska's most promising geothermal resource areas, and (2) to produce an integrated analysis of the resource with more accurate estimates of reservoir temperatures and the magnitude of energy available for future development.

As fossil fuels become scarce, industry may be forced to locate in regions with readily available energy. Thus, the Geyser Bight area may become attractive to energy-intensive industries such as ore-processing, hydrogen production by electrolysis of water (for later use in fuel cells at other locations), or seafood irradiation.

Altough the central Aleutians are sparsely populated and remote, rapid growth of the American bottom-fish industry in the Bering Sea and northern Pacific Ocean, and increased oil and gas exploration in the Bering Sea are generating an increased need for power in the region. This industrial growth may make development of high-quality, relatively remote geothermal resources attractive. Economic feasibility studies at Dutch Harbor (145 km east on Unalaska Island) show that the cost of electrical production using the Makushin geothermal resource is competitive with diesel-fired generators given sufficiently high flow rates in the geothermal wells (Spencer and others, 1982). The high cost of developing the Makushin geothermal resource is in part due to its relative inaccessibility; it is situated inland on the flanks of a rugged volcano.

We believe that Geyser Bight is a particularly attractive alternative to Makushin if the Makushin field proves insufficient for industrial development or if logistical expenses preclude development.

LAND STATUS AND ACCESSIBILITY

The Geyser Bight geothermal area is located on federal land under the jurisdiction of the U.S. Bureau of Land Management (BLM). It, as well as the Hot Springs Cove geothermal area 6 km to the northeast (fig. 1) are contained in the Geyser Springs Basin Known Geothermal Resource Area (KGRA). BLM, and under a cooperative agreement, the U.S. Fish and Wildlife Service, will be involved in lease sales, drilling permits and any further exploration or development of this resource.

Under the guidelines of the 1971 Alaska Native Claims Settlement Act (ANCSA), native Alaskan groups and the State of Alaska can select federal land up to their entitlement limits. The Aleut Native Corporation, the St. George Village Association, and Tanadquisix Village Association from St. Paul Island have each selected the entire KGRA and some surrounding areas. The State of Alaska has also tentatively selected land in the southern part of the KGRA, in an area that includes the superheated fumarole site (F3, sheet 1), but does not include any hot spring areas. The State has until January 2, 1994, to make additional selections. BLM is responsible for adjudicating land claims, and, by the rules of ANCSA, gives preference to native groups, once the State determines that its interests are not compromised.

Hot Springs Cove and Russian Bay are two (of several) semi-protected bays near the Geyser Bight geothermal area. With breakwater construction and/or dredging, a suitable deep-water harbor could be constructed at one or more of these sites. The flat floor and gentle slope of Geyser Creek valley would accommodate a road from the beach to the thermal area, a distance of only 5 km. In addition, a large airfield is located at Fort Glenn (World War II, abandoned) on the east end of the island, about 50 km from Geyser Creek valley, and an unimproved road leads from Fort Glenn to within 15 km of Geyser Bight.

Field work for this project was conducted on foot from a tent camp in the lower Geyser Creek valley. Field gear was flown from Fairbanks to Nikolski, the nearest village to Geyser Bight. Gear and personnel were transported from Nikolski to the field site by two inflatable boats and one aluminum skiff. We ran through light surf into the mouth of Geyser Creek and then lined and motored halfway through the dune field to our campsite. We also used the inflatable boats to locate a spike camp at Hot Springs Cove. Surf conditions at Geyser Bight generally make small boat operations unsafe. Any larger field effort, or a field effort requiring heavy equipment, would probably be best conducted using a landing craft from Dutch Harbor.

GEOLOGY OF THE GEYSER BIGHT AREA

OVERVIEW

The oldest rocks on central Umnak Island are fine-grained Tertiary volcanic and sedimentary rocks of low metamorphic grade (Tvs, sheet 1). These rocks, along with the late Miocene dioritic pluton that intrudes them (Tdp, sheet 1), form the base of a broad, wave-cut platform 100 to 200 m above sea level. Plutonic rocks as young as 9.5 Ma (this report) are cut by this surface at Geyser Bight. This major unconformity was formed in Pliocene time and is regional in extent (Scholl and others, 1987).

Quaternary volcanic rocks spanning at least 1.5 m.y. (this report) were erupted from several volcanoes and deposited on this platform. These volcanoes and their eroded remnants provide 600 m of relief in the immediate vicinity of Geyser Bight valley. The older of these volcanoes had vents northeast of Geyser Bight (fig. 2). The remnants of these volcanoes consist of central vent complexes surrounded by lava flows which dip radially outward. Extensive erosion has obscured the constructional morphology od these volcanoes.

Mt. Recheshnoi, the closest of the Pleistocene volcanoes, erupted in Holocene time. It is about 2,000 m high and its summit is 8 km southwest of Geyser Bight. Mt. Recheshnoi is predominantly calc-alkaline basalt and andesite. Flank eruptions of quartz-andesite, andesite, and rhyolite have occurred within the last 140 ka; the youngest flank eruption occurred 3,000 yr B.P. (Black, 1975). The rhyolite flank vents comprise one of only two known rhyolite occurrences west of the Valley of Ten Thousand Smokes (1,000 km to the east).

Mt. Vsevidof, 6 km west-southwest of Mt. Recheshnoi, is an active volcano that appears to be dominantly Holocene in age. Flows from Mt. Vsevidof do not crop out in the Geyser Creek area.

The hot springs, fumaroles, and geysers of the Geyser Bight area are located at the head of a large Pleistocene valley cut in the bedrock units discussed above.

The remainder of this report describes the geology of the Geyser Bight area in more detail. The discussion is organized by map unit (sheet 1) in chronologic order from youngest to oldest. Some rock units described in this section lie outside the area of the detailed geologic map. With few exceptions, the rock units are those of Byers (1959).

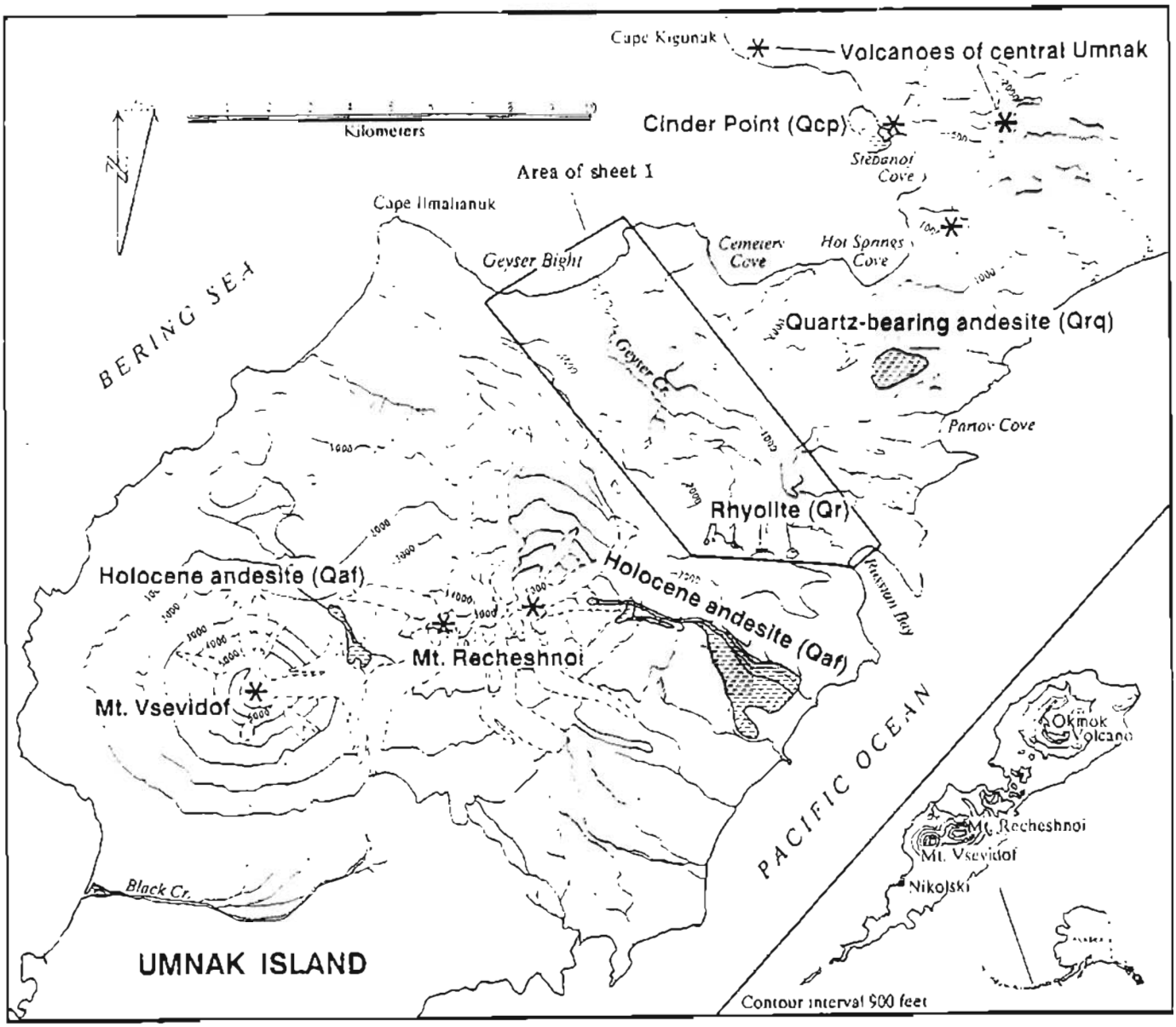

Figure 2. *Location of some volcanic centers on central Umnak Island.*

DESCRIPTION OF ROCK UNITS

BEACH SAND (Qb)

Active beaches at Geyser Bight and Russian Bay are composed of well-sorted, medium- to coarse-grained sand. Beach faces are moderately steep due to frequent moderate to heavy surf.

ALLUVIUM (Qal)

Alluvial silt, sand, and gravel fill the bottoms of Geyser Creek valley and Russian Bay valley. Modern streambeds contain pebbles up to a few centimeters in diameter. Areas adjacent from the streams can be underlain by peat and overbank mud of undetermined thickness.

These valleys presumably formed when the glacially carved Pleistocene valleys were drowned by post-glacial rise in sea level. The resultant deep bays were isolated by bay-mouth bars to produce lakes that were then filled by alluvium and overbank silt, lagunal and lacustrine deposits, and tephra. Till probably underlies the alluvium. If this model is correct, fill in Geyser Creek valley and Russian Bay valley may be quite thick and formed of a complex intertonguing of till, alluvial sand and gravel, very fine grained overbank and lacustrine silt and peat, and tephra. Because substantial deposition may have occurred at or below sea level, average grain-size may be quite small. Alluvium in Geyser Creek valley is probably very thin near the head of the valley.

Makushin valley is similar in size and, perhaps, history to Geyser Creek valley. Near its downstream end, it contains about 7 m of sod and organic-rich silt underlain by 22 m of water-saturated silt and fine sand, in turn underlain by 20 m of till(?) (Krause, 1986).

DUNE SAND (Qd)

The beaches at Geyser Bight and Russian Bay are backed by extensive fields of inactive, vegetated dunes composed of well-sorted, medium- to coarse-grained sand similar to beach sand. Older dunes (farther from the beaches) are often mantled by one-cm-thick red and black tephra layers with an aggregate thickness of a few meters. Dunes are typically 15-20 m high (locally as much as 45 m high) at Geyser Bight and 35 m high at Russian Bay.

TILL (Qgt)

Irregular piles and hummocks of unstratified, locally derived boulders and cobbles lie in shallow, gently sloping basins perched above major valleys. These deposits are probably latest Pleistocene in age. Total thicknesses of individual deposits are at least several meters. These are the only late Pleistocene glacial deposits in the map area. Byers (1959) shows Pleistocene and neoglacial moraines on the flanks of Mt. Recheshnoi, southwest of the area shown on sheet 1. Similar hummocky drift deposits occupy similar shallow alpine valleys elsewhere on the island, usually on the flanks of Mt. Recheshnoi. An older glacial drift unit (Qgd) is described below.

ALLUVIAL-COLLUVIAL FANS (Qf)

This unit comprises coarse, poorly sorted alluvial and colluvial material deposited in short, steep fans on the sides of main valleys at the mouths of minor streams and gullies.

UNDIFFERENTIATED COLLUVIUM (Qc)

Colluvium of undetermined origin was mapped where it was thick enough to prevent accurate determination of underlying bedrock. There are no associated landforms to indicate the nature of the material.

HOLOCENE TEPHRA (Qt)

Orange, brown, and black tephra units ≤ 4 m thick have accumulated in some low-relief upland areas. Individual beds are typically several centimeters thick, but can be several tens of centimeters thick. The tephra is primarily medium to coarse ash, with at least one prominent bed of lapilli-sized pumice. This unit was mapped where it was thick enough to obscure underlying bedrock units, and includes some small bedrock outcrops too small to show at map scale.

RHYOLITE (Qr)

At least seven small rhyolite bodies occur along an east-west zone south of Russian Bay valley. The outcrops range from 0.5 to 0.1 km^2 (sheet 1). The rhyolite forms dense, flow-banded outcrops in which the flow banding is typically subparallel to the trend of the outcrops and steeply dipping. The rhyolite is glassy to devitrified and sparsely phyric. Phenocrysts consist of plagioclase, biotite, quartz, and minor opaque oxides. The unit also contains rounded inclusions of typical Recheshnoi andesite up to several centimeters in diameter.

These inclusions contain approximately 10% plagioclose + clinopyroxene + olivine set in a fine-grained, quenched groundmass and appear to have been incorporated when the rhyolite was molten. Biotite from one rhyolite outcrop was dated at about 135 ka (see p. 16).

The strongly linear outcrop pattern, high density, steeply dipping and contorted flow banding suggest that all rhyolite outcrops may be part of a single, near-vertical, dike-like body. The lack of any associated subareal deposits or subhorizontal structure indicates that the rhyolite is not the eroded remnant of an ashflow or subareal lava flow. The larger bodies may be eroded remnants of domes, and the smaller bodies may be feeders to domes that were subsequently removed by glacial erosion. Rhyolite outcrops are spatially discreet, and rhyolite is not exposed in gullies between outcrops, which suggests that only fingers of the postulated dike reached the surface.

HOLOCENE ANDESITE (Qaf)

Holocene andesite flows extend from small vents high on the eastern and western slopes of Mt. Recheshnoi (fig. 2). None of these flows are within the map area of sheet 1. We sampled the two easternmost flows identified by Byers (1959). The older flow erupted from a vent at about 700 m elevation and flowed about one km horizontally and 350 m vertically down the flank of the volcano. The younger flow erupted from a vent at about 1260 m elevation and flowed 6 km down the flank of the volcano to terminate among Holocene beach ridges. The flows are narrow and were apparently quite fluid.

The flows are 58 percent SiO_2 andesite with 10 to 15 volume percent phenocrysts dominated by plagioclase and including clinopyroxene, olivine, orthopyroxene, and magnetite. Most plagioclase is normally zoned, but the older flow contains a small proportion of resorbed, reversely zoned, and/or spongy plagioclase phenocrysts. The younger flow contains rounded inclusions of highly vesicular olivine + clinopyroxene + plagioclase-phyric basaltic andesite (about 55 percent SiO_2). The inclusions which appear to have been mixed into a liquid host andesite, resemble the quenched basaltic blobs described by Eichelberger (1975) from Glass Mountain in Oregon.

Although moss and some grass cover the older flow, most aspects of flow morphology are unaltered. The younger flow is much less vegetated with well-preserved lateral levees and concentric ropy flow structures in its lower part; the upper part of the flow is blocky. Black (1975) states that the younger flow was deposited during a neoglacial advance and is thus about 3,000 yr old.

QUARTZ-BEARING ANDESITE (Qrq)

Basaltic andesite scoria and stubby lava flows erupted from a small vent on the ridge crest between Hot Springs Cove and Partov Cove. The outcrop area is about 2 km by 1 km, elongated to the east-northeast. A closed depression about 250 m diam and 10 m deep in the west-central part of the unit is probably the original vent. The northern part of the unit is composed of agglutinated scoria and bombs (a few to several centimeters diameter) that probably represent the remains of a cinder cone. Steep-fronted concentric lobes that represent stubby flows that issued from the base of the former cone make up the eastern part of the unit. Flow tops are massive andesite cut by shallow eastward drainages. Although rubbly flow tops and cinders were not found they probably formed during the initial eruption and were removed when Umnak Island was buried by glacial ice. Because these flows erupted about 89 ka (see p. 16), they were exposed to most of the last glacial cycle. However, glacial erosion was not severe enough to radically alter the initial volcanic morphology perhaps of its location at the top of a high ridge.

The unit is composed primarily of basaltic andesite with about 54 percent SiO_2. The lavas are compositionally similar to other lavas from the area except for the high MgO content which may reflect magma mixing within the unit. As noted by Byers (1959), the mineralogy of these lavas is unusual in that they contain plagioclase, magnesian olivine, clinopyroxene, orthopyroxene, magnetite, and some embayed beta-quartz. The complexity of this mineral assemblage suggests magma mixing.

The unit also contains mafic clots with about 65 volume percent crystals that are dominantly hornblende pseudomorphs. The clots also contain phenocrysts of plagioclase, olivine, and clinopyroxene. The groundmass consists of quenched plagioclase, pyroxene, and glass (mostly devitrified).

LAVAS OF CINDER POINT (Qcp)

Cinder Point is a small, 178-m-high cinder cone on the northeast edge of Inanudak Bay (fig. 2). Its two lobate lava flows are nearly circular in map view and about 200 m diam. Because the summit cone is only slightly modified by erosion, it is probably early Holocene in age. The Cinder Point cone is equi-distant from Okmok Caldera to the northeast and Mt. Recheshnoi. It is the westernmost of five aligned vents near Inanudak Bay (Byers 1959).

Cinder Point lavas are highly porphyritic, high-alumina basalts. Dominant phenocrysts are subhedral plagioclase crystals up to 5 mm long (average 1.5 mm) with thin, corroded rims; the crystals are free of spongy zones. There are occasional multigrain aggregates of plagioclase. Cinder Point lavas contain lesser amounts of clinopyroxene and olivine crystals that are subhedral, subequant, and 0.1 to 0.2 mm long.

LAVAS OF MT. RECHESHNOI (Qral, Qra, Qrd)

Mt. Recheshnoi is a large, heavily glaciated stratocone on central Umnak Island, southeast of Geyser Creek (fig. 2). It is mostly late Quaternary in age (see p. 15). The center of the cone is built on a 60-m-high flat erosional surface cut on Tertiary plutonic and sedimentary rocks. This surface is part of the regional Aleutian summit platform which formed since 5.3 Ma (Scholl and others, 1987). The east and northeast flanks of Mt. Recheshnoi overlie a $\leq$ 300-m-thick deposit of lava flows from older volcanoes. The central 40 to 50 km^2 (above 1000 m elevation) consist of pyroclastic beds and a vent complex (Byers, 1959) that has been heavily eroded by several small valley glaciers so that it retains no original constructional volcanic form. The summit area consists of a 4-km-long, east-west ridge that may reflect construction from an older eastern vent and a younger western vent (Byers, 1959). Below 1,000 m elevation the volcano consists of basalt and andesite flows with minor pyroclastic interbeds. The original constructional surface is preserved in some upland areas between glaciers, especially on the western flank, and some flows fill Pleistocene glacially carved valleys. The summit elevation is 1984 m, and deposits from the volcano cover 360 km^2.

In the Geyser Creek area, this unit consists of basalt and andesite lava flows interbedded with minor pyroclastic units. Flows typically have a thin, brick-red, rubbly bottom that grades upward into platy lava. Thicker or more mafic flows can have massive or columnar interiors, and upper parts of the flows are rubbly and oxidized. Intervals between flows are usually poorly exposed and contain pyroclastic material, soil, and colluvium. Individual flows are typically 4 to 12 m thick. Some flows are substantially thicker, presumably due to local ponding. Occasional zones several tens of meters thick are brick-red throughout with very thin platy flows in a rubbly matrix. These zones may have formed during single eruptive events when very rubbly aa flows continually overran their margins.

Except for the syneruptive brick-red oxidation on flow tops and bottoms, lavas from this unit are unaltered. All fractures in the flows are attributable to post-eruptive cooling; we observed no tectonic fractures. Flows dip to the north, northeast, and east, away from the summit of Mt. Recheshnoi, at gentle to moderate angles.

Most flows in the map area are truncated by the large glacial valleys that terminate at Geyser Bight and Russian Bay. These flows are shown as Qra on sheet 1. In contrast, valley-filling flows (Qral) occur near Russian Bay valley. These deposits consist of debris flows, lahars, ashflows, and minor lava flows. West of the head of Russian Bay valley, these poorly consolidated deposits are deeply incised by very steep-walled gullies. An ashflow is preserved in small benches on the northeast side of Russian Bay valley and in thicker deposits on the southern side of the valley. These flows are probably late Pleistocene to early Holocene in age and are, except for flows from flank vents, among the most recent deposits of Mt. Recheshnoi.

An unusually large, steeply dipping, northeast-trending dike (Qrd, sheet 1) was mapped south of the pass between Geyser Creek and Russian Bay valley. The dike, which is easily distinguished on small-scale radar images and photographs, forms a barrier to stream flow and has ponded a small patch of alluvium just below the pass into Geyser Creek. It is mantled by glacial drift.

Mt. Recheshnoi lavas are usually porphyritic and contain 25 to 40 volume percent phenocrysts. Aphyric lavas are rare. Plagioclase is ubiquitous and occurs in two major textural varieties. The first variety is characterized by euhedral, unzoned or normally zoned, twinned, inclusion-free crystals that occur as large tabular crystals and as smaller prismatic crystals. The second variety is characterized by tabular rounded and resorbed crystals that may be reverse zoned and often contain spongy zones or cores. Lavas with less than 56.5 percent SiO_2 contain prismatic euhedral to subhedral olivine crystals. Some high-silica andesites also contain olivine. Stubby, prismatic clinopyroxene crystals are ubiquitous. Most andesites-but few basalts-contain elongated prisms of subhedral orthopyroxene. Orthopyroxene concentrations are usually less than clinopyroxene concentrations. Titanomagnetite is a common accessory phase. Hornblende was found in one sample.

GLACIAL DRIFT (Qgd)

A section of glacial drift $\leq$ 800 m thick is exposed in the southwest wall of Geyser Creek valley, stratigraphically between lavas of Mt. Recheshnoi and the volcanics of central Umnak (see below). Thick massive sections of the drift are coarsely bedded and poorly sorted. These thicker sections contain rounded andesitic blocks up to 1 m diam in a matrix composed primarily of sand-sized material. Thinner, very fine-grained, well-sorted, tuffaceous(?), laminations about 1 cm thick are also present.

Lava flows (DT88-17 and DT88-5) that provide younger and older limiting ages for the drift have been dated at 499 $\pm$ 14 and 1,104 $\pm$ 37 ka, respectively (sheet 1; p. 16). The drift was probably deposited between the intervals of volcanic activity on central Umnak Island and Mt. Recheshnoi. Geochronologic data suggest that this time was between 500 and 800 ka.

VOLCANICS OF CENTRAL UMNAK ISLAND (Qcuv)

The volcanics of central Umnak lie stratigraphically beneath Mt. Recheshnoi (Qcuv, sheet 1) and are stratigraphically equivalent to Byers' (1959) QTv. We use a different unit label than Byers on sheet 1 because the unit does not contain Tertiary rocks (p. 17).

Lavas and pyroclastic rocks were erupted from several small, early Pleistocene vents on central Umnak Island (fig. 2). Because the vents are outside the map area of sheet 1, much of this discussion relies on Byers (1959). Four to six of the vents are now exposed. This unit is covered by Okmok Volcano to the northeast and Mt. Recheshnoi to the southwest: thus additional vents may be hidden. The exposed volcanoes are heavily eroded, 3 to 7 km diam, and < 800 m high. Individual vents have outwardly dipping basalt and andesite flows and a central core dominated by breccia, tuff, and feeder dikes. Byers (1959) mapped several zones of altered, silicified, or K-feldspathized rocks. We did not visit these areas.

In the Geyser Bight area, the unit consists of south- to southwest-dipping basaltic and andesitic lava flows with minor pyroclastic and brecciated interbeds. Vent areas like those exposed east of Inanudak Bay do not occur in the area of sheet 1. Lava flows are similar in appearance and composition to those from Mt. Recheshnoi (see above), but aphyric and sparsely phyric lavas are more common, and resorbed and corroded plagioclase is less abundant.

This unit is recognized in the field by the south to southwest dip of its lavas (into Mt. Recheshnoi and away from central Umnak Island) and by the lack of both alteration and persistent tectonic fracture pattern exhibited by the underlying Tvs unit.

QUARTZ DIORITE AND QUARTZ MONZONITE PLUTON (Tdp)

Dioritic and monzonitic plutonic rocks-in part of Late Miocene age (see p. 17)-crop out at low elevations on the western and eastern walls of the lower half of Geyser Creek valley (sheet 1). These rocks may be part of a larger plutonic body that crops out in a few locations at the base of Mt. Recheshnoi and Mt. Vsevidof (Byers, 1959). This larger plutonic body may be a single large pluton or an amalgamation of several smaller bodies of Oligocene to Miocene age. Because outcrop is not continuous, field evidence of multiple plutons could not be obtained. For convenience, we will refer to all plutonic rock as a single pluton. The pluton lies unconformably

below the volcanic rocks. This unconformity represents the regional wave-cut platform at the summit of the Aleutian ridge (Scholl and others, 1987). The lower contact of the pluton is not exposed. Plutonic rocks in the Geyser Bight area are, at least in part, much younger than, and therefore not related to, the Oligocene quartz diorite and diorite stocks described by McLean and Hein (1984) on southwestern Umnak Island.

Our mapping shows that plutonic rock occurs much farther up Geyser Creek valley than previously mapped by Byers (1959), thus increasing the probability that plutonic rock may host the geothermal system. Individual outcrops of plutonic rock are fairly homogeneous, medium grained, and equigranular. Fractures are usually spaced a few to a few tens of centimeters apart. Individual outcrops often bear several fracture sets at different azimuths and dips. There is no single pervasive joint orientation on either outcrop or regional scale. Steeply dipping mafic and andesitic dikes a few tens of centimeters to a few meters across are common, but there is no strongly preferred orientation.

Plutonic samples in the Geyser Creek valley and on the shore of Geyser Bight are pyroxene-hornblende quartz monzonite and pyroxene-biotite-hornblende quartz diorite (table 1, fig. 3). Samples from near Geyser Bight are quartz diorite or plagioclase-rich quartz monzonite. Samples from further up-valley are plagioclase-poor quartz monzonite. Up-valley samples have moderately higher SiO_2 content and dramatically higher K_2O content than samples from Geyser Bight. On the K_2O-SiO_2 plot (fig.4) the trend defined by the quartz diorite and quartz monzonite steeply cuts the medium-K to high-K boundary of Gill (1981) and is much steeper than can be produced by fractional crystallization.

The more potassic samples have higher modal concentrations of K-feldspar (table 1), which is presumably the major site of potassium in these units. The K-feldspar occurs as large, discrete subhedral grains and in micrographic and myrmekitic intergrowths with quartz. These igneous textures indicate that the anomalous K_2O contents have an igneous rather than metamorphic or metasomatic origin. Much of the K-spar occurs as late-stage intergrowths with quartz, which suggests that the K_2O-rich nature of the rocks is related to the evolution of a K_2O-rich magma rather than to the accumulation of feldspar phenocrysts. If the K_2O-rich and K_2O-poor magmas are related to each other, it must be by some process other than fractional crystallization. They probably are not genetically related, but rather reflect independent periods of stock emplacement. Although high-K magmas rarely erupt in the modern Aleutian arc, they are found in some plutonic rocks elsewhere in the arc (Kay and others, 1982). McLean and Hein (1984) report 31-33 Ma plutonic and hypabyssal high-K rocks of similar composition from southwestern Umnak Island (fig. 4).

Table 1. *Modal abundance of minerals in plutonic rock samples*[a]

	DT88-01	DT88-01	DT88-02	DT88-03	DT88-04	88CNU10	88CNU11
Plagioclase	60.3	49.7	52.0	60.0	46.0	44.3	44.0
K-feldspar	3.7	6.7	14.7	6.0	19.7	19.0	22.0
Quartz	10.0	8.7	13.3	13.3	12.7	8.3	11.7
Biotite	3.7	0.3	1.3	9.0	0.0	0.0	0.0
Amphibole	15.7	29.0	12.0	0.0	16.3	9.0	9.7
Chlorite	1.7	3.7	4.3	0.3	0.7	2.3	5.7
Pyroxene	3.0	0.3	0.0	8.0	0.3	3.7	3.3
Opaque oxides	1.7	1.0	1.3	2.7	3.7	4.0	3.0
Accessories	0.3	0.7	1.0	0.7	0.7	0.0	0.7
Myrmekite[b]	0.0	0.0	0.0	0.0	0.0	9.3	0.0

[a]Modes are based on petrographic determination of 300 grains per sample.

[b]Myrmekite was only counted as a separate phase when intergrowths were of fine enough scale to preclude accurate counting of individual mineral species.

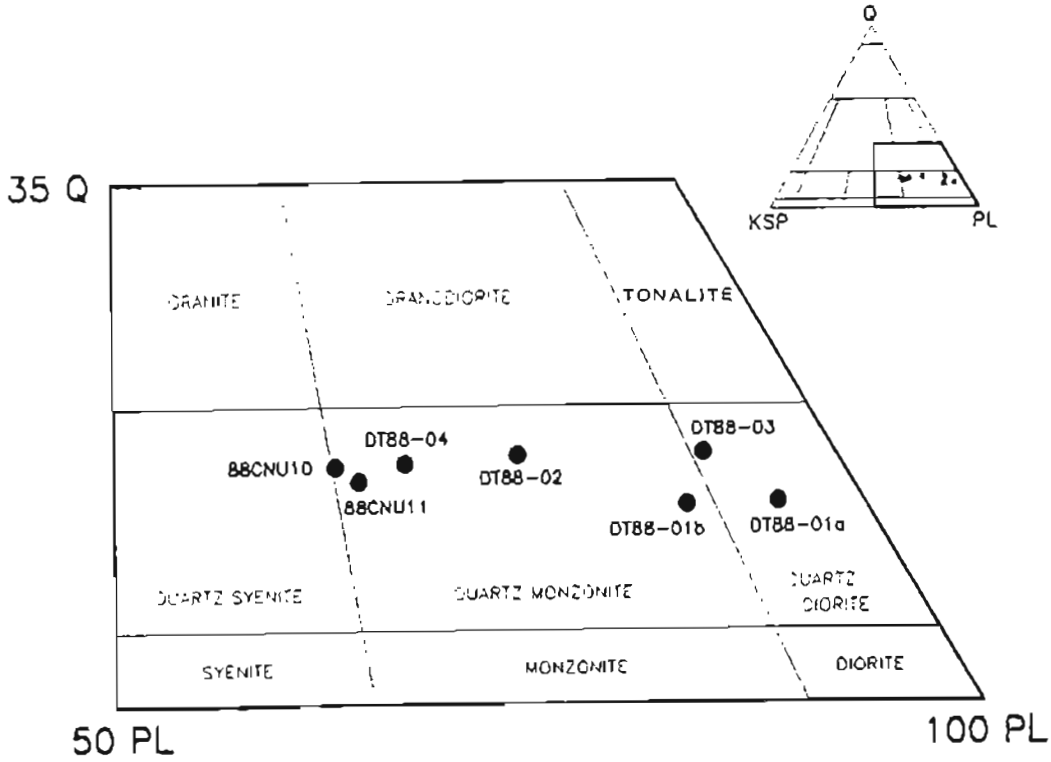

Figure 3. *Part of the IUGS plutonic rock classification diagram; apices are quartz (Q), alkali feldspar (KSP), and plagioclase (PL). Samples are plotted according to modal mineralogy (table 1) rather than normative mineralogy from the chemical composition.*

TERTIARY SEDIMENTARY AND VOLCANIC ROCKS (Tvs)

The oldest rock unit in the Geyser Bight area consists of lightly metamorphosed lava flows, dikes, sills, and sedimentary and volcanogenic clastic rocks of Tertiary age. The largest exposures of this unit are at the southwestern end of Umnak Island where there are no overlying volcanic units. According to Byers (1959), the unit consists of gently dipping mafic lava flows with subordinate beds of argillite and tuff, all of which were intruded by gabbro and diorite that were subsequently albitized. These rocks are gently folded and crosscut by minor faults (Byers, 1959), fracturing is pervasive. McLean and Hein (1984) report late Eocene to early Oligocene ages for these rocks.

In the Geyser Bight area, the unit is dominantly composed of fine-grained, equigranular to porphyritic hypabyssal and extrusive mafic and intermediate igneous rocks. The unit occurs as screens and blocks within the pluton and overlies the pluton on the east and west sides of Geyser Creek valley. The maximum thickness exposed in the Geyser Bight region is about 150 m. The upper surface has gently rolling topography identical to that elsewhere on the broad, wave-cut platform that truncates this unit. The contact between the Tertiary volcanic sequence and the pluton is irregular and occasionally of moderate relief.

In the Geyser Bight area, alteration of these Tertiary rocks is common. In one exposure on the southwestern side of Geyser Creek valley, hornblende quartz diorite in the lower valley wall crops out immediately below highly altered andesite (Tvs) that contains 70 percent quartz veinlets that appear to originate in the quartz diorite. Pyroxene-plagioclase andesite overlying the pluton on the east side of Geyser Creek valley is pervasively chloritized and in some localities silicified or pyritized. Quartz veining is pervasive. On the east side of the Geyser Bight beach, the unit is fine grained, but the presence of elongated plagioclase microlites suggests that the unit is volcanic rather than sedimentary. Unequivocally sedimentary units of Tvs were not seen in the Geyser Bight area.

Tvs is distinguished from overlying volcanic rocks by its pervasive tectonic fracture pattern and lack of well-preserved volcanic features. In addition, it is usually highly altered.

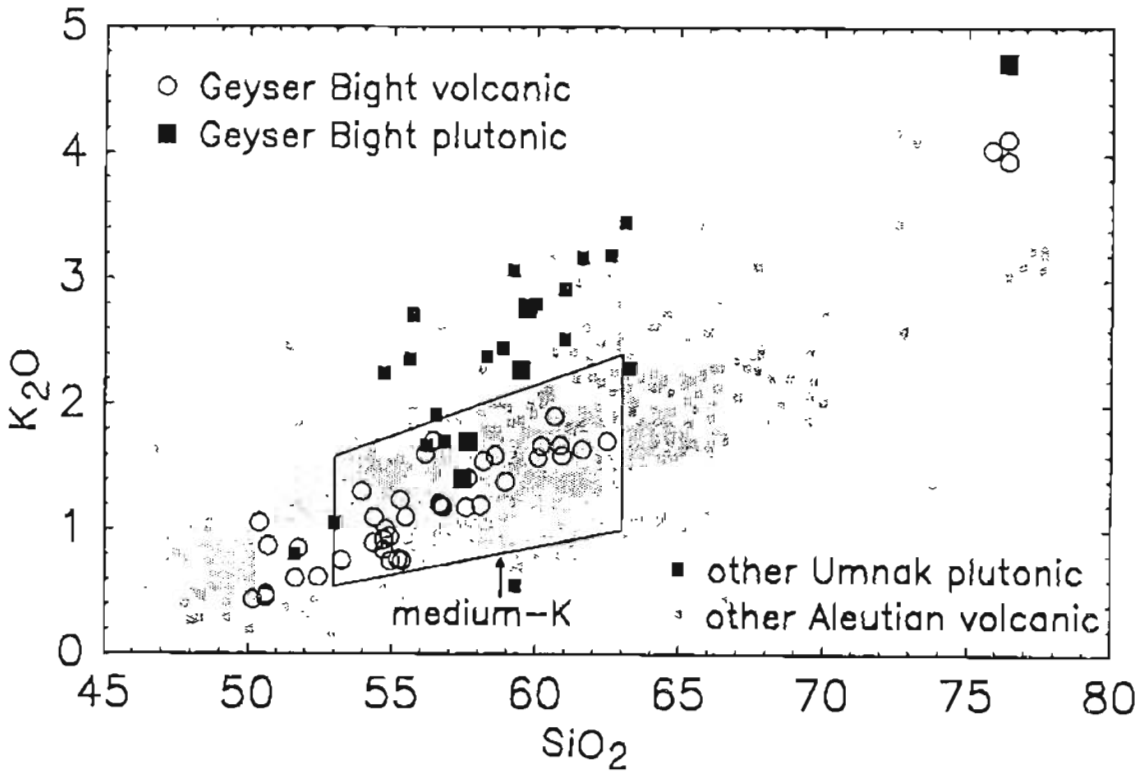

Figure 4. *K_2O vs. SiO_2 diagram of Geyser Bight plutonic and volcanic rocks (this study; Byers, 1959). Plutonic rock compositions from southwestern Umnak Island (McLean and Hein, 1984) and literature values for Quaternary Aleutian volcanic centers are shown for comparison.*

STRUCTURE

Only the oldest rocks (Tvs) on central Umnak Island have been deformed, and these only gently. Beds usually have gentle dips, folds are open, and faults and fractures, although numerous, do not have large displacements (Byers, 1959). South of Mt. Vsevidof, folds trend northwest and large fractures trend northeast (Byers, 1959). The amount of Tvs outcrop in Geyser Creek valley was not sufficient to allow recognition of folds or faults.

Plutonic rocks are well fractured in surface outcrops. Fractures are spaced a few centimeters to a few tens of centimeters apart. Most outcrops have several rather than a prominent joint set; we did not observe any jointing in a preferred direction in the map area. Dikes in the pluton have no preferred alignment.

The only fractures seen in the volcanics of central Umnak Island (Qcuv) and the lavas of Mt. Recheshnoi (Qra) resulted from volcanic cooling.

Motyka and others (1981) note that Geyser Creek valley trends northwest at the same azimuth that Nakamura and others (1980) suggest is the azimuth of principal compressive stress due to subduction of the Pacific sheet. The "Nakamura" stress trajectory is based on the alignment of parasitic and flank volcanic vents of Aleutian and other Alaskan volcanoes, and on Quaternary fault orientations. Nakamura and others (1977, 1980) suggest that dilational fractures should appear parallel to the axis of principal compression and allow easier rise of magma to the surface. Such fractures could form local zones of weakness and localize a geothermal resource. We found no obvious northwest-trending fractures or faults, but the thick, continuous tephra and vegetation cover at low elevations may obscure some structures.

An important feature of the Nakamura and others (1977) hypothesis is that flank volcanic features are expected to be aligned parallel to the maximum compressive stress. In the Geyser Bight area, this does not appear to be the case. The 3-km-long linear zone of rhyolite plugs above Russian Bay trends N.85°W., rather than

N.47°W., which is the convergence direction between the Pacific and North American sheets (Jacob and others, 1977). This east-west trend is also reflected in the attitudes of many near-vertical dikes at Geyser Bight, Cemetery Cove, and Stepanof Cove. The largest dike we observed in the Geyser Creek area is part of Mt. Recheshnoi volcano and crops out between Geyser Creek valley and Russian Bay valley. Its trend is nearly orthogonal to that predicted by Nakamura and others (1977).

Our geologic mapping and cross sections (sheet 1) indicate that valley fill is very thin at the head of the valley and that plutonic rock extends much farther up the valley than shown by Byers (1959). We propose that geothermal reservoirs will most likely occur in the highly fractured plutonic rock. Tvs may also be present, as shown on cross section B-B' (sheet 1). Exploratory drilling at Makushin volcano demonstrated the ability of plutonic rocks to sustain fracture permeability sufficient to host a geothermal reservoir.

VOLCANIC HAZARDS

Because the Aleutian arc is the locus of intense volcanism, volcanic hazards may be present anywhere within the arc. However, at Geyser Bight and in Geyser Creek valley, the volcanic hazards are surprisingly slight despite the presence of two active volcanoes. Mt. Vsevidof, which is unglaciated and therefore has had numerous Holocene eruptions, is 18 km southwest of Geyser Creek valley, but the large size of Mt. Recheshnoi and the 300-m-high ridge southwest of Geyser Creek protect Geyser Creek from flow hazards from Mt. Vsevidof. Historic volcanic activity at Mt. Vsevidof has been restricted to minor explosions and steaming. If this pattern of eruption continues, future activity may deposit minor amounts of ash in Geyser Creek valley.

Okmok Volcano, 30 km to the northeast, is the most active volcano on Umnak Island. Following two mid-Holocene, caldera-forming eruptions, activity has been restricted to steaming, minor ash emissions, and the emplacement of basaltic lava flows on the caldera floor. Future activity is expected to follow the same pattern-quiet, effusive flows accompanied by minor ash eruptions. The caldera wall is about 300 m high and breached only to the northeast. If lava erupts in sufficient volume to leave the caldera, it will probably exit through the northeast breach. We lack adequate data to judge the probability of explosive eruptions or eruptions from centers outside Okmok Caldera. Geyser Creek valley is separated from Okmok Volcano by Inanudak Bay and a 600-m-high ridge. Thus it is well protected from volcanic activity originating at Okmok (fig. 2).

Mt. Recheshnoi (10 km southwest of Geyser Creek valley) is the closest volcano to the geothermal area. Because the central cone is highly eroded, it is probably entirely Pleistocene in age. A few Holocene flank eruptions, including andesite flows on the east and west flanks have occurred. The rhyolite bodies and quartz-andesite flows, considered Holocene in age by Byers (1959), are actually 135 ka and 89 ka old, respectively. These flank flows did not enter Geyser Creek valley. Insufficient data preclude estimating the recurrence interval of Holocene eruptions, but the probability of volcanic flows entering Geyser Creek valley seems small. Geyser Creek valley is protected from flowage hazards by a high ridge between the valley and Mt. Recheshnoi. No Holocene mass-flow deposits have been found in Geyser Creek valley or Russian Bay valley.

The most likely volcanic hazard is ash fall, which could present a temporary hazard to machinery and aircraft operation. Holocene tephra 3-4 m in cumulative thickness occurs throughout the Geyser Creek area.

GEOCHRONOLOGY OF VOLCANIC AND PLUTONIC EVENTS

BACKGROUND

We have completed ^{40}K-^{40}Ar age analyses for 23 andesite flows, one rhyolite plug, and the plutonic rock that may host the reservoir for the Geyser Bight geothermal system. These results provide a time framework for the mapped rock units and for the evolution of the magmatic system that drives the geothermal resource.

ANALYTICAL METHODS AND RELIABILITY OF YOUNG AGES

All andesite samples were dated as whole rocks. Biotite from the rhyolite plug was dated, and biotite and hornblende from the pluton were dated. Replicate potassium was measured using $LiBO_2$ flux fusion and flame photometry with a lithium internal standard. Mineral standards were used to calibrate the photometer. Argon

isotopes were measured by isotope dilution on a computerized, 6-in.-radius mass spectrometer. Analytical data for the ^{40}K-^{40}Ar age determinations are given in table 2, and sample localities are shown on sheet 1.

Several modifications of our analytical techniques allowed us to obtain reproducible, stratigraphically consistent ages on some whole-rock andesite samples as young as 60,000 yr. These modifications are listed below.

1. Reducing air-argon contamination from the extraction system by replacing quartz-lined, air-cooled fusion bottles with water-cooled, unlined bottles.

2. Boiling whole-rock samples (crushed to 16-48 mesh) for 1 hr in distilled water immediately before loading them in the extraction system resulted in significantly lower atmospheric argon per unit sample weight in about 30 percent of the samples. The reason for this effect is not well understood; it was observed empirically by G.H. Curtis, R.E. Drake, and A.L. Deino (University of California, Berkeley) and communicated to Turner, who produced similar results. One possibility is that the atmospheric argon in cracks in the sample may be replaced by hydrogen during boiling (R.E. Drake, oral com.).

3. As a general procedure, argon from one sample fusion is split into two to four aliquots that are sequentially analyzed on the mass spectrometer. The first split is used to "flush" the spectrometer to reduce the memory effect in static gas analysis. This effect is particularly important when analyzing young samples with small amounts of radiogenic ^{40}Ar, such as most of the Umnak Island andesites. Results from these "flushing splits" were averaged with the subsequent splits only when they were statistically equivalent. Results from the remaining splits were averaged to calculate the values of radiogenic ^{40}Ar, percent radiogenic ^{40}Ar, and age (table 2). With one exception (88CNU55), the argon analyses in this study represent single fusions of each sample.

Two recent test studies of suites of young andesites from Mt. Spurr, Alaska, and the Nevados de Payachata volcanic group in the Chilean Andes (both done in our laboratory by the methods described above) produced results that are reproducible within analytical uncertainty and fit the volcanic stratigraphy observed in the field (Worner and others, 1988; Nye and Turner, 1990). However, dating andesites this young is definitely pushing the limits of the K-Ar method, as evidenced by problems we encountered with some Umnak samples.

RESULTS

With some exceptions, ages of the 23 dated samples agree with observed stratigraphic relationships. The dates provide a well-constrained time framework for the area's eruptive history and a cooling age for the plutonic rock that may host the geothermal system. Ages are discussed from youngest to oldest, in the approximate order shown in table 2.

The youngest flows (Qrf) from Mt. Recheshnoi proved too young to date, but three of the upper cone-building flows (Qra) yielded ages of 75, 121, and $\geq$ 110 ka (minimum age based on petrographic criteria). Lower in the Qra section, we obtained an age of 258 ka from the northeast side of Geyser Creek valley, and ages of 285 and 478 ka from flows above Hot Springs Cove. Basal Recheshnoi flows on the southwest side of Geyser Creek valley yielded ages of 472, 489, 534, and 499 ka. These radiometric ages for Mt. Recheshnoi flows range from 75 $\pm$ 11 to 534 $\pm$ 13 ka at the base of the section.

The 478-ka Qra age is problematic because it is from a flow that is located only one or two flows below the flow dated at 285, ka in the same section. We observed no evidence of a paleosol or fault separating the two dated flows, and field relations suggest that these flows should be similar in age. Because the 478-ka age is consistent with the 472-534-ka Qra ages from the southwest side of Geyser Creek valley it cannot be entirely rejected on the basis of the geologic observations discussed above. The sample meets petrographic reliability criteria for whole-rock K-Ar dating. Excess argon is not normally found in significant amounts in subaerial lava flows and is unlikely to be present in the dated sample. At present, we cannot resolve this problem. Fortunately, it does not affect the documented age span for Mt. Recheshnoi flows (Qra) discussed above.

Table 2. *Agetable*

Lab no.	Field no.	Material dated[a]	K_2O[b] (wt %)	Sample weight[c] (g)	$^{40}Ar_{rad}$ (mol/g) x 10^{-11}c	$\frac{^{40}Ar_{rad}}{^{40}K \times 10^{-3}c}$	$\%^{40}Ar_{rad}$	Age (ka) ± 1 δ
				Upper cone-building flows (Qra), south flank Mt. Recheshnoi				
88101	88cnu85	wr	0.613	12.2853	0.0067	0.0044	0.90	75 ± 11
88084	88cnu83	wr	0.869	11.5900	0.0152	0.0071	5.56	121 ± 6
88102	88cnu80	wr	0.875	11.7469	0.0144	0.0067	3.41	110 ± 7
88099	88cnu06	wr	1.232	10.0537	0.0459	0.0150	1.35	258 ± 35
				Recheshnoi flows (Qra) above Hot Springs Cove				
88073	88cnu56	wr	1.547	10.2845	0.0636	0.0166	2.94	285 ± 9
88100	88cnu57	wr	1.450	10.5823	0.0999	0.0278	6.24	478 ± 12
				Basal Recheshnoi flows (Qra), southwest Geyser Creek valley				
88153	DT88-10	wr	1.560	9.1595	0.1061	0.0275	12.20	472 ± 14
88107	DT88-14	wr	1.667	9.0659	0.1173	0.0284	7.31	489 ± 15
88103	DT88-16	wr	1.212	10.3391	0.0930	0.0310	5.35	534 ± 13
88108	DT88-17	wr	1.189	10.8868	0.0854	0.0290	4.03	499 ± 12
				Rhyolite (Qr)				
88138	88gpu07	bi	8.398	0.4002	0.1633	0.0079	1.47	135 ± 15
				Quartz andesite (Qrq)				
88105	88cnu55	wr	1.260	10.2996	0.0167	0.0054	0.96	92 ± 9
88160	88cnu55	wr	1.260	9.8800	0.0150	0.0050	0.64	78 ± 17
				Volcanics of central Umnak (Qcuv) above Hot Springs Cove				
88106	88cnu59	wr	1.550	10.0698	0.0951	0.0248	14.04	426 ± 13
				Volcanics of central Umnak (Qcuv), northeast Geyser Creek valley				
88076	88cnu02	wr	0.695	12.1284	0.0787	0.0457	6.58	786 ± 12
88104	88cnu04	wr	0.648	10.7349	0.0779	0.0485	19.37	835 ± 25
88077	88cnu03	wr	0.775	12.1601	0.0954	0.0497	13.39	854 ± 22
				Volcanics of central Umnak (Qcuv), southwest Geyser Creek valley				
88110	DT88-05	wr	0.759	11.3441	0.1200	0.0639	7.13	1,104 ± 48
88111	DT88-07	wr	0.717	6.1810	0.1163	0.0655	4.92	1,124 ± 48
				Pyroclastic rocks (Qcup), Stepanof Cove				
88117	DT88-36	wr	1.087	7.1607	0.2145	0.0797	7.72	1,368 ±54*
				Dikes intruding pyroclastic rocks (Qcup), Stepanof Cove				
88114	DT88-30	wr	1.072	10.8711	0.2105	0.0793	10.30	1,365 ± 41
88116	DT88-30P	wr	1.085	5.7325	0.2512	0.0935	3.90	1,613 ± 56
				Plutonic rocks (Tdp), east side of Geyser Bight				
88167	DT88-1A	bi	7.846	0.2255	10.9100	0.5614	63.61	9,640 ±290
88164	DT88-1A	hb	0.392	1.5531	0.5315	0.5476	19.08	9,400 ±280

[a]Abbreviations are wr (whole-rock), bi (biotite), hb (hornblende).
[b]Averages of 2 replicate analyses/sample except for 88138 (6 replicates), 88167 (3 replicates), and 88164 (4 replicates).
[c]Averages of 2 analyses per argon extraction except for 88099 (3 analyses) and 88105, 88167, 88164 (1 analyses each).
*denotes minimum age based on petrographic criteria

Sample 88GPU7 is from the easternmost and largest of the seven biotite rhyolite plugs (Qr) above Russian Bay (sheet 1). Biotite from the rhyolite yielded an age of 135 ± 15 ka.

Sample 88CNU55 is from the quartz-olivine andesite flows (Qrq) that overlie Qra above Hot Springs cove. The 89 ka age for this unit is older than expected but geologically feasible. The well-preserved, concentric flow fronts visible on air photos suggest that the unit is unglaciated, but, field inspection shows that rubbly flow tops have been removed, presumably by glacier ice. The position of this unit on a high, broad ridge uncut by canyons suggests that it was probably overlain by a broad, slow-moving icefield that only slightly eroded the underlying rocks, thus preserving the concentric flow-front morphology. The uppermost Qra section directly below this unit was dated at 285 ± 9 ka and provides the only available older age constraint for the Qrq unit.

Volcanic flows of central Umnak Island (Qcuv) underlie the Qra unit. Their attitudes indicate source vents north of Geyser Creek valley. Five samples from the Qcuv unit that flanks Geyser Creek valley range from 786 ± 21 ka yr in the upper part of the section to 1,124 ± 48 ka at the base of the section. A sample from near the top of the Qcuv section (above Hot Springs Cove) yielded a minimum age of ≥ 426 ka B.P. The age span of Qcuv flows is therefore documented at ≤ 786 ± 21 to 1,124 ± 48 ka.

Pyroclastic rocks (Qcup) at Stepanof Cove, presumed by Byers (1959) to be equivalent in part to the Qcuv unit, yielded a minimum age of ≥ 1,368 ± 54 ka. The dated sample is from a radially fractured andesite block believed to have cooled in place within the pyroclastic deposit. This minimum age-about 140 ka older than the oldest age we obtained from the base of the Qcuv section.

Two samples from a single, 1.3 m-thick dike that intrudes the dated pyroclastic unit (Qcup) at Stepanof Cove yielded ages of 1,365 ± 41 and 1,613 ± 56 ka. The significantly different ages are due to variations in radiogenic ^{40}Ar content per gram of sample (potassium contents are essentially identical). We conclude that the quickly chilled dike rock contains variable amounts of excess argon and that the younger age probably better reflects the true cooling age of the dike. The younger age is concordant with the minimum age of ≥ 1,368 ± 54 ka for the pyroclastic unit intruded by the dike. These data suggest two interpretations for the age of the pyroclastic (Qcup) unit: (1) the pyroclastic unit may be significantly older than the minimum age of ≥ 1,368 ± 54 ka, or (2) the concordant Qcup and younger dike ages may reflect the true cooling age for these units (about 1.4 Ma), and the dike may have been a feeder for the pyroclastic eruption.

Sample DT88-1A from the plutonic rock unit (Tdp) collected at the east side of Geyser Bight yielded concordant biotite and hornblende ages of 9.64 ± 0.29 and 9.40 ± 0.28 Ma, respectively. These concordant ages indicate that the dated pluton had a simple cooling history; it cooled through the argon-blocking temperatures for hornblende and biotite (from 530° ± 40°C to 280° ± 40°C) at about 9.5 Ma. Cooling must have occurred in less than 300 ka (standard deviation of ages) for the ages to be concordant.

McLean and Hein (1984) report 31-33 Ma plutonic and hypabyssal rocks from southwestern Umnak Island. Our much younger date for plutonic rock at Geyser Bight indicates that there have been at least two episodes of Tertiary plutonism on the Island. The 9.5 Ma pluton is the youngest rock on Umnak truncated by the regional wave-cut surface of the Aleutian summit platform.

GEOCHEMISTRY OF VOLCANIC ROCKS

INTRODUCTION

The chemical compositions of magmas change in response to igneous processes. By measuring the composition of erupted magmas, we can recognize the processes that operated during the life of the volcanic system. This approach provides direct information about the magmatic plumbing system that is the source of geothermal heat. Among the recognized processes are fractional crystallization, magma mixing, and variations in partial melting. During fractional crystallization, crystals with compositions different than the host magma separate and drive the composition of the remaining liquid along a specific path. Mixing of chemically distinct magma batches also produces recognizable chemical trends. Initial melts produced in the source region have recognizable chemical features that reflect the origin and mode of melting. In addition, temporal variations in

chemistry provide direct information about the evolution of the plumbing system. In some cases, inferences about the location and size of the dominant magma chamber can be made.

In this report, we describe the chemical composition of Geyser Bight magmas and interpret variations in chemical composition in terms of igneous processes that can constrain the geologic evolution of the geothermal system. Data were obtained by X-ray fluorescence spectroscopy at the University of California, Santa Cruz. Duplicate analyses of all samples indicate that mean analytical precision is less than 1.5 relative percent for SiO_2, TiO_2, Fe_2O_3, Al_2O_3, CaO, and K_2O; less than 2 percent for MgO; and about 5 percent for Na_2O and P_2O_5. Extreme values for Na_2O imprecision exceed 20 percent relative. Sample locations are shown on sheet 1 and figure 5. All analytical data are shown in table 3.

CHEMICAL VARIATION OF LAVAS

Harker diagrams of Geyser Bight lavas are shown in figure 6. Most samples are medium-K andesite, as defined by Gill (1981), with some basalt and rare rhyolite but no dacite. In most respects the basalt and andesite are compositionally similar to other Aleutian lavas. FeO^t (total iron as FeO), MgO, CaO, and Al_2O_3 fall with increasing SiO_2; K_2O increases dramatically; and Na_2O and TiO_2 are scattered. Scatter in Al_2O_3 and, to a lesser extent TiO_2, is probably related to differential crystal accumulation. Scatter in Na_2O is partially due to analytical imprecision.

Most samples fall within the calc-alkaline field of Miyashiro (1974). Most samples that fall above or near the Th-Ca dividing line are part of a chemically anomalous high FeO^t, high TiO_2 group described below. Samples from Mt. Recheshnoi are strongly calcalkaline; Mt. Recheshnoi is among the most calcalkaline volcanoes in the Aleutian arc and bears many similarities to the calcalkaline volcanoes of the eastern arc. A continuum of compositions existsbetween 50 percent and 63 percent SiO_2, but no magmas have between 63 percent and 76 percent SiO_2, which constitutes a major compositional gap. Rhyolitic samples were taken from the rhyolite domes west of Russian Bay valley and from granophyres within the pluton. Rhyolite is rare in Pleistocene Aleutian volcanoes, and is only known from 4 centers other than Recheshnoi: (1) a small pod on the flank of Okmok caldera, 35 km to the northeast; (2) a few pumice samples from Shishaldin; (3) Novarupta, the site of the climactic 1912 eruption of the Valley of Ten Thousand Smokes; and (4) a single pumice sample from Augustine volcano. Only Novarupta (1000 km east along the arc) has erupted more silicic magma.

A group of samples most noticeable in FeO^t vs SiO_2 (fig. 6) defines a trend parallel to the main evolutionary trend but with higher iron contents. These samples are also characterized by high TiO_2; relatively low MgO (and therefore high FeO^t/MgO); relatively low Al_2O_3 concentrations (which form a linear trend between 52 percent SiO_2 and 17.5 percent Al_2O_3, and 63 percent SiO_2 and 15.5 percent Al_2O_3); and fewer phenocrysts than other samples. These samples are referred to as the high FeTi group. Samples in this group include lavas erupted from the central Umnak Island vents at intervals throughout their lifetimes (but not all Qcuv samples); some recent lavas from Mt. Recheshnoi; the Holocene Recheshnoi andesite flows (Qrf); and samples from quenched blobs within the rhyolite. Quartz andesite samples are not part of the high FeTi group.

The group of samples at lower FeO^t are probably not related to the sparsely phyric, high FeTi group by simple crystal accumulation because that accumulation should raise both FeO^t and MgO. Instead, crystal-rich samples have lower Fe and higher Mg.

Plutonic rocks are compositionally similar to Recheshnoi and central Umnak andesites except for the high K_2O content of quartz monzonites and granophyres, but not quartz diorites. This presumably reflects some unspecified difference in petrogenetic processes between plutonic and volcanic rocks. Because the plutonic samples are not related to the present magmatic plumbing system, they are not discussed here; their composition is described in the discussion of map units (p. 11).

Cinder Point is a small, monogenetic cone on the flanks of Okmok Volcano whose composition and history probably have little bearing on the Recheshnoi geothermal system. Cinder Point samples differ from most other samples; they have high Al_2O_3, CaO, and normative plagioclase and low MgO. They also have large, monomineralic, polycrystalline, plagioclase aggregates, often rounded and embayed, up to 5 mm diam. The composition of the Cinder Point samples probably reflects selective crystal accumulation.

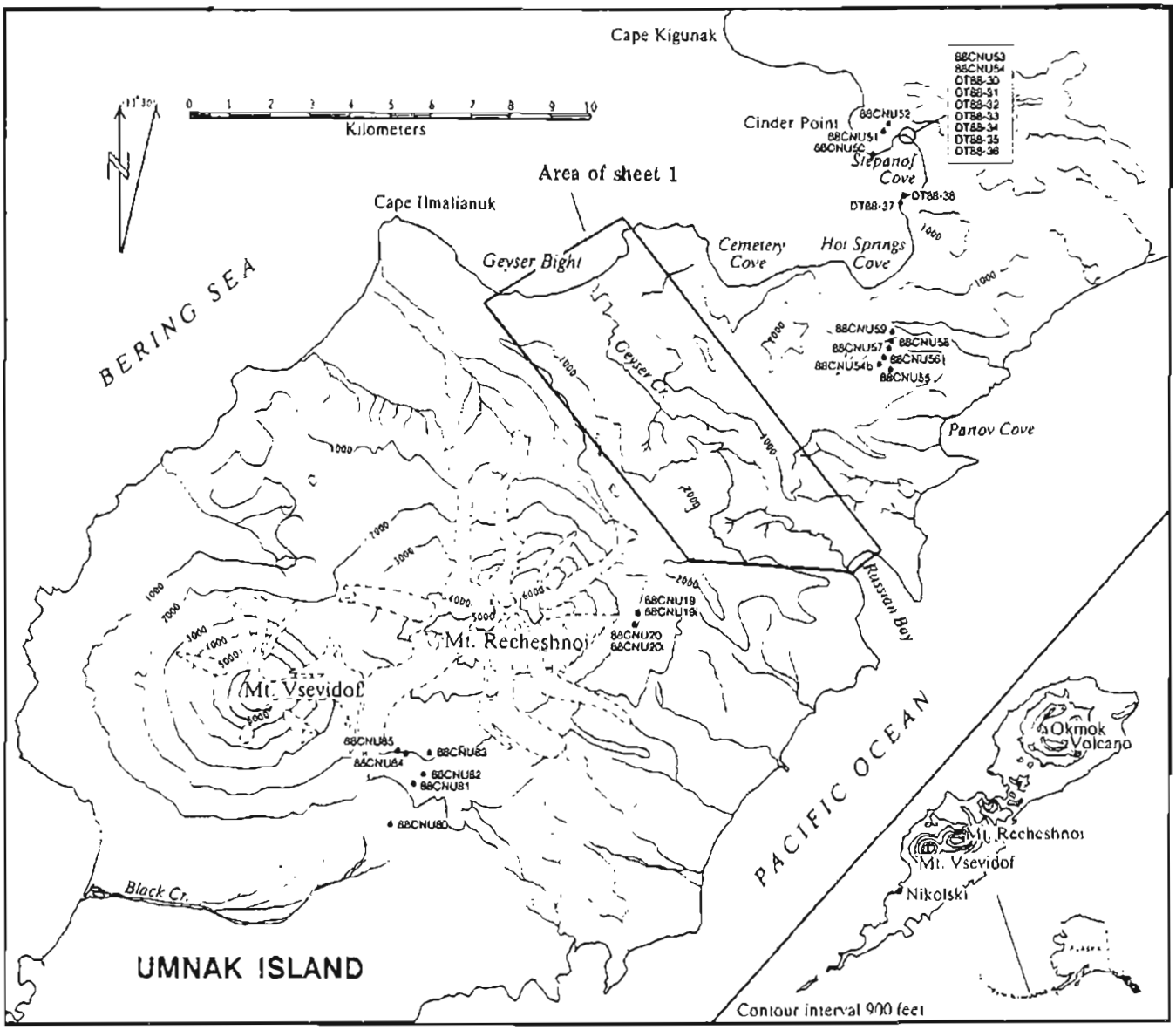

Figure 5. *Location of samples outside the area on sheet 1; analytical data are shown in table 3.*

PETROGENESIS OF LAVAS

Processes that may interrelate these lavas include fractional crystallization, variable P-T-P_{H2O} fractionation path, magma mixing, crystal sorting, crustal assimilation, crustal melting, and variations in primary magmas. Each process is discussed below. It is difficult to identify the correct operational process without additional trace element and isotopic data, and even with that data, it is often difficult to construct exact petrogenetic models. Nevertheless, we can make some first-order qualitative observations.

CRYSTAL FRACTIONATION

Much compositional variation among the basalts and andesites is probably due to fractional crystallization. Separation of 70 percent of plagioclase ± olivine + clinopyroxene ± orthopyroxene + magnetite crystals (by weight) can account for similar compositional variations in other Aleutian volcanoes of similar bulk composition (for example Kay and others, 1982; Nye and Turner, 1990). However, scatter about expected fractionation trends in most variation diagrams requires the involvement of other secondary processes.

Table 3. *Compositional data on samples from the Geyser Creek area and surrounding regions*

ID	88cnu51	88cnu19	88cnu19i	88cnu20	88cnu54[b]	88cnu55	88cnu14	88cnu17	88cnu18i	88cnu13	88cnu06	88cnu07
unit	Qcp	Qrf	Qrf	Qrf	Qrq	Qrq	Qr	Qr	Qr	Qra1	Qra	Qra
Chemical composition[a]												
SiO_2	50.62	56.79	54.91	56.73	50.39	53.94	75.82	76.36	58.93	61.61	55.27	.
TiO_2	0.75	1.18	1.27	1.18	0.77	0.70	0.15	0.13	1.19	0.85	0.96	.
Al_2O_3	21.67	16.97	17.16	16.87	15.35	15.91	13.16	13.11	16.14	17.00	17.60	.
FeOt	7.27	8.09	8.83	8.10	7.95	7.00	1.23	1.17	7.97	5.75	7.32	.
MgO	4.00	3.87	4.47	3.88	10.89	8.00	0.17	0.15	3.33	2.28	5.07	.
CaO	11.60	7.46	8.10	7.41	9.96	9.38	1.01	1.04	6.53	5.79	8.07	.
NaO	3.54	4.30	4.14	4.46	3.49	3.62	4.39	3.91	4.39	4.93	4.32	.
K_2O	0.46	1.18	0.94	1.19	1.05	1.30	4.04	4.12	1.38	1.64	1.24	.
P_2O_5	0.10	0.16	0.18	0.18	0.15	0.13	0.03	0.01	0.14	0.13	0.16	.
MnO	na	na	na	na	na	na	na	na	na	na	na	.
LOI	na	na	na	na	na	na	na	na	na	na	na	.
Total[b]	**100.99**	**100.75**	**100.29**	**101.59**	**99.00**	**99.28**	**102.19**	**101.17**	**99.37**	**100.14**	**101.05**	.
Fe_2O_3	8.10	8.98	9.75	9.07	8.68	7.67	1.39	1.31	8.72	6.36	8.15	.
Modal composition												
Gms[c]	60	85	40	90	35	75	.	85	90	70	65	50
Plag1[d]	++	+	+	=	=	.	.	+	+	+	=	++
Plag2[e]	.	.	==	==	+	+	.	.	+	+	++	=
Ol	=	=	+	==	+	+	.	.	.	.	=	==
Cpx	=	=	+	=	+	+	.	.	+	+	+	+
Opx	.	==	.	=	.	=	.	.	.	.	=	+
Hb	.	.	.	.	++	.	.	.	.	.	.	.
Bi	.	.	.	.	.	.	.	+	.	.	.	.
Qz	.	.	.	.	.	==	.	+	.	.	.	.
Oxide	==	==	.	=	.	=	.	==	.	=	==	==
Comments	.	.	50% vesicles	.	.	gabbroic clots				glomerocryst	.	.

[a]Whole-rock chemical composition is normalized to 100% anhydrous.
[b]Original Fe_2O_3, total, and LOI reported.
[c]Gms is estimated percent groundmass.
[d]Plag1 is well formed and inclusion free.
[e]Plag2 is resorbed, reversely zoned, or spongy

Proportions of minerals denoted by ++ (dominant), + (common), = (uncommon), == (rare), and · (not observed).

Table 3. *Compositional data on samples from the Geyser Creek area and surrounding regions-Continued*

ID	88cnu08	88cnu09	88cnu15	88cnu21	88cnu56	88cnu57	88cnu58	88cnu80	88cnu81	88cnu82	88cnu83	88cnu84
unit	Qra	Qra	Qra	Qra	Qra	Qra	Qra	Qra	Qra	Qra	Qra	Qra
Chemical composition												
SiO_2	.	51.74	.	50.70	56.44	58.18	.	54.71	.	.	54.36	51.65
TiO_2	.	0.95	.	0.74	1.05	0.97	.	0.96	.	.	0.94	1.22
Al_2O_3	.	16.14	.	15.52	16.49	16.97	.	18.65	.	.	18.87	17.53
FeOt	.	8.04	.	7.97	7.07	6.43	.	7.45	.	.	7.26	9.28
MgO	.	8.08	.	10.93	4.76	4.01	.	4.47	.	.	4.48	5.83
CaO	.	9.84	.	10.11	8.15	7.45	.	8.88	.	.	9.05	9.68
NaO	.	4.19	.	3.05	4.13	4.27	.	3.84	.	.	4.02	4.04
K_2O	.	0.85	.	0.87	1.71	1.54	.	0.92	.	.	0.89	0.61
P_2O_5	.	0.16	.	0.12	0.20	0.17	.	0.12	.	.	0.13	0.16
MnO	.	na	.	na	na	na	.	na	.	.	na	na
LOI	.	na	.	na	na	na	.	na	.	.	na	na
Total	.	**100.66**	.	**100.84**	**100.47**	**99.21**	.	**98.53**	.	.	**100.30**	**101.40**
Fe_2O_3	.	8.92	.	8.85	7.84	7.04	.	8.09	.	.	8.03	10.36
Modal composition												
Gms	70	75	60	40	70	50	50	65	65	70	70	99
Plag1	=	+	++	+	+	+	+	++	++	+	+	=
Plag2	++	=	.	.	=	=	=	=	=	=	+	.
Ol	.	+	.	++	=	=	=	=	+	+	=	=
Cpx	+	=	+	=	+	+	+	+	=	+	=	==
Opx	+	==	+	.	+	+	+	=	=	=	==	.
Hb	.	.	.	.	.	.	.	.	.	.	.	.
Bi	.	.	.	.	.	.	.	.	.	.	.	.
Qz	.	.	.	.	.	.	.	.	.	.	.	.
Oxide	.	.	=	.	=	=	=	.	=	==	==	.
Comments	clots	.	clots	.	.	.						

Table 3. *Compositional data on samples from the Geyser Creek area and surrounding regions-Continued*

ID	88cnu85	dt88-10	dt88-12	dt88-13	dt88-14	dt88-15	dt88-16	dt88-17	88cnu02	88cnu03	88cnu04	88cnu05
unit	Qra	Qra	Qra	Qra	Qra	Qra	Qra	Qra	Qcuv	Qcuv	Qcuv	Qcuv
Chemical composition												
SiO_2	52.44	60.07	.	60.84	60.16	56.64	58.08	57.58	54.95	55.21	55.35	60.65
TiO_2	0.89	0.74	.	0.73	0.73	0.78	0.84	0.83	0.83	0.70	0.83	1.26
Al_2O_3	18.17	17.11	.	16.96	17.31	18.23	18.05	18.25	20.88	18.81	20.89	15.86
FeOt	7.90	5.55	.	5.45	5.50	6.58	6.10	6.10	6.43	6.73	6.57	7.20
MgO	6.42	3.62	.	3.56	3.61	4.14	3.67	3.68	2.97	5.22	3.14	2.43
CaO	9.78	6.93	.	6.81	6.99	8.78	7.89	8.12	9.44	9.19	9.60	5.65
NaO	3.69	4.27	.	3.85	3.93	3.51	4.03	4.12	3.62	3.28	2.74	4.85
K_2O	0.62	1.57	.	1.67	1.66	1.20	1.19	1.18	0.75	0.76	0.75	1.90
P_2O_5	0.10	0.14	.	0.13	0.12	0.14	0.15	0.15	0.13	0.09	0.13	0.20
MnO	na	na	.	na	na	na	na	na	na	na	na	na
LOI	na	na	.	na	na	na	na	na	na	na	na	na
Total	**99.43**	**98.83**	.	**99.01**	**100.45**	**97.52**	**99.41**	**100.24**	**98.34**	**98.93**	**97.93**	**101.18**
Fe_2O_3	8.65	6.06	.	5.98	6.11	7.08	6.69	6.75	6.98	7.35	7.10	8.03
Modal composition												
Gms	60	70	60	60	65	70	75	75	65	50	55	95
Plag1	+	=	+	+	+	+	+	+	+	+	+	+
Plag2	=	+	+	+	+	=	+	+	.	=	=	.
Ol	+	.	.	.	.	.	.	.	+	.	+	.
Cpx	=	+	+	+	+	=	+	+	+	+	.	+
Opx	.	=	=	=	+	=	=	=	=	=	= =	+
Hb	.	.	.	.	.	+	.	.	.	= =	.	.
Bi	.	.	.	.	.	.	.	.	.	.	.	.
Qz	.	.	.	.	.	.	.	.	.	.	.	.
Oxide	= =	= =	= =	= =	= =	= =	.	.	.	.	= =	.
Comments				.	.	.	.	.	.	.	.	.

Table 3. *Compositional data on samples from the Geyser Creek area and surrounding regions-Continued*

ID	88cnu52	88cnu53	88cnu54	88cnu59	dt88-05	dt88-06	dt88-07	dt88-08	dt88-34	dt88-35	dt88-36	dt88-37
unit	Qcuv	Qcuv	Qcuv	Qcuv	Qcuv	Qcuv	Qcuv	Qcuv	Qcuv	Qcuv	Qcuv	Qcuv
Chemical composition												
SiO_2	55.48	54.78	.	58.58	54.73	.	53.24	.	.	.	54.37	62.48
TiO_2	1.10	1.17	.	0.97	0.74	.	0.88	.	.	.	1.18	1.28
Al_2O_3	16.67	16.94	.	17.05	17.73	.	18.99	.	.	.	17.26	15.54
FeOt	8.64	8.75	.	6.33	6.83	.	7.90	.	.	.	8.85	6.81
MgO	4.16	4.39	.	3.90	5.79	.	5.94	.	.	.	4.46	2.00
CaO	8.70	9.32	.	7.24	8.69	.	9.61	.	.	.	9.01	4.61
NaO	3.99	3.47	.	4.18	4.54	.	2.56	.	.	.	3.57	5.07
K_2O	1.10	1.00	.	1.59	0.84	.	0.75	.	.	.	1.09	1.71
P_2O_5	0.17	0.18	.	0.18	0.12	.	0.12	.	.	.	0.21	0.50
MnO	na	na	.	na	na	.	na	.	.	.	na	na
LOI	na	na	.	na	na	.	na	.	.	.	na	na
Total	**98.84**	**98.02**	.	**99.23**	**98.50**	.	**100.12**	.	.	.	**98.88**	**99.41**
Fe_2O_3	9.40	9.44	.	6.93	7.43	.	8.72	.	.	.	9.63	7.47
Modal composition												
Gms	95	90	99	50	60	95	85	80	99	95	80	99
Plag1	+	+	+	+	+	+	+	++	+	+	=	+
Plag2	+	.	.	=	=	.	=	.	.	+	+	.
Ol	.	=	.	==	+	.	+	.	.	.	+	.
Cpx	+	+	+	.	+	.	.	.	+	+	+	+
Opx	+	.	.	.	+	.	.	.	.	=	.	.
Hb	.	.	.	.	.	.	.	.	.	.	.	.
Bi	.	.	.	.	.	.	.	.	.	.	.	.
Qz	.	.	.	.	.	.	.	.	.	.	.	.
Oxide	.	.	.	=	==	.	.	.	.	.	.	.
Comments	.	clots	.	.	.	.	.	.	.	.	.	.

Table 3. *Compositional data on samples from the Geyser Creek area and surrounding regions-Continued*

ID	dt88-38	dt88-30	dt88-31	dt88-32	dt88-33	88cnu10	88cnu11	dt88-01a
unit	Qcuv	Qcuv dike	Qcuv dike	Qcuv dike	Qcuv dike	Tdp	Tdp	Tdp
Chemical composition								
SiO2	.	.	.	.	.	59.67	59.47	57.44
TiO2	.	.	.	.	.	1.06	1.26	0.86
Al2O3	.	.	.	.	.	17.33	17.05	17.59
FeOt	.	.	.	.	.	5.90	6.04	6.54
MgO	.	.	.	.	.	3.43	3.52	4.42
CaO	.	.	.	.	.	5.81	6.38	7.85
NaO	.	.	.	.	.	3.67	3.59	3.57
K2O	.	.	.	.	.	2.77	2.27	1.40
P2O5	.	.	.	.	.	0.24	0.29	0.18
MnO	.	.	.	.	.	0.11	0.12	0.14
LOI	.	.	.	.	.	1.85	1.16	0.85
Total	.	.	.	.	.	**100.02**	**100.36**	**99.93**
Fe2O3	.	.	.	.	.	6.40	6.61	7.15
Modal composition								
Gms	98	98	90	85	98	.	.	.
Plag1	+	+	+	+	+	.	.	.
Plag2	.	.	.	=	=	.	.	.
Ol	.	.	.	=	?	.	.	.
Cpx	+	+	+	+	+	.	see table 2-1	.
Opx	.	.	=	+	.	.	for modes	.
Hb	.	.	.	.	.	.	.	.
Bi	.	.	.	.	.	.	.	.
Qz	.	.	.	.	.	.	.	.
Oxide	.	.	.	.	.	.	.	.
Comments	.	.	.	.	ol altered	.	.	.

MAGMA MIXING

Magma mixing is difficult to quantify with only major element whole-rock geochemical data and petrographic data. Quantitative tests of magma mixing require modelling of incompatible and compatible trace elements and through knowledge of phenocrysts composition. However, some compositional aspects of Geyser Bight lavas suggest that magma mixing may be common.

First, two textural types of plagioclase commonly occur within the lavas (table 3). One population is euhedral to subhedral, normally zoned, and inclusion free; the other population is rounded and resorbed (often with euhedral rims), has reversals in zoning, and usually contains discrete concentric zones of glassy inclusions. The morphology of the latter plagioclase reflects a period of disequilibrium that may be associated with magma mixing or xenocryst entrainment. Measuring the chemical difference between the two plagioclases or the amount of chemical change across the boundary between the spongy zone and the euhedral rim would allow assessment of the magma-mixing hypothesis. In andesitic systems, these differences are often greater than those caused by polybaric fractionation or changes in the partial pressure of water (see Gill, 1981, for discussion).

Second, the covariation of K_2O with MgO is not as expected for magmas related by fractional crystallization. Figure 7 shows all Geyser Bight samples and a calculated path for about 70 percent fractional crystallization from a parent with 0.4 percent K_2O and 10 percent MgO. The path assumes that MgO behaves as a compatible trace element with a solid/liquid distribution coefficient (Kd) of 2.2, and that K_2O has a Kd of 0. Because K_2O is not an essential constituent of any fractionating mineral (until biotite crystallizes in the rhyolite), it can be treated as a trace element. All Geyser Bight samples diverge from the strong curvilinear path that is predicted. Samples that lie on chords on the concave side of the model line may be partly explained by intertrend mixing of basalt and silicic andesite. Divergence from the predicted trend may also result from variations in K_2O content of parent magmas and minor accumulation of mafic minerals. Samples that fall below the curve have anomalously high Al_2O_3 and may have selectively accumulated plagioclase. Certainly the quartz andesite flows are so far above the model fractionation line that magma mixing must be involved. The extreme disequilibrium of the mineral assemblage in this unit provides strong evidence of this mixing.

Also shown in figure 7 are data from Okmok Volcano, whose magma is highly tholeiitic and probably not significantly affected by magma mixing (for example, Kay and others, 1982; Kay and Kay, 1985). While the Okmok Volcano data conform more closely to the calculated fractionation line, there is still considerable scatter. For most Geyser Bight samples, magma mixing is probably not a dominant process for units other than the quartz andesite; it may be a common minor process.

CRYSTAL ACCUMULATION

The possibility that differential accumulation of crystals within the host magmas modified the composition of those magmas is a concern when describing porphyritic magmas. Indeed, plagioclase accumulation is probably a major factor in determining the final composition of lavas from Cinder Point (as discussed above). Most scatter in Al_2O_3 for Mt. Recheshnoi samples can be explained by about 10 percent plagioclase accumulation, an amount far less than the modal amount of plagioclase. Selective crystal accumulation should primarily influence Al_2O_3 and normative plagioclase because plagioclase dominates the modal mineralogy. The lack of correlation between Al_2O_3 or normative plagioclase and the percentage of phenocrysts in the rock indicates that crystal accumulation is not a major influence on magma composition.

CRUSTAL MELTING

While repeated transit of basaltic and andesitic magma through the arc crust might be expected to partially melt that crust, magmas that clearly owe their origin to this process are rare in the Aleutians. One possible exception is the rhyolite from Russian Bay valley (Qr, sheet 1). The prominent compositional gap between 63 and 76 percent SiO_2 indicates that this rhyolite is probably not derived from the acid andesites by fractional crystallization. Instead, the rhyolite was probably produced by partial melting of the arc crust by heat provided by the more mafic magmas (see Smith and Leeman, 1987, for a discussion of a similar mechanism at Mt. St. Helens). If rhyolite was produced over much of the lifetime of the volcano, there should be back-mixed dacites or

andesites. Such rocks are rare, the best example being the quartz andesite (Qrq) exposed between Hot Springs Cove and Partov Cove. This lack of back-mixed magmas suggests that rhyolite production was temporally restricted.

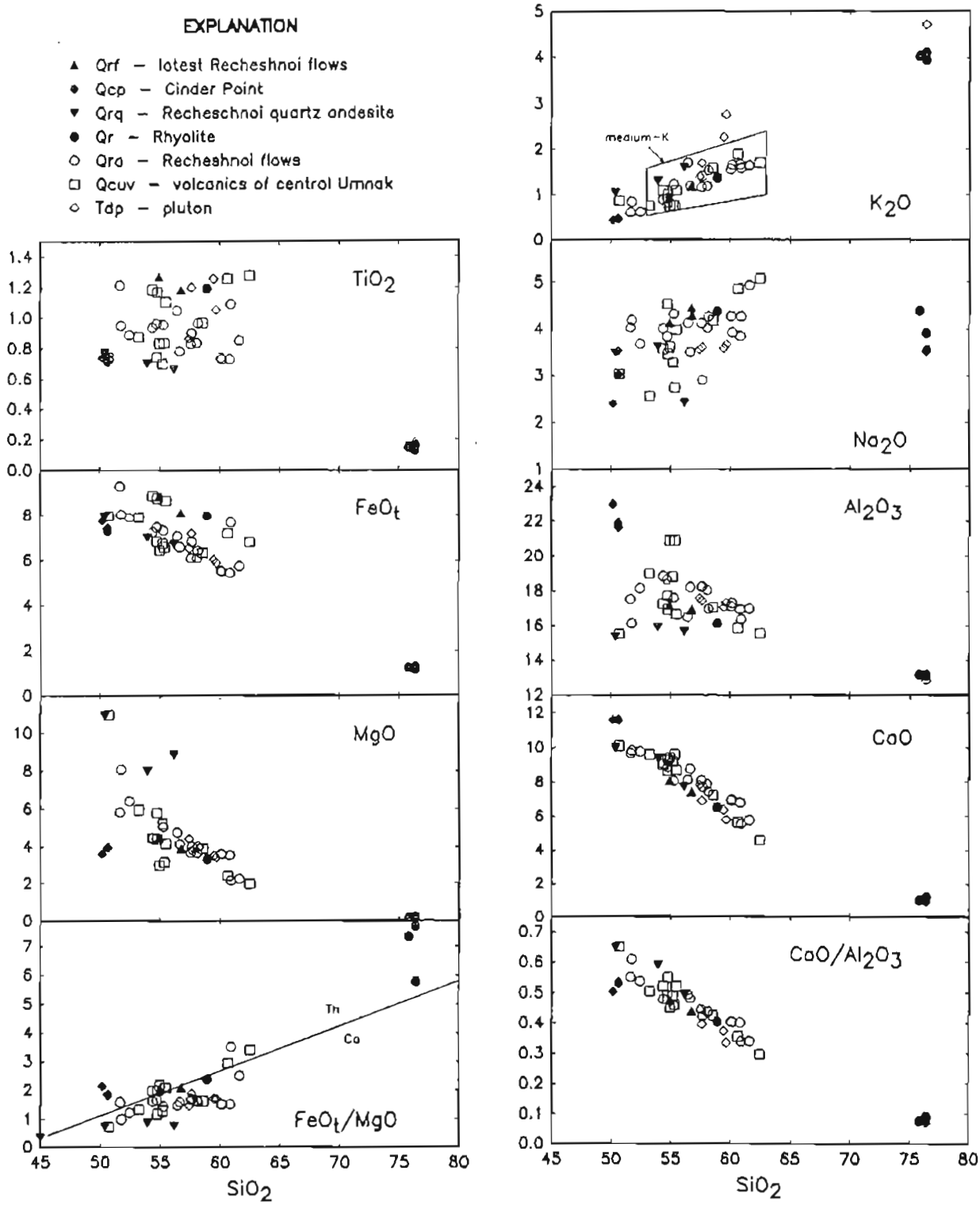

Figure 6. *Silica variations of igneous rocks from Geyser Bight valley and the surrounding region. The Th-Ca dividing line is from Miyashiro (1974), and the medium K region is from Gill (1981).*

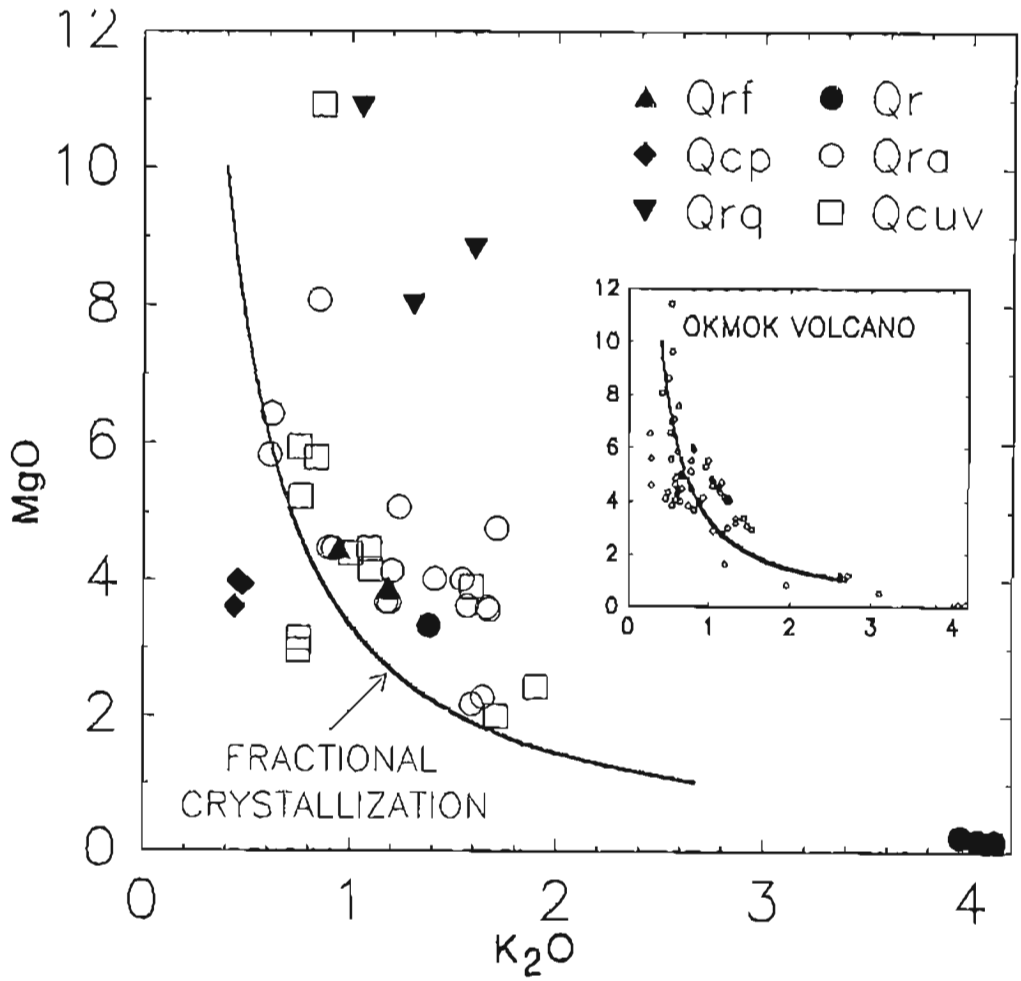

Figure 7. *K_2O and MgO variations in Geyser Bight area magmas. Parameters of the fractional crystallization path are discussed on page 25. Okmok Volcano data are from the literature.*

OTHER PROCESSES

The high FeTi magmas cannot be related to other magmas by fractional crystallization, magma mixing, or crystal accumulation. Their petrographic and geochemical similarities to the tholeiitic series rocks described by Kay and others (1982) include high FeO^t and TiO_2, high FeO^t/MgO, and low crystal content. Kay and others (1982) and Kay and Kay (1985) suggest that these rocks are the result of crystallization at low pressure, low water content, and high temperature. The position of the cotectic that governs the evolution of these magmas, as deduced from experimental work, does not seem to shift from that governing the evolution of other magmas (fig 8). Thus, if the Kay and others (1982) explanation is correct, the magnitude of lowered pressure and/or water pressure is not sufficient to be reflected in normative mineralogy. The origin of the high FeTi magmas remains enigmatic.

Variations in parental magma chemistry are expected, but with these data we cannot evaluate the magnitude of their effects. Similarly, crustal assimilation may affect the final compositions of some magmas. In fact, if the presence of rhyolite signals mobilization and eruption of partial crustal melts, then crustal contamination is quite likely. Recognition of crustal contamination requires additional data.

INFERENCES FOR DEPTH OF FRACTIONATION

Understanding the size, depth, and mean lifetime of crustal magma chambers is obviously important to understanding the geothermal energy of active volcanoes, but these aspects of magmatic evolution are among the most difficult to quantify. Observations of the magnitude and direction of shifts of cotectics in multiply- saturated systems with changes in pressure and water pressure are made by equilibrating natural melts with their phenocryst assemblages in a laboratory at known P_{total} and P_{H2O} and measuring the composition of the equilibrium liquid. There are abundant data for mid-ocean ridge basalts (MORB) at low pressure with no water. Data on andesitic compositions at moderate P_{total} and P_{H2O} are much less common, in part due to the difficulty of the experiments.

Available data are summarized in figure 8 on a projection onto normative diopside, silica, and plagioclase from within the tetrahedron diopside, silica, plagioclase and olivine. The dry, 1 atm cotectic is given by the MORB data (see fig. 8 for references). Additional anhydrous experiments at 8 kilobars (kb) and hydrous experiments at 2 and 5 kb are plotted. The cotectic shifts towards plagioclase with increasing pressure and water pressure because both reduce the stability of plagioclase. The 2 to 5 Kb "damp" cotectic shifts farther than the 8 Kb dry cotectic. All Geyser Bight data shift towards plagioclase and overlap the 2 and 5 Kb cotectics which indicates that most chemical evolution of Geyser Bight magmas, and thus most of their residence time in the crust, must have been at a minimum depth of 6 to 15 km. If the magmas were anhydrous, that depth must be well over 25 km. The presence of relict amphibole in several samples suggests the magmas were hydrous. Plutonic samples plot along the same inferred cotectic as Geyser Bight lavas, which suggests that the magmas principal crustal residence is at a depth similar to that of pluton formation. The Cinder Point samples plot much closer to the plagioclase apex than others, which probably reflects plagioclase accumulation rather than a deeper origin.

TEMPORAL VARIATIONS IN MAGMA COMPOSITION

Figure 9 shows a series of variation diagrams that illustrate the composition of Geyser Bight magmas as a function of age. There are no major monotonic variations in chemistry over the 1.4 m.y. that lavas have erupted at Geyser Bight, but there are some minor trends that deserve comment. Lavas from central Umnak Island show a very slight decrease in FeO^t and CaO/Al_2O_3, and, perhaps, MgO over time, and there is a very faint hint of concomitant increase in SiO_2. These changes are very slight, marred by the eruption of some silicic magmas early in the history of the central Umnak Island vents; they could prove to be an artifact of the small number of analyses. These apparent trends probably do not signal a slight increase in fractionation of a homogeneous magma batch because K_2O contents of 800 ka lavas are not higher than those of 1100 ka lavas. They do suggest that these temporal variations, if real, reflect variations in the composition of parental magmas, and in the amount of fractionation.

Chemical changes within the lifetime of Mt. Recheshnoi are more pronounced and are probably real. Figure 9 shows that over much of the 0.5 m.y. lifetime of Mt. Recheshnoi, magmas have become more mafic, with a few notable exceptions. Over this time, SiO_2 dropped from approximately 60 to approximately 53 percent and FeO^t, MgO, CaO, and CaO/Al_2O_3 increased. TiO_2 increased for about the first 200 ka and then decreased, while K_2O remained steady for 200 ka and then decreased. The lack of strict monotonic correlation between K_2O and SiO_2 suggests variations in parent magma composition through time. The lack of monotonic correlation between TiO_2 and SiO_2 may reflect either variable parent magma composition or a slight change in magnetite stability (and thus probably oxygen fugacity) through time. It is impossible to quantify these processes with the data in hand. In addition, we do not have samples from the northwest, west, and southeast sides of the volcano. The temporal changes of magma chemistry with time may well be more complicated than our data shows. We do not have ages for a few basalt flows from the Geyser Creek valley that are presumably at least a few hundred thousand years old and may fall off the perceived temporal trend. These flows may represent the periodic influx of mafic magma into a quasi-steady system that is evolving toward more mafic average composition. Periodic eruption of mafic magmas from steady-state systems has been observed elsewhere (for example, Nye and Turner, 1990) and is not unexpected.

Three exceptions to the trend towards more mafic compositions-with time-of Mt. Recheshnoi lavas are discussed below. The first is the rhyolite, which erupted about 135 ka. Quenched andesite blobs within the rhyolite suggest that mafic magma was still present in the system as the rhyolite erupted. This andesite may

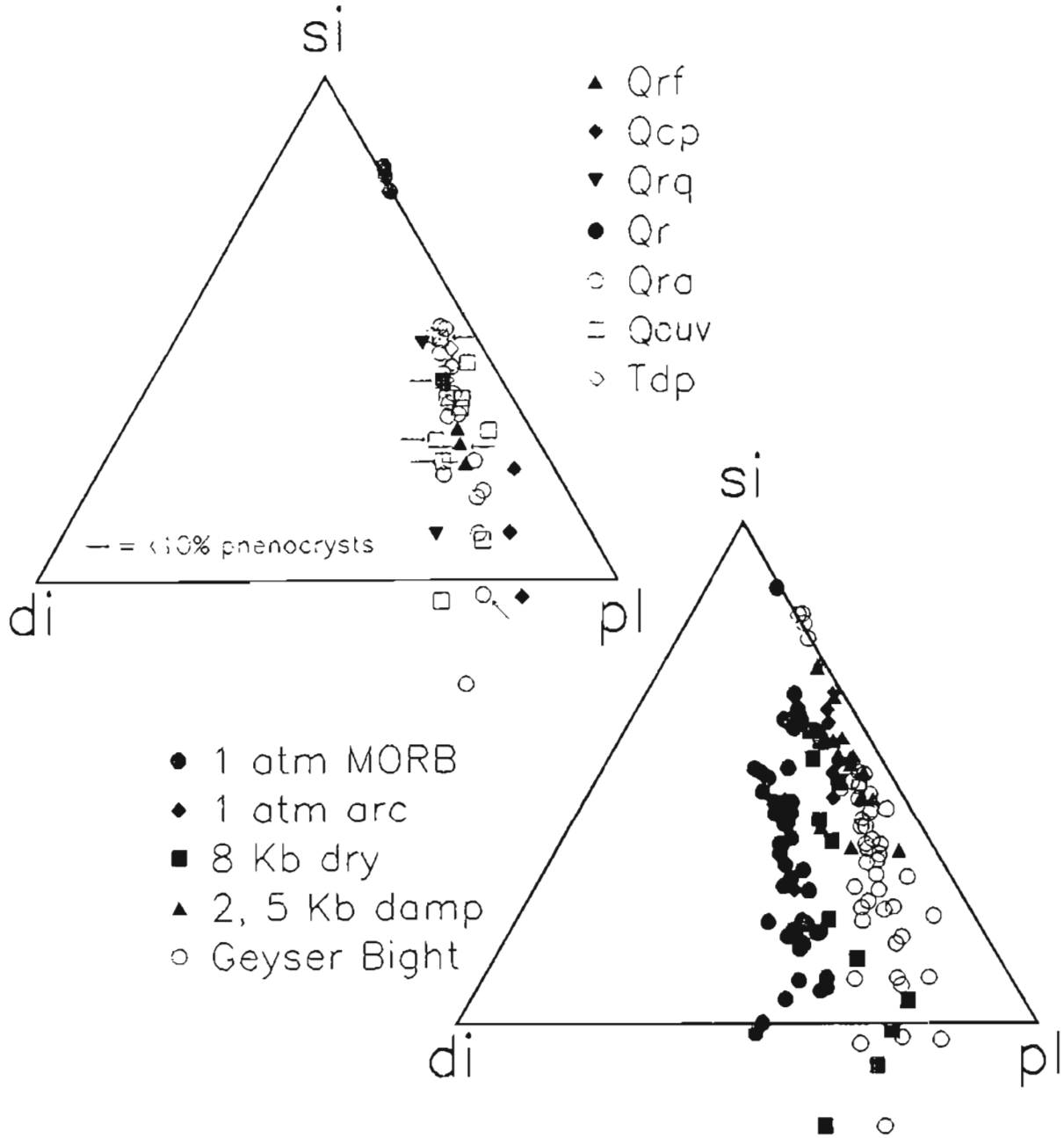

Figure 8. *Projections from olivine onto the plane diopside-silica-plagioclase within a normative tetrahedron (Grove and others, 1982). Non-Geyser Bight data are from Baker and Eggler (1987), Grove and others (1982), Grove and Bryan (1983), and Walker and others (1979).*

conform to the overall temporal trend, especially if corrected for minor contamination of the basalt with rhyolite. Secondly, the andesite flows from the east flank of the volcano (Qrf) are more silicic than the youngest lavas from the Mt. Recheshnoi central vent (57 percent compared to 52 percent SiO_2). These flows contain inclusions of more mafic andesite, which indicates that the entire system is not moving towards more silicic compositions. Note that the included blobs in the rhyolite and the young flank andesite are quenched magma within their host, as opposed to stoped conduit material or country rock. The third exception is the felsic andesite clasts in young, valley-filling ash flows in Russian Bay valley (Qra1). The petrology and geochemistry of this unit are not well known.

All Mt. Recheshnoi samples that belong to the high FeTi group are young. Thus, the most tholeiitic of the Mt. Recheshnoi samples are young compared to the bulk of Mt. Recheshnoi lavas. On a FeO^t/MgO vs. SiO_2 diagram, however, Mt. Recheshnoi as a whole is very calcalkaline.

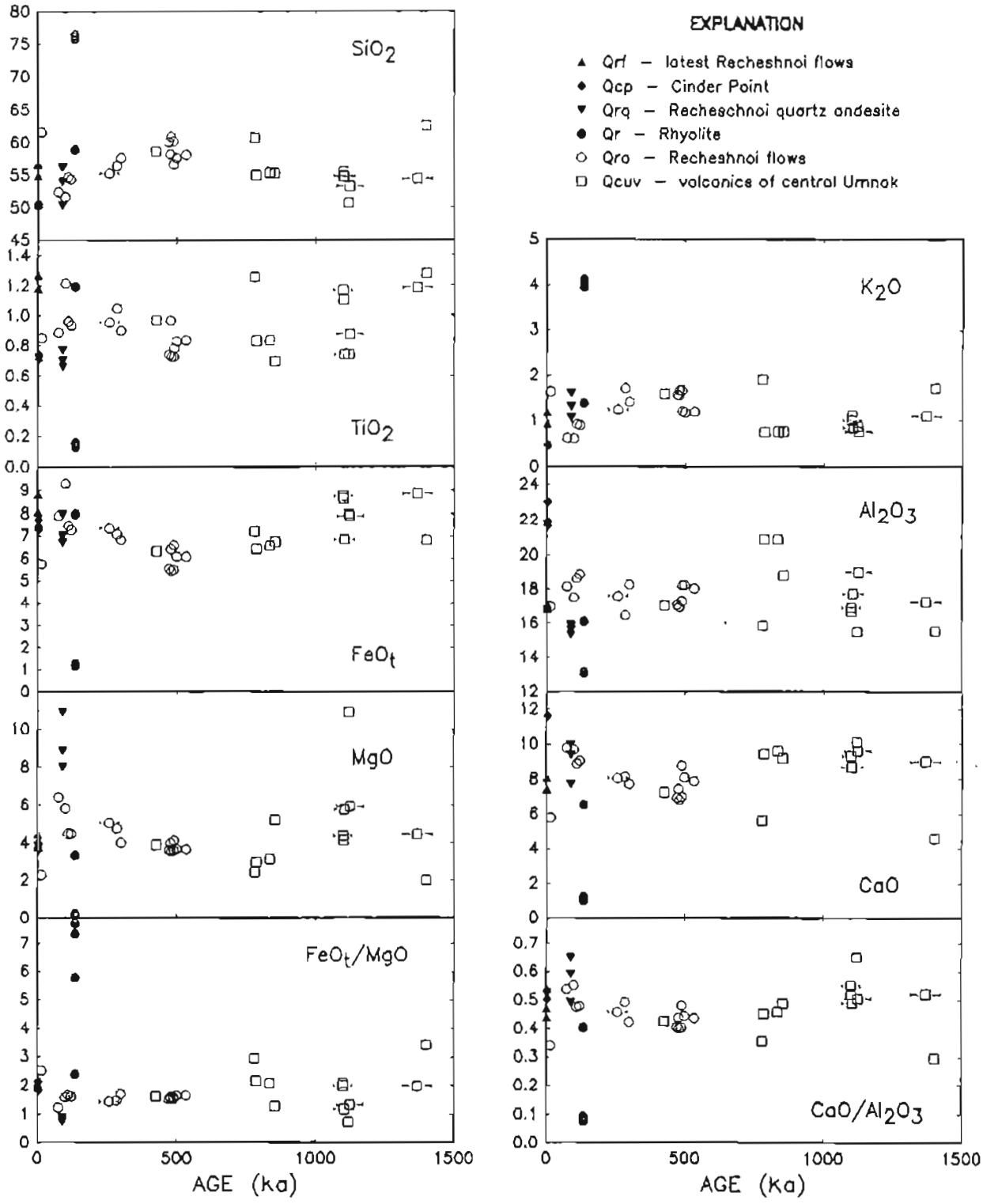

Figure 9. *Temporal variation in composition of volcanic rocks from Geyser Bight valley and the surrounding region.*

EVOLUTION OF THE MAGMATIC SYSTEM

The magmatic system most relevant to understanding the Geyser Bight geothermal system is that of Mt. Recheshnoi. The vents of central Umnak Island have been dormant for 500 to 750 ka, and any magma chambers that were associated with them are probably fully crystallized and near the temperature of the surrounding country rock.

Mt. Recheshnoi magmas have become more mafic with time, although some anomalously felsic magmas have erupted within the last 150 ka. This evolutionary trend is unlike that of the few other Aleutian volcanoes for which we have abundant age and geochemical data. Mt. Spurr steady-state andesite magmas remain nearly constant in composition for the 250-ka lifetime of that volcano, although mafic magmas were periodically erupted, most notably during and after avalanche caldera formation late in the history of the volcano (Nye and Turner, 1990). Early Mt. Wrangell lavas are mafic, but the lavas have remained nearly constant in composition over the last 500 ka (Nye and Turner, unpub. data). Holocene Makushin magmas are on average more silicic than Pleistocene magmas, which are variable in composition. Myers and others(1985) and Myers and Marsh(1987), based on studies of two separate volcanoes of different sizes, and thus presumed different ages, suggest that volcanoes may evolve from early calc-alkaline (presumably andesitic) compositions to late tholeiitic (more basaltic) compositions. Mt. Recheshnoi may be an example of the volcano type Myers proposes, but the magnitude of the compositional shift is less than he anticipated.

One model for the evolution of the Mt. Recheshnoi magmatic system is discussed below. As new magma intruded a realatively cool crust early in Mt. Recheshnoi's history, the large thermal contrast resulted in significant fractionation and heat loss to the crust. Successive batches of melt entered and passed through the crust, fractionating and loosing heat. Through this process the crust heated to provide less thermal contrast, which decreased fractionation of subsequent batches of rising melt. Successive magmas are less fractionated and more mafic, and ultimately, the crust heated to the point of partial fusion to produce the rhyolite. Once the crust started to melt, it generated a silicic component that could be mixed with incoming basaltic magmas to produce hybrid silicic magmas such as the most recent Mt. Recheshnoi's magma. This model is similar to that of Myers and others (1985) because it suggests that thermal maturation of the conduit system is important in volcanic evolution. It differs from that of Myers and others (1985) because it predicts increasing, rather than decreasing, chemical coupling with the crust.

THERMAL AREAS: DESCRIPTION, SPRING DISCHARGE, AND CONVECTIVE HEAT FLOW

LOCATION

Six zones of thermal springs and small geysers are dispersed over an area of about 4 km^2 in the upper reaches of Geyser Creek valley at elevations that range from 30 m to 110 m (sheet 2, fig. 10). Letters designate spring groups according to the nomenclature established by Byers and Brannock (1949). Previous investigations of the geothermal springs at Geyser Bight include Byers and Brannock (1949), Ivan Barnes (1975 - U.S. Geological Survey, unpub. data, written commun., 1975; 1981), and Motyka and others (1981). Most hot springs emanate along Geyser Creek and its tributaries and emerge in the valley floor and at the base of steep valley walls. Two small areas of steaming ground and weakly pressurized fumaroles are located at elevations of 275 and 310 m in a tributary valley at the headwaters of Geyser Creek (F1 and F2, sheet 1).

During geologic field mapping (1988) a previously unreported fumarole field was discovered at approximately 450 m elevation on the lower northeast flank of Mt. Recheshnoi (F3, sheets 1 and 2). The field is about 4 km south of Geyser Bight valley and is separated from the valley by a broad ridge. The fumaroles lie near the head of a rugged canyon that drains towards Russian Bay. One fumarole was superheated, with a temperature > 125°C. Weather conditions and time constraints prevented sampling the fumarole gases.

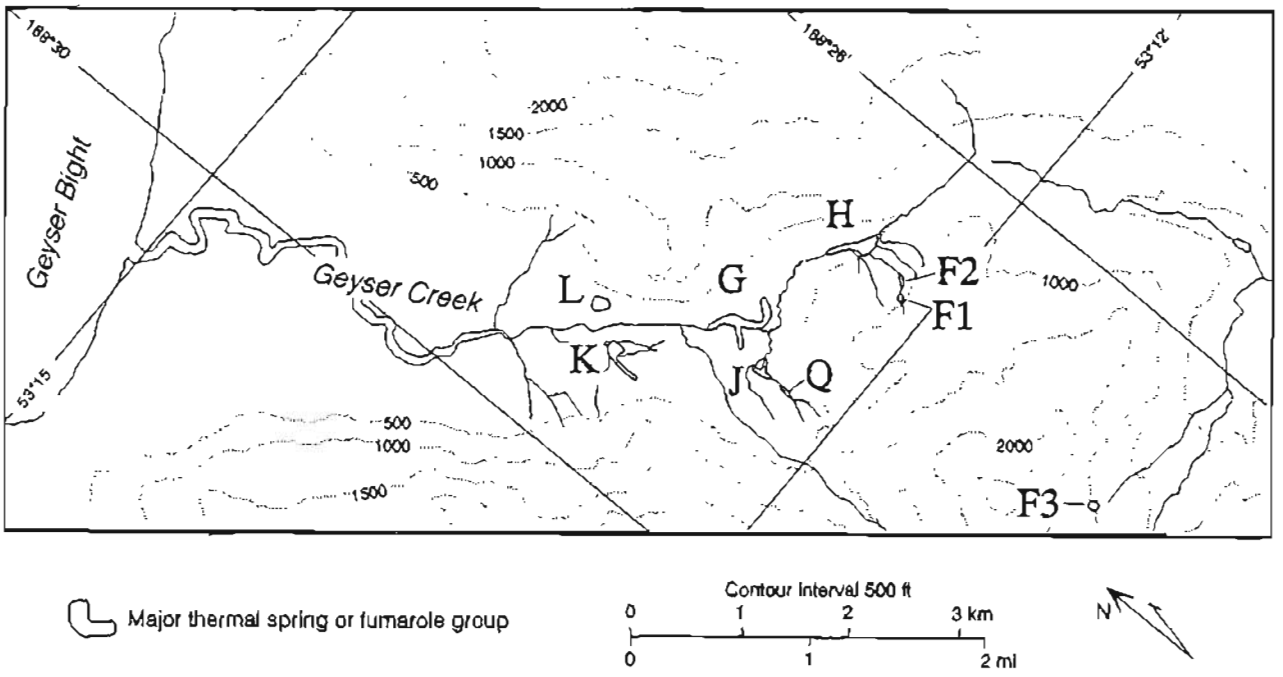

Figure 10. *Location map of the thermal springs and fumaroles of Geyser Bight, central Umnak Island.*

SPRING DESCRIPTIONS

Geothermal activity at Geyser Bight (table 4) appears to vary over time; in 1980 there was substantially less output than either 1947 or 1988. For the 1988 activity column in table 4, the following conventions are used. Seeps (s) describes hot water quietly flowing from alluvium, colluvium, bedrock, or any combination thereof, at rates of ≤ 5 lpm (liters per minute). Springs (sp) are larger flows than seeps. Pools (p) are small, open bodies of water fed by a spring or by numerous indistinguishable seeps. At ebullient boiling springs (eb), gas and steam violently break the surface. Fountain (f) refers to springs in which, in addition to ebullition, hot water is ejected above the normal surface of the water. Using White's (1967) definition, a geyser (g) is a "hot spring characterized by intermittent discharge of water ejected turbulently and accomplished by a vapor phase." Some authors believe ebullition and fountaining are a type of geyser activity. Some springs that were pulsing and almost continuous fountains in 1988 were described as geysers with 50 to 60 cycles per min in 1980 (Motyka and others, 1981). Because the Geyser Bight geothermal area is relatively unknown, detailed descriptions of the thermal spring sites are provided for future reference. Descriptions of activity refer to our period of observation (July 1988) unless otherwise stated.

SITE F1

Fumarole field 1 (fig. 11) is located at approximately 300 m elevation in a slightly circular depression, mostly on the left bank of a creek informally referred to as Fumarole Creek. Immediately above F1, the temperature of Fumarole Creek is 9.2°C. In comparison to other local snow-fed creeks that have temperatures of 4°C, the 9.2°C temperature of Fumarole Creek indicates that it has some geothermal heat input above F1. Visual estimates of creek flow are 400 lpm above and 450 lpm below F1; the creek temperature below F1 is 19.5°C . The most prominent feature at F1 is a 100°C pressurized vent. A slight odor of H_2S is noticeable. Adjacent to this vent is a 6 by 8 in area of altered hot ground with active steam vents and mud pots.

SITE F2

Fumarole field 2 (fig. 12) is located at approximately 275 m elevation and extends about 150 m along Fumarole Creek about 1/2 km downstream from F1. Fumarole Creek temperatures measure 17°C above F2 and 21°C below F2. Visual flow estimates are 450 lpm above F2 and 500 lpm below F2. The most prominent feature at F2 is a 102°C pressurized vent. F2 has low-chloride hot springs and mud pots and fumaroles. A 20-m diam fossil fumarole field is located on the left bank of Fumarole Creek about 20 to 30 m below the last steam vent of F2.

Table 4. *Comparison of Geyser Bight spring characteristics; 1947, 1980, and 1988*

Site	1988			1980			1947		
	Temp °C	Flow[a] l/min	Activity	Temp °C	Flow l/min	Activity	Temp °C	Flow l/min	Activity
G1	81-102	70	f	100	20	g	101	260	sp
G2	102	25	f	79	5	g	88	6	sp
G3	101	20	f	100	16	g	100.5	18	sp
G4	97	15	f	92	5	s	98	36	sp
G5	u	0	eb	nr	nr		u	none	eb
G6	75-94	36	sp,eb	97	20	eb	95	80	sp
G7	not	found		not	found		82	85	sp
G8[b]	100	150	g	100	75	g	101	170	g
G8A	65-96	15	s,eb	92-98	nr	sp,s	nr	nr	
G9	102	36	f	99		sp	101	6	sp
G10	103	54	f	100		sp	99	170	eb,f
G11	88	18	sp	81		sp	77	170	sp
G12	51	u	p	nr	u	p	51	u	p
H0	nr	nr	sp	97	30	sp	nr	nr	
H1	102	400	f	100	300	g	102	660	g
H2	99-102	95	f	99	100	g,f	101	600	g
H3	48	150	sp	45	60	sp	53	none	
H4	102	400	g	100	45	eb	101	340	sp
H5	not	found		101	nr	g	101	85	sp
H6	104	50	eb	99	30	f,eb	100	66	sp
H7	101	135	sp	99	70	eb	90	260	g
H8	99	100	g	nr	nr		nr	nr	
H9	67	200	sp	nr	nr		nr	nr	
H10	97	150	f	nr	nr		nr	nr	
H11	71-96	165	g	nr	nr		nr	nr	
H12	75-81	5-30	sp,s	84	1	s	nr	nr	
H13	70	40	sp	nr	nr		nr	nr	
J1	80	10	p	82	nr	p	88	720	nr
J2	80	32	s	77	nr	s	nr	nr	
J3	55-80	41	sp,s	77-88	10	sp,s	nr	nr	
J4	65	20	p	69	5	p	nr	nr	
J5	90	25	g	92	15	g	nr	nr	
J6	85	25	p	83	15	p	nr	nr	
K1	61		p	62		p	70	170	
K2	50		p	59		p	58	85	
K1+K2		30			100				
K3	80	10	sp	nr	nr		nr	nr	
K3-seeps	63	50	s	nr	nr		nr	nr	
L	40-78	250	sp,s,p	45-85	200	p,sp,s	67-69	170	
Q	30-80	131	sp,s	70-75	25		nr	nr	
Total flow est.		**3,250**			**1,150**			**4,150**	

[a]Most 1988 flows were visually estimated. L, H7, G11, were measured with standard pygmy flow meter.
[b]Flow for G8 is at maximum activity. See discussion on page 36.
Abbreviations: sp=spring, s=seep, f=fountain, g=geyser, eb=ebullient boiling, p=pool, u = unable to make measurement, nr = not reported

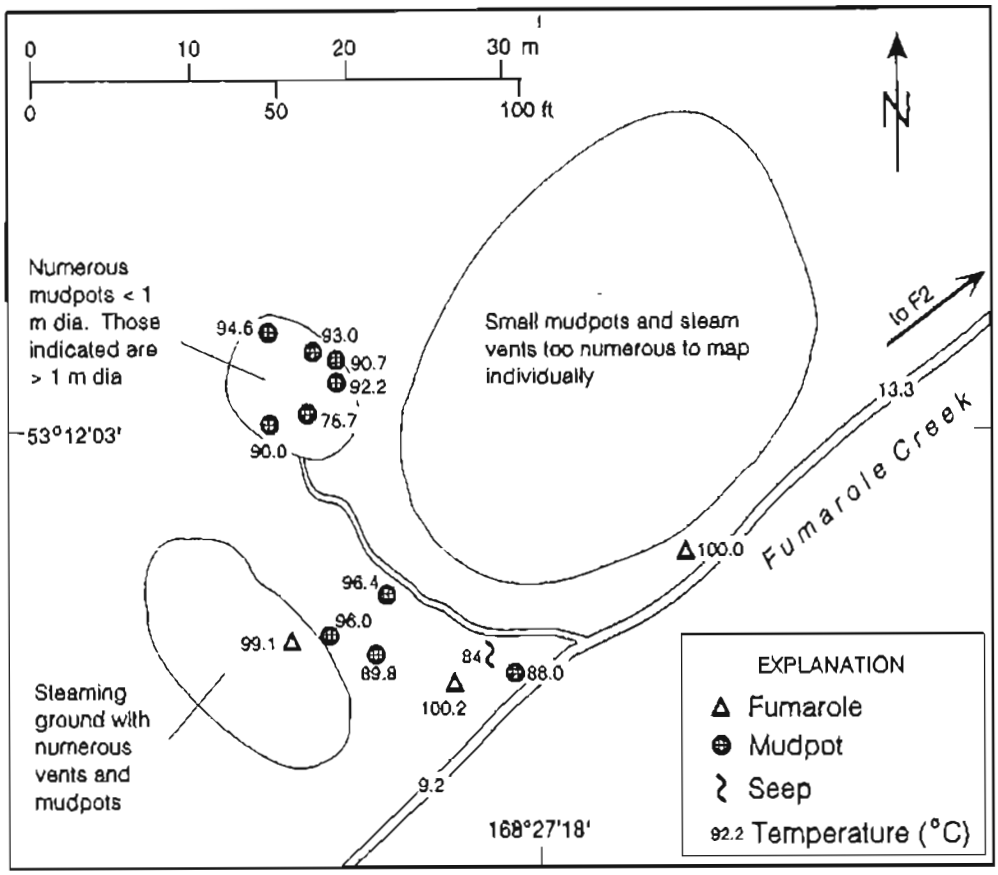

Figure 11. *Map of Geyser Bight fumarole field 1, central Umnak Island.*

SITE F3

Fumarole field 3 (fig. 13) is located at approximately 425 m elevation on a creek in the central part of upper Russian Bay valley. The most prominent feature at F3 is a superheated, pressurized fumarole with a > 30 plume and a minimum temperature of 125°C. Five-cm diam rocks thrown into the vent were forcefully ejected by the fumarole jet. H_2S odor is noticeable, but not overpowering. The temperature of the creek that drains the fumarole field is 7°C above and 43°C below the geothermal area. Two fossil fumarole areas are located about 10 m above the main active area, one on each side of the main creek. About 40 m east of the large fumarole is an area of altered steaming ground 40 by 25 m with numerous active boiling-point fumaroles.

SITE G

Site G (fig. 14) is located 5.5 km from Geyser Bight at the southeastern end of the main glacial valley. Two groups of thermal springs emerge at the base and on the lower slopes of the east valley wall. Thermal waters emanate from numerous small pools, orifices, and seeps in the cemented alluvium and colluvium. Several small steam vents also occur in the area. Fossil geothermal areas, the largest measuring 100 by 50 m, indicate that the geothermal activity was more extensive in the past or has migrated. Several warm seeps and numerous sinter-covered rocks are located in an old channel across the east fork of Geyser Creek, towards site J.

The up-valley series of springs is clustered at the base of a low ridge adjacent to two small, warm water ponds of (fig. 15). Spring G1 consists of several vents at the upstream edge of the larger pond. Springs G1b, c, and e exhibit ebullient boiling and have fountains to 30 cm. Spring G1c has the largest flow and was sampled for water chemistry. In 1988, spring G1c was pulsing almost continuously; in 1980 it erupted every 1 to 3 s. G1a was fountaining with occasional bursts of steam. The pH of the thermal-spring waters at G1 ranges from 6.8 to 9.2 which reflects the boiling and loss of acid gases.

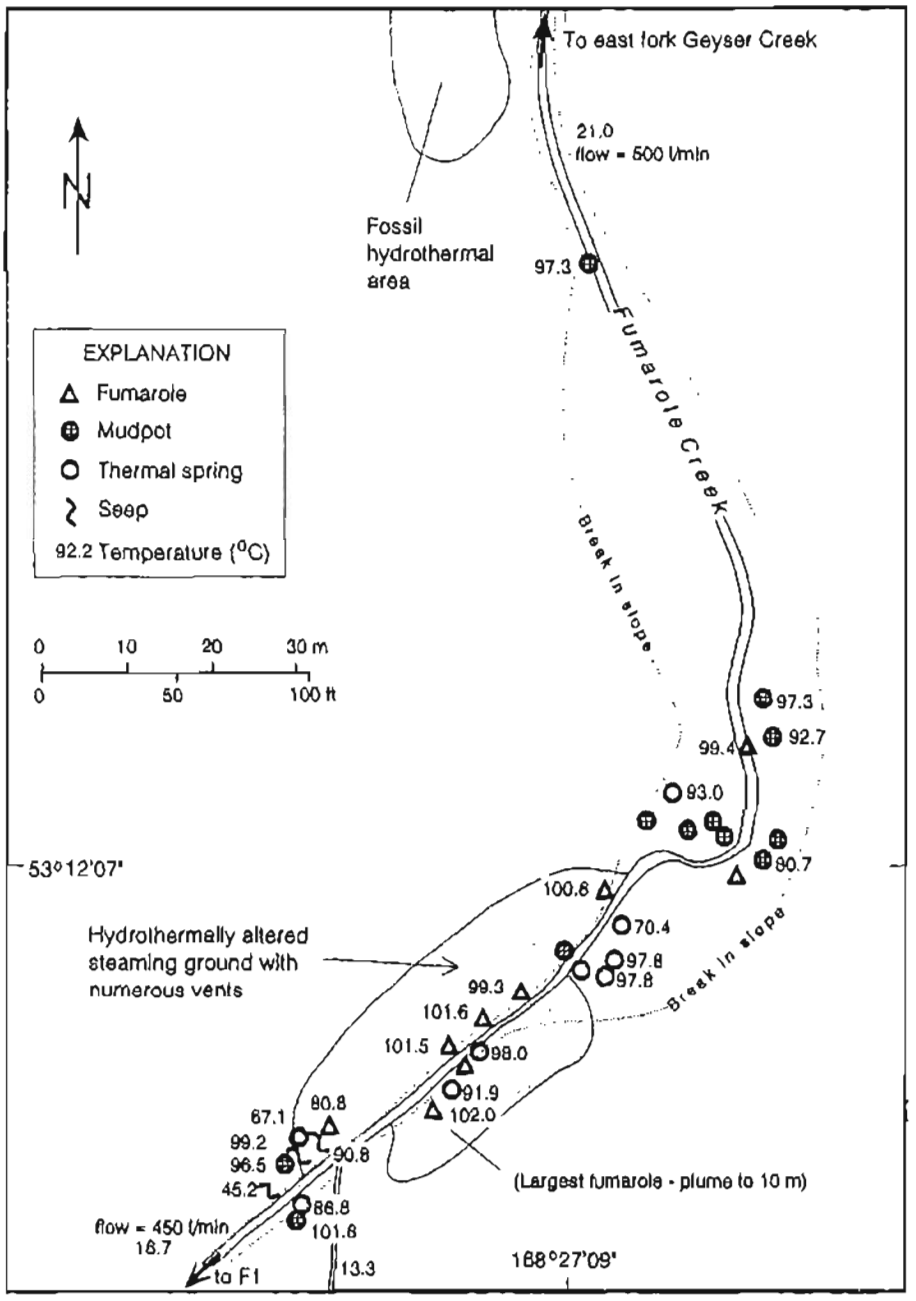

Figure 12. *Map of Geyser Bight fumarole field 2, central Umnak Island.*

Vigorously boiling fountains, springs G2, G3, and G4, and several smaller vents lie above and 10 m from G1 (fig. 15). A silica apron ≤ 5 m wide extends downslope from this cluster, and an area of steaming ground ≥ 25 m in lateral extent lies immediately east. G5, a steaming vent ≥ 2 m diam, lies further upslope. Water that was heard boiling below the surface could not be reached with a 2-m probe. The ground in the immediate area is warm, moss covered, and altered to clays. Between the two warm ponds, spring G6 emerges from a 50-cm-diam sinter cone. The pH of spring G6 is 7.2; 0.5 m away is a small bubbling vent with pH of 1.9. Several seeps with flows ≤ 10 lpm emanate along the shore of the smaller pond, and gas bubbling in the pond points to locations of additional vents.

Down-valley from G1-G6 is an area of diffuse geothermal activity (fig. 14). Numerous seeps occur along 150 m of an unnamed creek. One seep had sufficient flow in 1947 to be called G7 by Byers and Brannock (1949). Between these seeps and the east fork of Geyser Creek, a 40-m-diam unvegetated area of warm, bare ground yeilds temperatures of 38°C. Nearby are two large mud pots, and 10 m farther is spring G8.

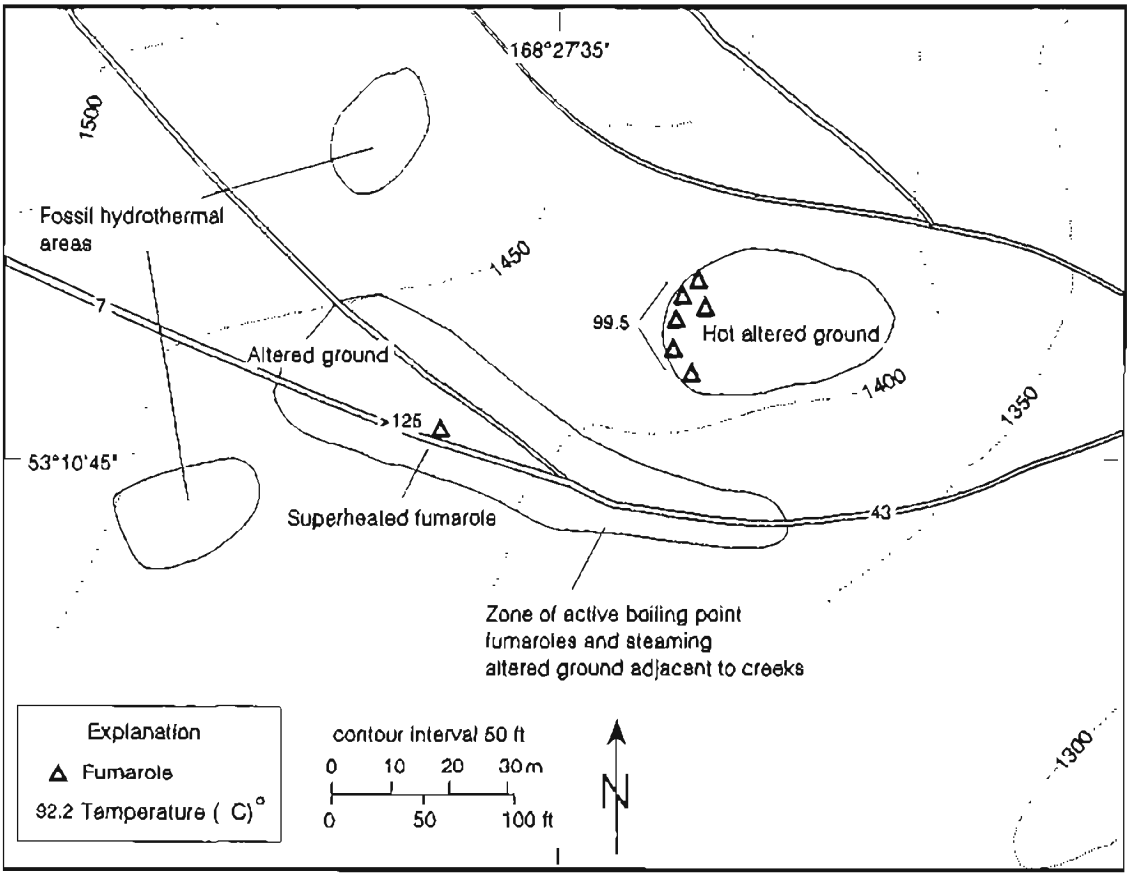

Figure 13. *Map of fumarole field 3, upper Russian Bay valley, central Umnak Island.*

Spring G8 is a geyser that emerges in a 1-m-diam bowl composed of sinter-cemented rock (fig. 16). In a typical eruptive cycle, approximately 750 l of water are discharged every 12 min for an average minimum flow of 60 lpm. The height of the fountaining was 60 cm in 1870 (Dall, 1870) and 1947; it decreased to 20 cm in 1988. A 5-m-wide, 25-m-long silica apron extends from the geyser towards the east fork of Geyser Creek. Adjacent to spring G8 (fig. 16) is a 4-m-diam cluster of acid springs with pH values from 1.5 to 5.9. Two springs are vigorously boiling, two are muddy, and all have low flows with a combined discharge of approximately 15 lpm. These springs appear to result from condensation of steam and acid gases into and warming near-surface meteoric waters.

Springs G9, G10, G11, and a warm pool, G12, are located farther downstream (fig. 17). Several vents also discharge directly into the east fork of Geyser Creek and along its banks. The creek bottom has algal growth at least 50 m below the last seep. Warm ground was found as far as 200 m downstream from G12. Springs G9 and G10 are fountaining and have siliceous sinter cones and terraces, while spring G11 emanates from a cluster of boulders. Water in pool G12 has a maximum temperature of 51°C, but temperatures to 72°C were found in bottom sediments.

SITE H

Site H springs (fig. 18) are located along the east fork of Geyser Creek and in a narrow tributary valley, elevation approximately 100 m. The intensity of thermal activity at H has been irregular. In 1947, Byers and Brannock (1949) reported seven springs with total output of approximately 2,000 lpm. In 1980, Motyka and others (1981) reported eight springs, but total output was only 650 lpm. In 1988, six additional springs and numerous seeps were observed. Several previously reported vents were dry, but total output was at least 1900 lpm in 1988. The temperature of the east fork of Geyser Creek was 8.3°C above site H and 16.9°C below site H.

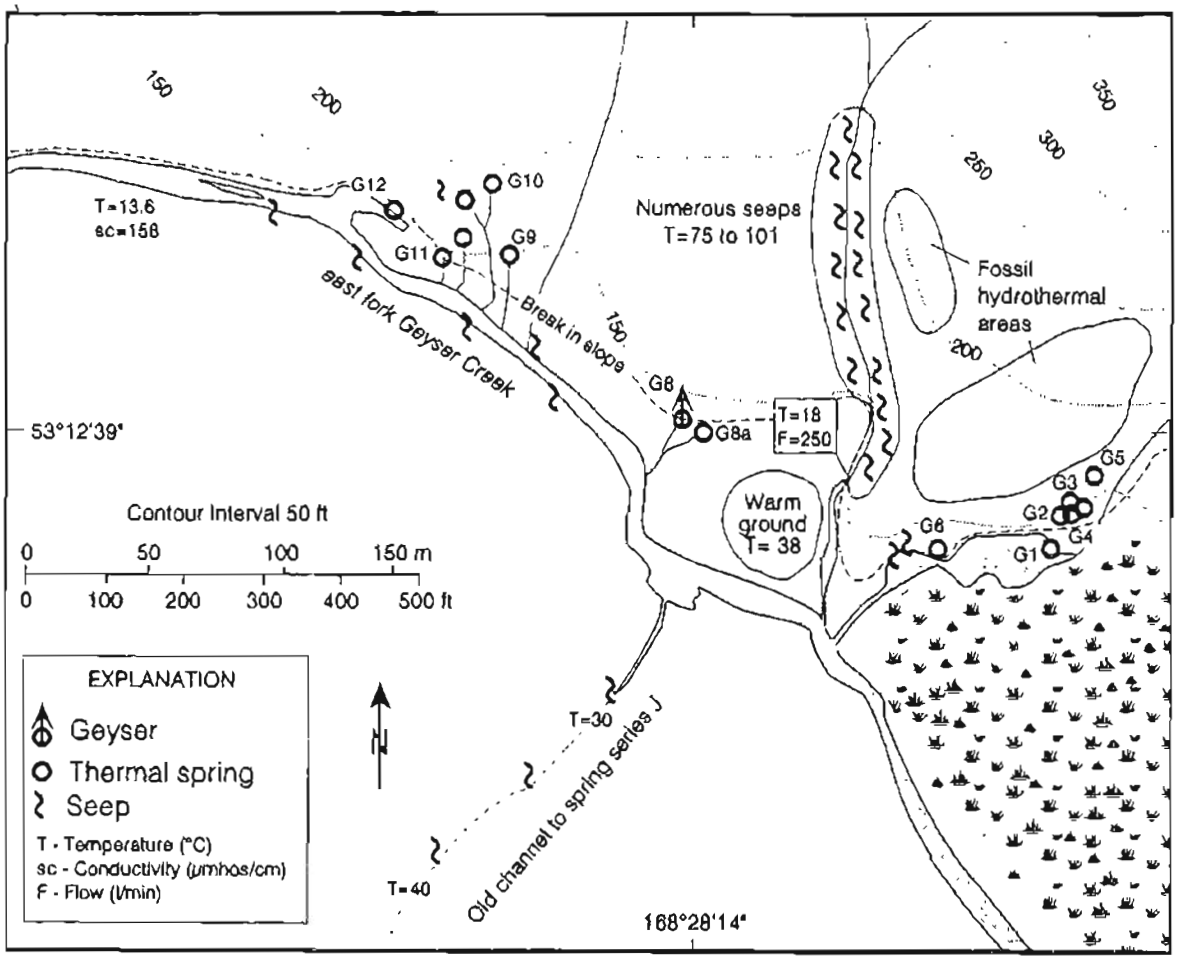

Figure 14. *Map of Geyser Bight spring series G, central Umnak Island.*

The uppermost springs and seeps emerge from volcanic bedrock that flanks a 15-m waterfall (fig. 19). Most vents are inaccessible because of cliffs, but their presence can be inferred by dark green algae and steam. Springs also discharge directly into the creek as evidenced by bubbling gas in a relatively calm area between two steps of the waterfall. Temperatures (where measured) range from 40° to 80°C; flow was ≤ 40 lpm.

At the base of the waterfall, a small creek ("H" Creek) enters the east fork of Geyser Creek from the south (fig. 19). The most active H springs line the banks of this creek. Above the highest visible seep, the temperature of "H" Creek is 16°C, which indicates that some hot water is seeping directly into the streambed above the visibly active thermal zone. At the mouth of "H" Creek, the temperature rises to 53°C from the addition of boiling water from the visible springs. Except for H3 and H0, the other numbered springs along "H" creek exhibit ebullient boiling and fountaining.

Spring H2 is immediately upstream from the mouth of "H" Creek along the east fork of Geyser Creek. Two vents (flows 40 to 50 lpm each) and several smaller spouting vents comprise this spring group. One larger vent discharges into a quiet pool and the other (H2) constantly bubbling with a 10-cm fountain. Along "H" Creek, the first set of vents is labeled H3 (fig. 19). H3 and all other numbered springs along "H" Creek emanate from its west bank. The largest and most active spring along "H" Creek is H1, a set of three interconnected, 1-m-diam cauldrons set within a 10-m-diam patch of large, mostly volcanic boulders up to 2-m diam. The cauldrons contain vigorously boiling water with 70-cm fountains. The 12-m-long channel that drains H1 contributes about one-third of the flow in "H" Creek. H1 was a geyser with period of 2.5 to 3.5 min in 1947, and a geyser with period of 1 min in 1980; it continuously fountained in 1988. Ten meters upstream from H1, spring H0 emerges in a small, 1-m-diam bowl perched about 5 m above "H" Creek. In 1980, this spring had a flow of 30 lpm, but by 1988 its flow had diminished to a trickle.

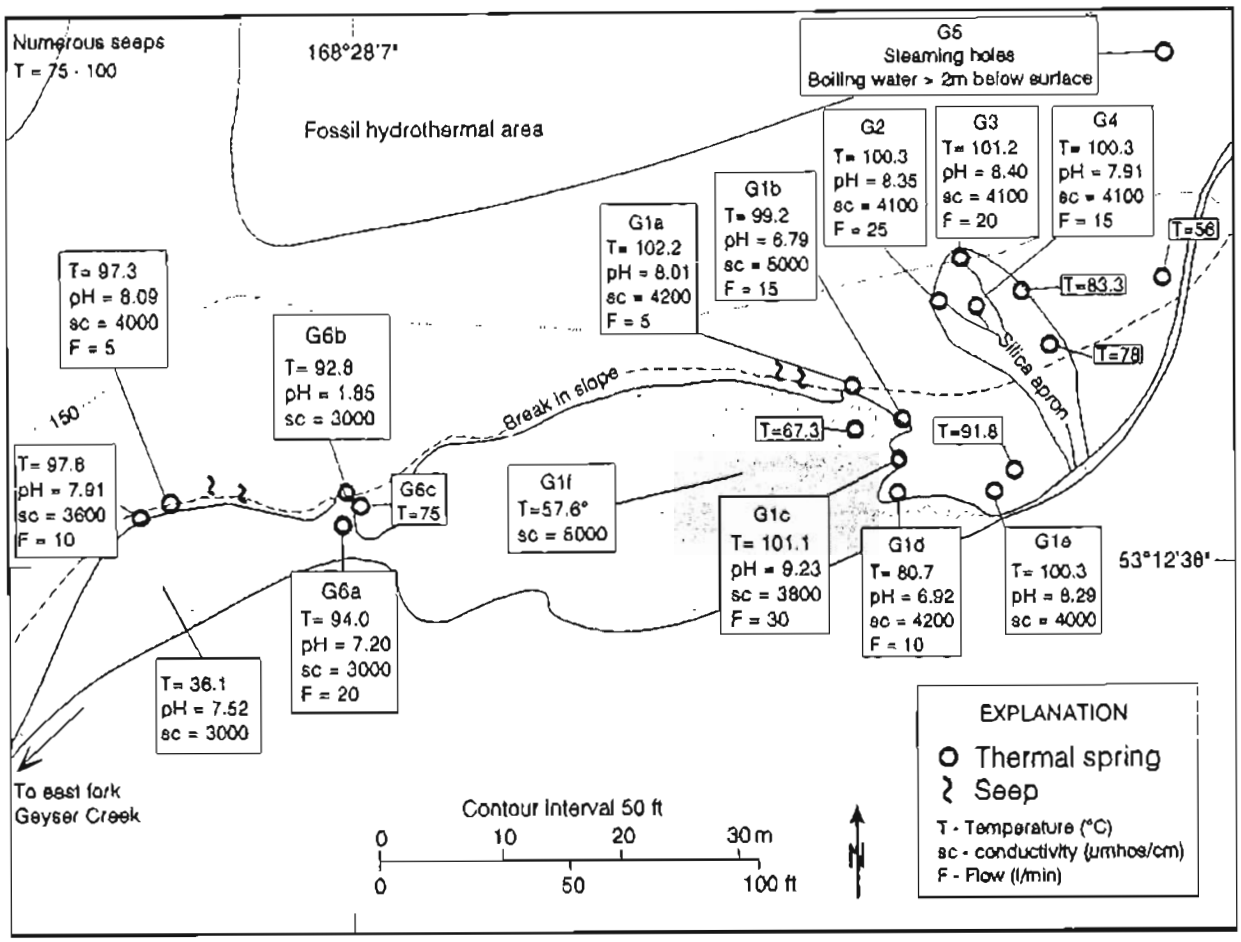

Figure 15. *Map of Geyser Bight springs G1 to G6, central Umnak Island.*

H10 has an algae-covered silica apron located about 20 m upstream from H0. The principal spring has a 30-cm fountain in a 60-cm-diam bowl located about 5 m above "H" Creek. Ten meters upstream, H11 emerges from the alluvium and colluvium. Located in a 1-m-diam bowl about 4 m from the "H" Creek, this geyser fountains to 40 cm with irregular periods one to several minutes. Although H11 is the last large springs along this creek, seeps with temperatures of 70° to 90°C are found for another 20 m upstream.

About 100 m downstream from the mouth of "H" creek-along the east fork of Geyser Creek-is a previously unreported area of geothermal activity (fig. 20). Along the north bank, for approximately 25-30 m, numerous seeps discharge 40° to 60°C water at 2 to 20 lpm. Across the east fork of Geyser Creek (south side), H8 is normally a 1.3 by 0.5-m steaming pool of hot water with bubbling gas and no outflow. However, in 1988 it erupted as a spectacular geyser with a 2-m fountain and water discharge of ≥ 100 lpm for about 10 min. Spring H9 emerges from colluvial cover about 15 to 20 m south of H8. Its outflow enters a narrow, 40- to 50-cm-wide channel, with several seeps and discharges into the east fork of Geyser Creek immediately upstream from H4.

H4 is a geyser of irregular period. When first sampled in 1988, H4 boiled and fountained continuously to 40 cm while discharging about 400 lpm of water during the 5-hr observation. Two days later, H4 was initially dry and then became active, geysering to 50 cm for 2 min before going dry. Three minutes later, it geysered to 50 cm for 3 min. Fountain height then decreased to 10 to 20 cm for 6 min before going dry again. After 11 min, it geysered to 50 cm for 3 min before decreasing to 10 to 20 cm. That fountain level lasted at least 30 min, until the end of the observation period. The next day, H4 had a 40-cm fountain and behaved as it had when first observed.

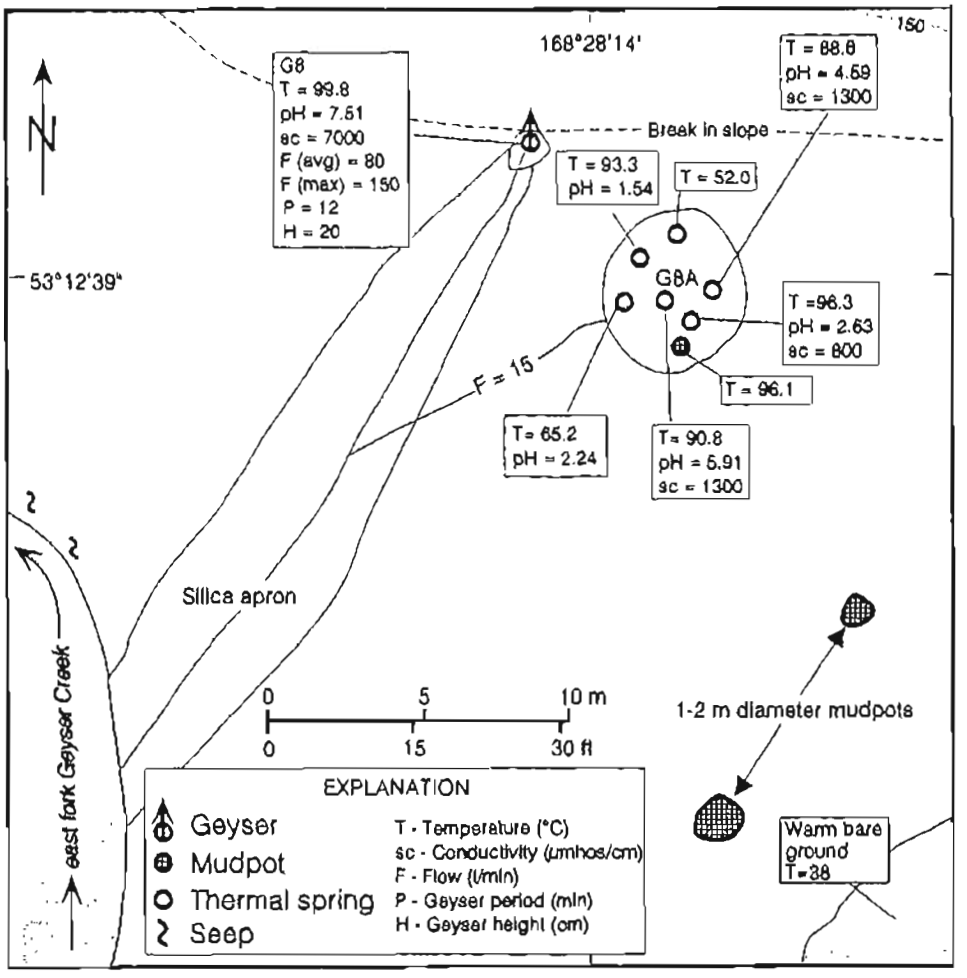

Figure 16. *Map of Geyser Bight spring G8, central Umnak Island.*

Downstream 20 to 25 m is the last concentration of site "H" springs. A 10 by 15 m bare patch in lush vegetation marks the area where the H6 springs emerge from the cemented colluvium and glacial debris that covers the valley on the north side of the creek. The main vent issues boiling water with a 10-cm fountain; a smaller vent (3 m away) is quiet with gas slowly rising to the surface. On the south side, across from H6, are the two steaming pits called A and B in 1980. Both are about 2 m diam with water level 1.5 m below the surface. The level of the water oscillated 25 cm in 1980; in 1988 it did not. Spring H7, about 5 m away, changed from an active geyser in 1980 to a quiet pool with gas slowly bubbling to the surface. H5, a geyser in 1980, could not be found. The temperatures of A, B, and H7 were within a degree of each other in 1980 and 1988, and are at or slightly above boiling.

SITE J

Site J (fig. 21) is located in the southwest corner of Geyser Creek valley across from site G. J1, the most prominent thermal spring at the site emanates from a 3-m-diam, 5-m-deep, funnel-shaped aquamarine pool set in valley alluvium. A large silica apron extends east of the spring. Byers and Brannock (1949) estimated 720 lpm discharge from the pool in 1947, but by 1988 flow had decreased to 10 lpm. Low, rumbling concussions could be heard and felt from beneath the ground surface around J1. The geometry, size, and temperature of the J1 pool suggest that J1 was a geyser that has become inactive or is presently a geyser whose eruptive cycle has not been observed.

Other springs and seeps at site J are dispersed over a distance of 250 m along the slope break at the base of a low ridge. Above the currently active springs is a fossil hydrothermal area about 5,000 m^2 in size. The active

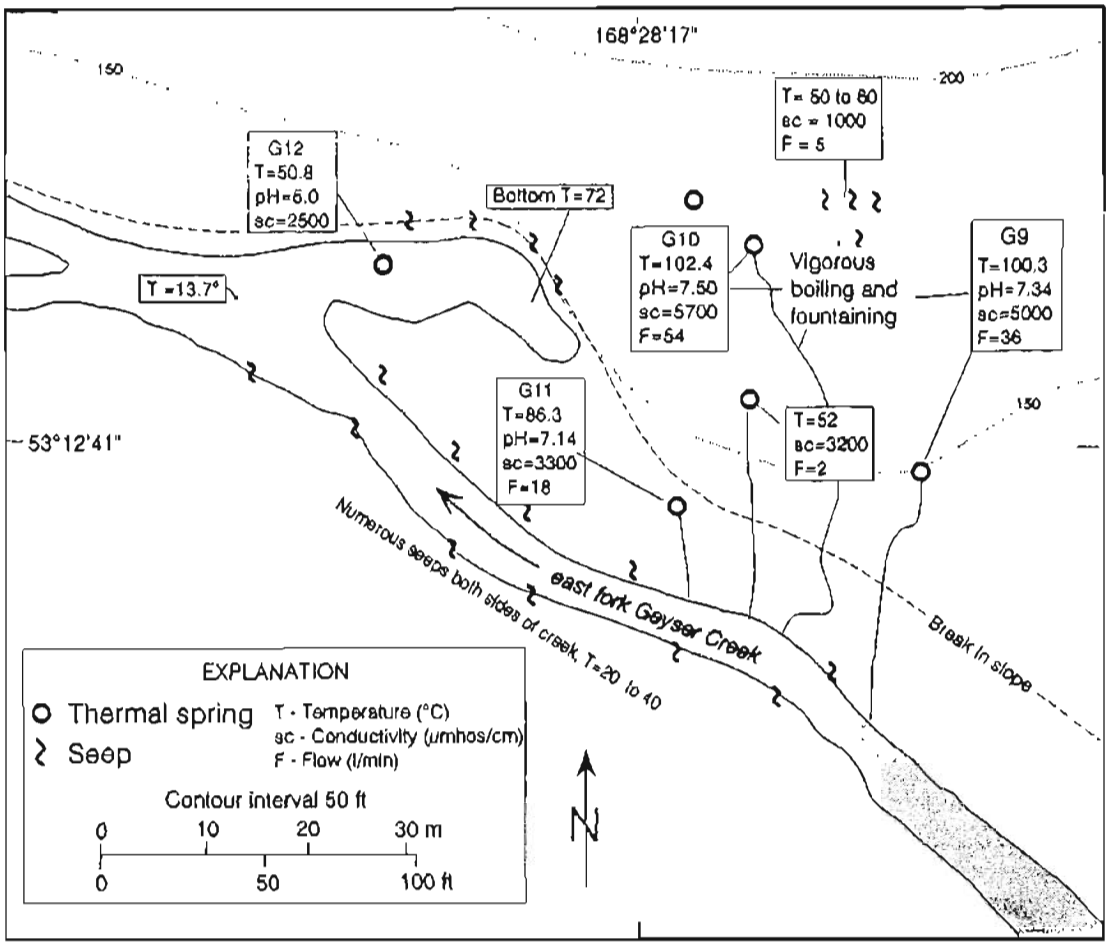

Figure 17. *Map of Geyser Bight springs G9 to G11, central Umnak Island.*

springs typically emerge from pools that range from 0.5 to 2.5 m diam with deep, funnel-shaped bottoms set in valley alluvium. Spring J6 emerges from a 1-m-diam vent in the center of a 4-m-diam pool. Gas occasionally breaks the surface of the calm pool. An oblong pool 1 by 1.5 m at the head of a 20 by 20 m silica apron marks the location of geyser J5. Every hour or so, gas and steam burst from the vent, and the water flow doubles to 50 lpm for about a minute. The temperature at J5 was 90°C, but may increase during geysering. A puncture through the surface silica apron of J5 revealed a second silica surface 0.5 to 0.75 m beneath the upper surface. The irregular lower surface may be the bottom of an old pool. We observed water between the two silica layers. The adjacent spring, J4, at 60°C, is cooler than J5 but similar to it in pH, conductivity, flow rate, the form of the pool from which it emanates, and the presence of a silica apron. A deep gurgling can be heard coming from beneath the surface around J4. J3 (flow rate 10 lpm) is the last spring emerging from a pool. J2 is one of several seeps that lie 150 m farther along the slope break; temperatures decrease with distance. Compared to other springs in Geyser Bight, site J is characterized by almost no algal growth. As with J1, the geometry and pool size of several of the other J springs suggest they may also have been or are geysers whose activity has not been observed.

SITE K

Site K (fig. 22) is located 4.8 km inland from Geyser Bight near the valley center. The springs flow directly from alluvium near the terminus of a large alluvial fan. At K1, 61°C water emerges in an oval 2.5-m-wide, 4-m-long and ≤ 1.5-m-deep pool, and flows down a narrow channel into two successively large oval pools covered with thick, dark algal growth. The lower pool, (spring K2) was 59°C and bubbling in 1980. In 1988, K2 was a quiet 50°C pool clogged with algae. Overflow (100 lpm in 1980; 30 lpm in 1988) from these pools and a fourth small, irregularly shaped pool with 40°C water spills into a nearby cold-water stream.

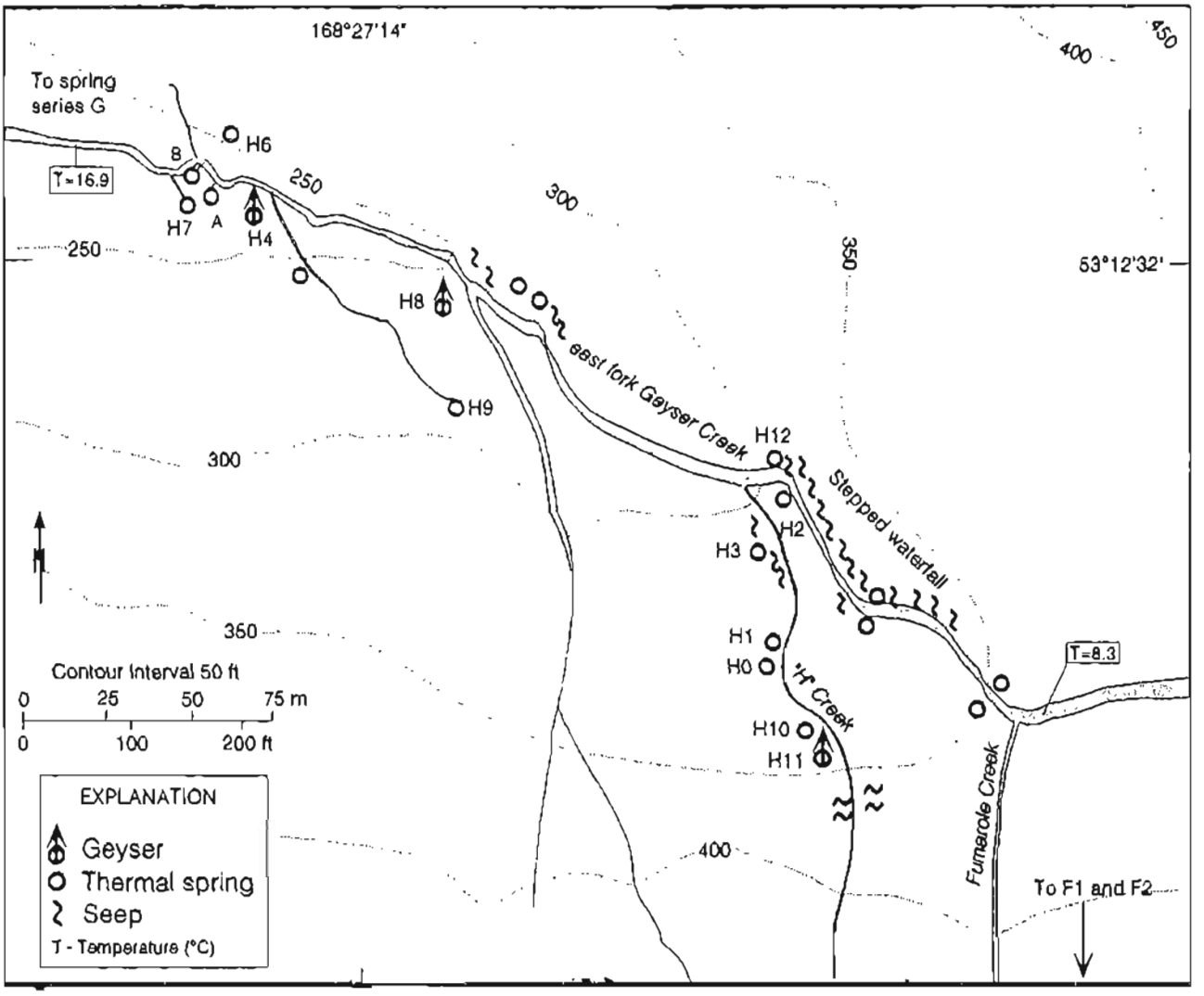

Figure 18. *Map of Geyser Bight springs series H, central Umnak Island.*

A second cold stream of similar size joins this stream 20 m downstream from the outflow of K1 and K2. Spring K3, on the small delta between these two streams, drains into the second stream. K3's 30-cm-diam vent is hidden at the end of a 3-m-long, 0.7-m-wide, 1.25-m-deep cut in the grass-covered alluvium. Numerous 50° to 70°C seeps emerge from the left bank of the second stream. Stream water increases temperature from 12° to 18°C as it passes through the seep area. Numerous small ponds ≤ 0.5 m diam with temperatures of 30° to 40°C are found between this creek and the channel that connects K1 and K2. A slight odor of H_2S is evident at site K.

SITE L

Hot-spring site L lies almost directly across from site K, in an indentation on the northeast side of the valley (fig. 23). The concavity of the hollow in which the site is located and the warmth and muddiness of the soil in and around the springs suggest the area is a small, shallow slump caused by warm-water injection. Several small springs emerge around the upper back wall of the depression, and a few muddy seeps emerge at its center. Numerous vents, 36° to 86°C, discharge water directly into a 1-m-deep, 20 by 7 m pool. This pool supports abundant bacteria and algal flora. Spring L3 has the greatest flow. The most active site in 1980 was L1; by 1988 this vent had cooled to 25°C with no water in its outflow channel. Combined discharge from site L totaled 250 lpm. The H_2S odor is noticeable at least 100 m from the site, which has the strongest H_2S odor in Geyser creek valley.

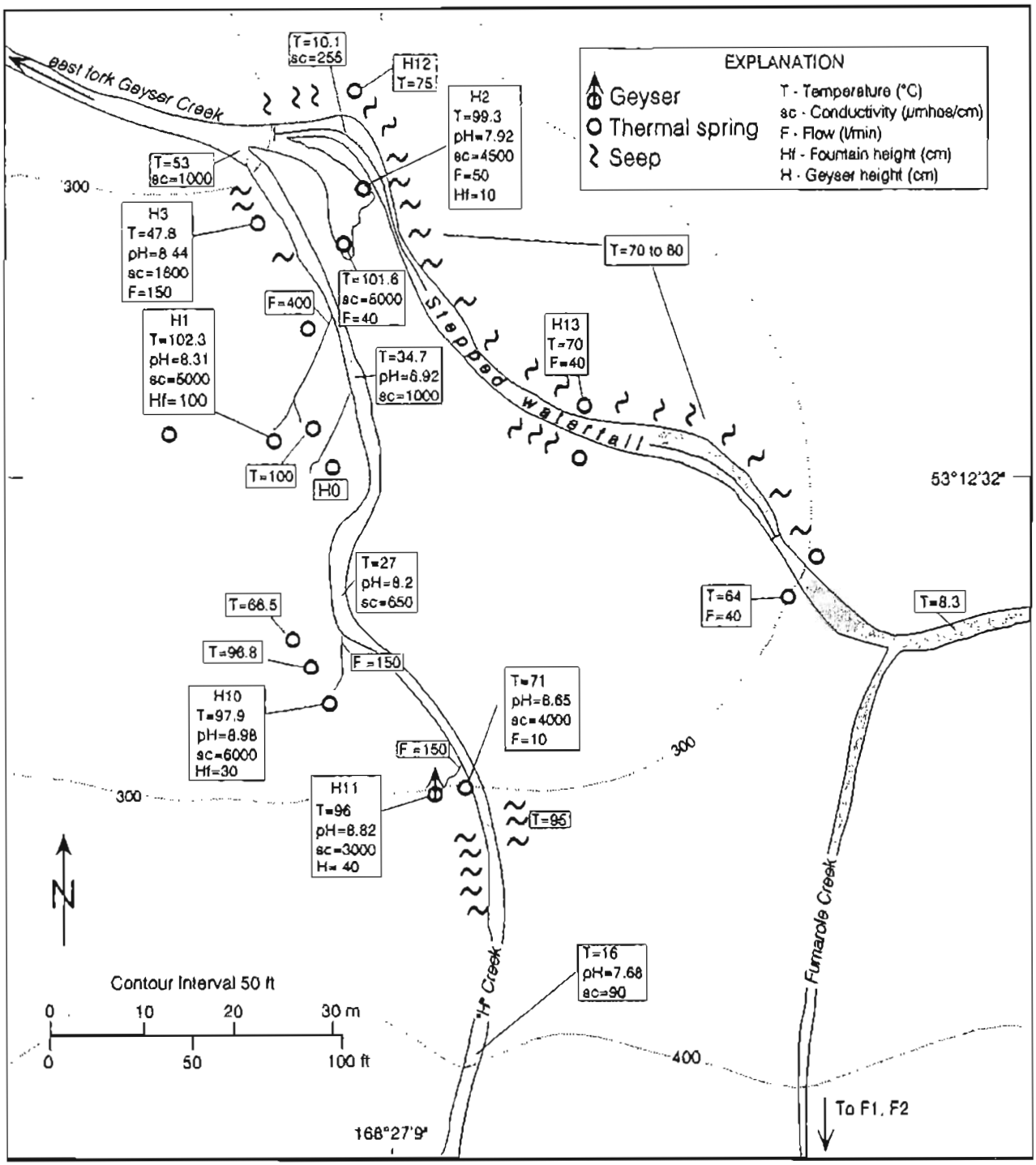

Figure 19. *Map of Geyser Bight springs H0 to H3 and H10 to H13, central Umnak Island.*

SITE Q

Two small springs and several seeps discharge in a narrow tributary valley located about 0.3 km above site J (sheet 2). They emerge from the valley alluvium for a distance of 50 m at the slope break and are found only on the west bank (fig. 24). Volcanic rock that crops out along the creek between sites J and Q and shows signs of previous thermal-spring activity. The most prominent springs, Q1 and Q2, have temperatures of 80° and 79°C, flows of 30 and 25 lpm, and similar conductivities and pH. A slight H_2S odor is evident. Above Q, the creek temperature is 4°C, which suggests no additional geothermal activity up-valley.

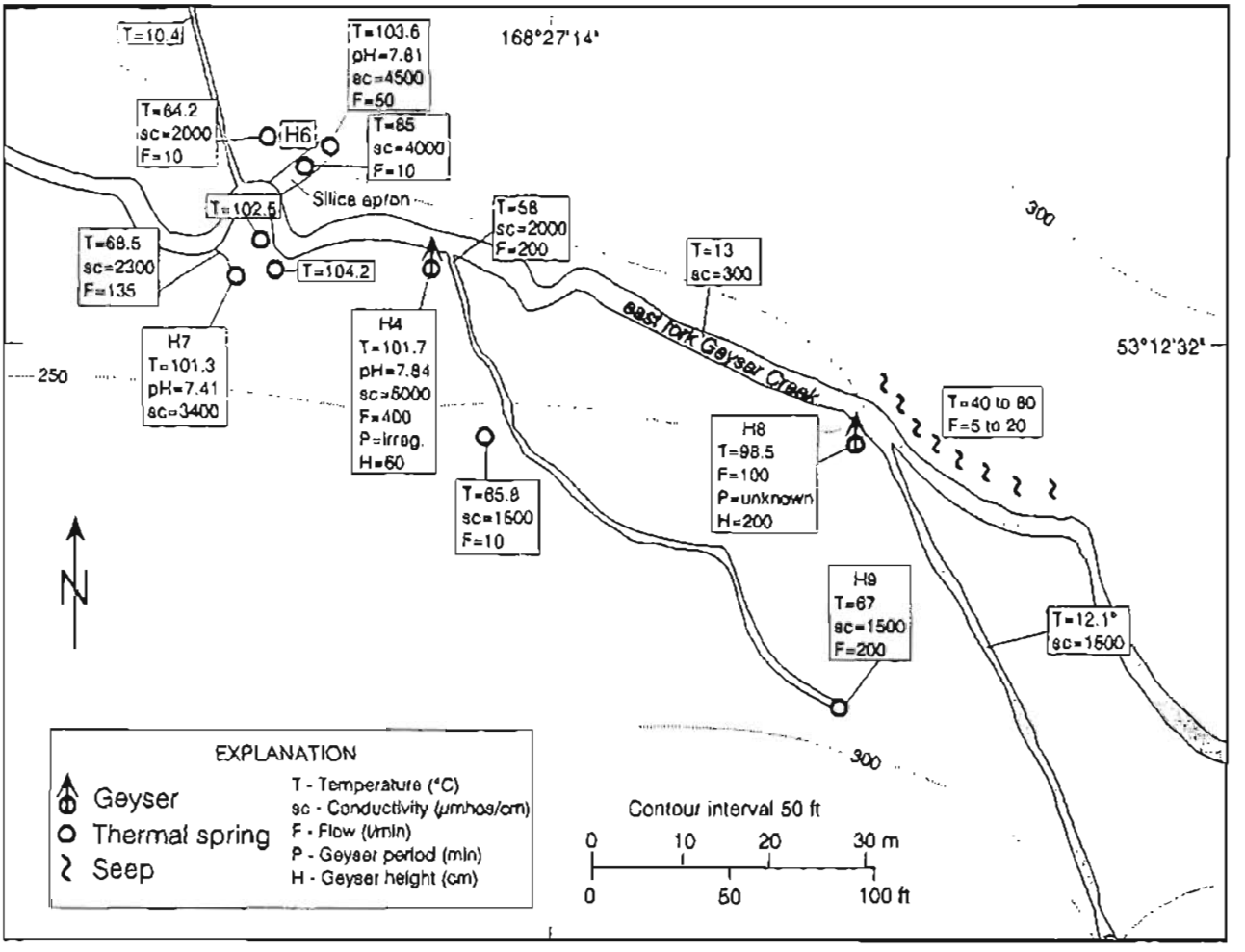

Figure 20. *Map of Geyser Bight springs H4 to H9, central Umnak Island.*

CONVECTIVE HEAT DISCHARGE BY SPRING FLOW

The results of our 1988 thermal-spring-discharge measurements are shown in table 5. For comparison, thermal-spring discharges measured by Motyka and others (1981) in 1980 are given in table 6 and those by Byers and Brannock (1949) in 1947 are shown in table 7. Reported spring temperatures are the hottest measured at the site. The calculated heat discharged by spring flow (table 5) is referenced to the enthalpy of water at 10°C, the approximate average annual temperature in the central Aleutian Islands.

Because of problems with our flow meter, most 1988 discharges were visually estimated and may be subject to substantial error (25 - 50 percent); those sites that were measured by catchment or flow meter are noted in table 5. The heat discharge by spring flow calculated for 1988 (16.7 MW) is much greater than for 1980 (6.1 MW), partly because more springs were included in the 1988 calculations. Variations in spring flow may also contribute.

Convective surface heat discharge, which was also estimated from stream-flow measurements made in 1981, is included in table 6. Geyser Creek flow was measured below the point of input of thermal waters that drains from G and J (sheet 2). Stream-water samples were collected at this site and from a site above H. The hottest and most chemically concentrated thermal-spring waters at G (G8), J (J5), and H (H6) were taken to represent the undiluted thermal water that discharges into the stream drainage. The average analyzed concentrations of Cl and B in these waters and in the stream waters above H and below G were used in mass-balance calculations to determine the hot-water fraction. To calculate the convective heat discharge, we assumed the hot-water fraction

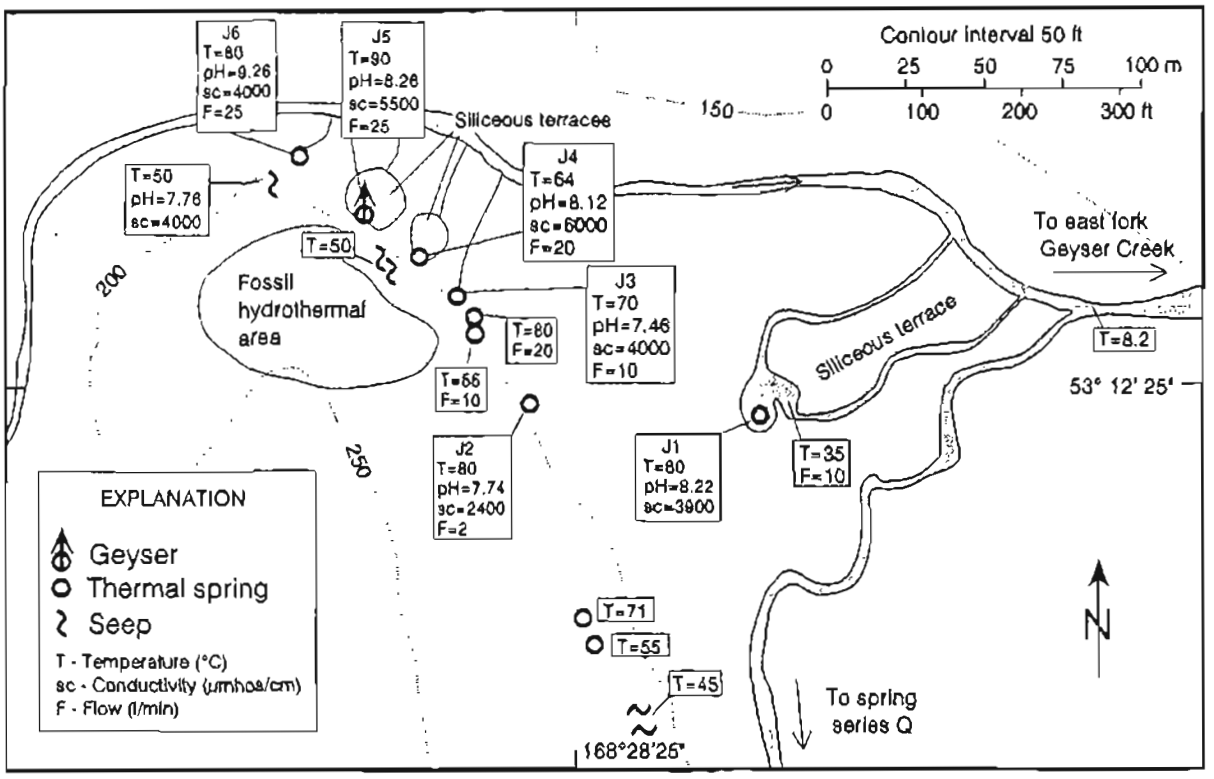

Figure 21. *Map of Geyser Bight springs series J, central Umnak Island.*

was at the surface boiling point. The estimated 13.3 MW of discharged heat does not include contributions from spring groups K, L, and Q nor from any thermal waters that may enter the creek below the flow-measurement point.

When the heat discharge from spring groups K, L, and Q is subtracted from the 1988 estimates, the result, 15.1 MW, compares reasonably well with the 1981 estimate of 13.3 MW determined by mass-balance calculations. The 1988, 1981, and 1980 estimates are substantially lower than the heat discharge by spring flow calculated using 1947 estimates of spring flow (table 7) (Byers and Brannock, 1949). Although Byers and Brannock (1949) do not report the method or precision of their measurements, the differences in flow rate in some cases appear too large to be explained by differences in measuring techniques; the variations in spring discharge appear to be real. For example, flow-meter measurement of spring discharge at H7 was 135 lpm in 1988 and 70 lpm in 1980 vs. Byers and Brannock's (1949) report of 260 lpm in 1947; discharge from hot spring pool J1 was visually estimated at 10 lpm in 1988 vs. 760 lpm in 1947. Geyser activity, particularly at H, was more subdued in 1980 than observed in 1988 or reported by Byers and Brannock (1949). Silica sinter is being deposited at many boiling point vents and also forms large aprons in outflow channels. Silica and other hydrothermal alteration deposits may periodically choke some spring and geyser conduits. Periodic vent opening and increase in discharge could be triggered by seismic activity or build-up of steam pressure similar to that observed at Yellowstone National Park.

GEOCHEMISTRY OF GEOTHERMAL FLUIDS

INTRODUCTION

Reports of the Geyser Bight hot springs appear in Grewingk (1850) and Waring (1917), and their existence was probably known to Aleut villagers at Nikolski since ancient times. Byers and Brannock (1949) conducted an extensive survey of the thermal-spring areas during their reconnaissance geologic mapping of Umnak Island in 1946-48 and reported analyses on water samples from two springs. Samples from four thermal springs were collected and analyzed by Ivan Barnes (written commun., U.S. Geological Survey, 1981) in 1975 as part of a U.S. Geological Survey reconnaissance investigation of hot-spring sites in the Aleutian arc.

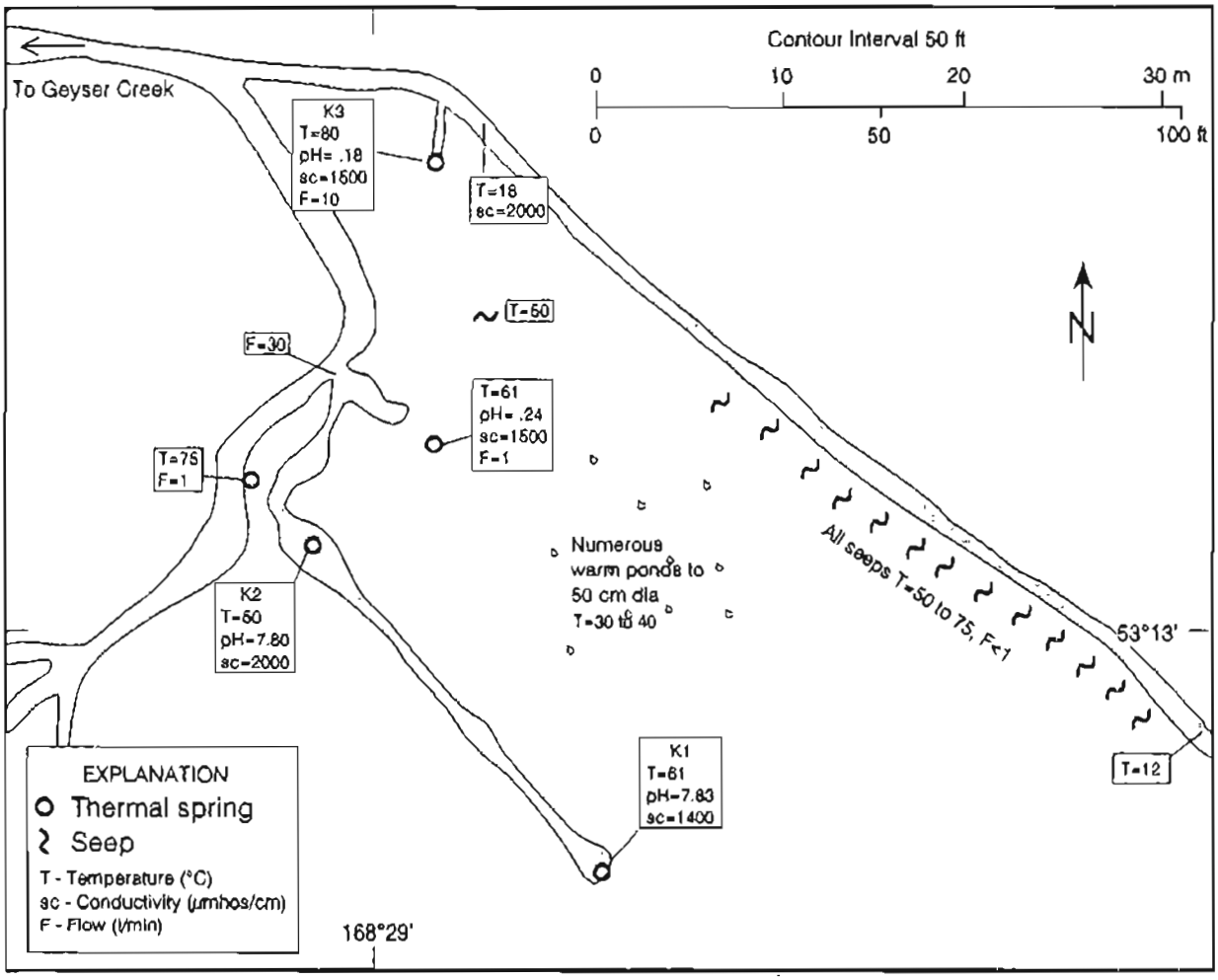

Figure 22. *Map of Geyser Bight spring series K, central Umnak Island.*

In 1980, we sampled and analyzed seven Geyser Bight thermal springs and measured spring discharges during a regional assessment of geothermal resources in the Aleutian Islands for the State of Alaska (Motyka and others, 1981). These preliminary studies suggested that the hot springs are fed by multiple reservoirs with temperature ranges from 160° to 190°C. The multiple reservoirs are related to a deeper parent reservoir with a temperature as high as 265°C. In this fluid geochemistry study of the Geyser Bight geothermal area, waters from 14 thermal springs and numerous surface waters were sampled and analyzed to more conclusively determine if multiple reservoirs exist and to determine the geochemical, isotopic, and temperature parameters of these reservoirs. These data were also used to examine chemical equilibria, determine the source of water charging the reservoirs, and estimate heat loss by surface and near-surface thermal water discharge.

The results of this investigation confirm the existence of at least two chemically and isotopically distinct intermediate reservoirs with temperatures of 200° and 165°C. Evidence for deep reservoirs at temperatures of 265° C and possibly 225° C also exists, but we are unsure if these deep reservoirs are related or interconnected.

METHODS

SAMPLING PROCEDURE

Thermal-spring waters were collected as close to the issuing vent as possible, and surface waters were sampled directly from streams or creeks. The samples, normally filtered through 0.45μ filters, consisted of 500 ml or 1 liter each of filtered, untreated and filtered, acidified (HCl) waters; 100 ml 1:10 and 1:5 diluted

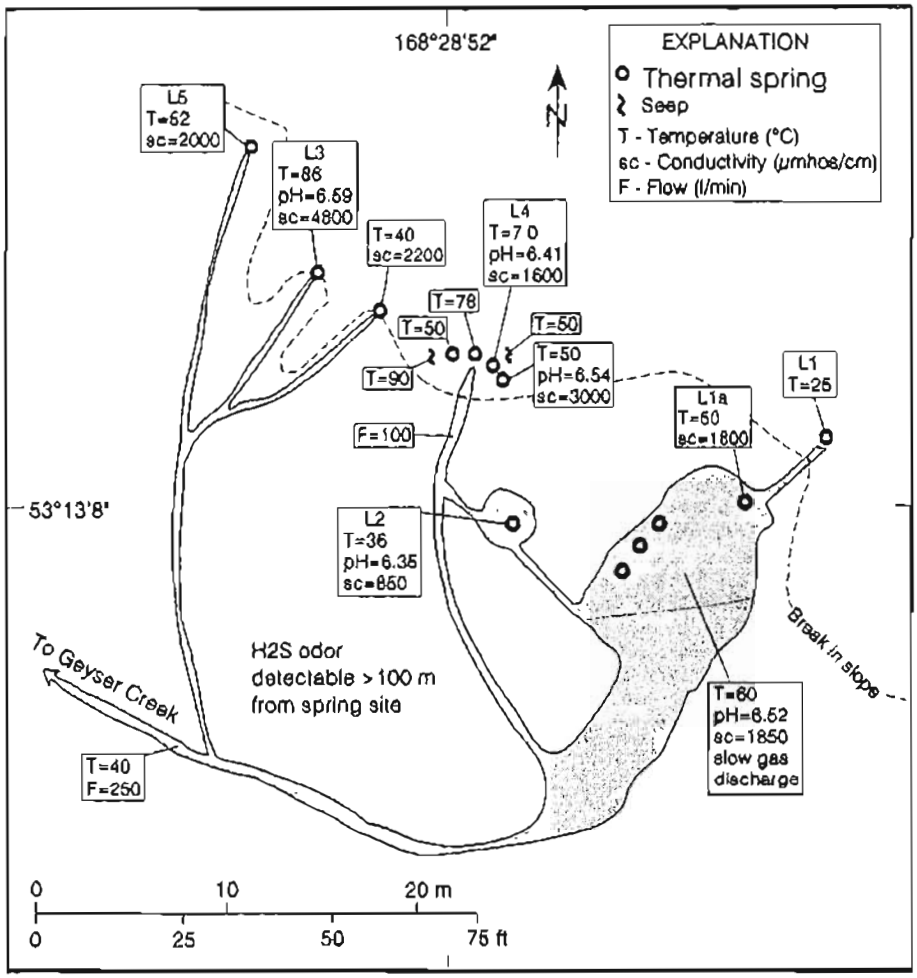

Figure 23. *Map of Geyser Bight spring series L, central Umnak Island.*

samples for silica determinations; and 30 ml samples for oxygen and deuterium isotopic analyses. At three springs (G8, H6 and L3), 500 ml of water were filtered through 0.1µ filters and treated in the field with methyl isobutyl keytone (MIBK) for later aluminum analysis following methods described by Presser and Barnes (1974). At several sites (G8, H1, H4, J1 and L3), 1 liter of filtered water was collected and treated with formaldehyde for later determination of oxygen-18 composition of the sulfate species. One liter of unfiltered, untreated water was collected for tritium determinations from two springs (G8 and H4) and two streams.

Gases were collected in 1980 and 1981 by immersing a plastic funnel in the spring-water pool. The funnel was placed over a train of bubbles and connected to an evacuated gas-collecting flask with tygon tubing. The gas sample was taken by allowing the gases to displace water in the funnel, purging the sampling line of air, then collecting the gas in the evacuated flask. Samples were collected in 50 to 100 cc flasks of helium-impermeable Corning 1720 glass.

ANALYTICAL PROCEDURES

All thermal-spring water samples collected in 1980 were analyzed at the DGGS water laboratory in Fairbanks. Procedures are described in Motyka and others (1981).

For 1981 and 1988 stream waters, HCO_3, temperature, and pH were determined in the field following methods described by Presser and Barnes (1974). The remaining constituents were analyzed at the DGGS water laboratory in Fairbanks. Na, K, Li, and Sr were determined using a Perkin-Elmer atomic absorption spectrometer following procedures outlined in Skougstad and others (1979) and in the Perkin-Elmer reference manual.

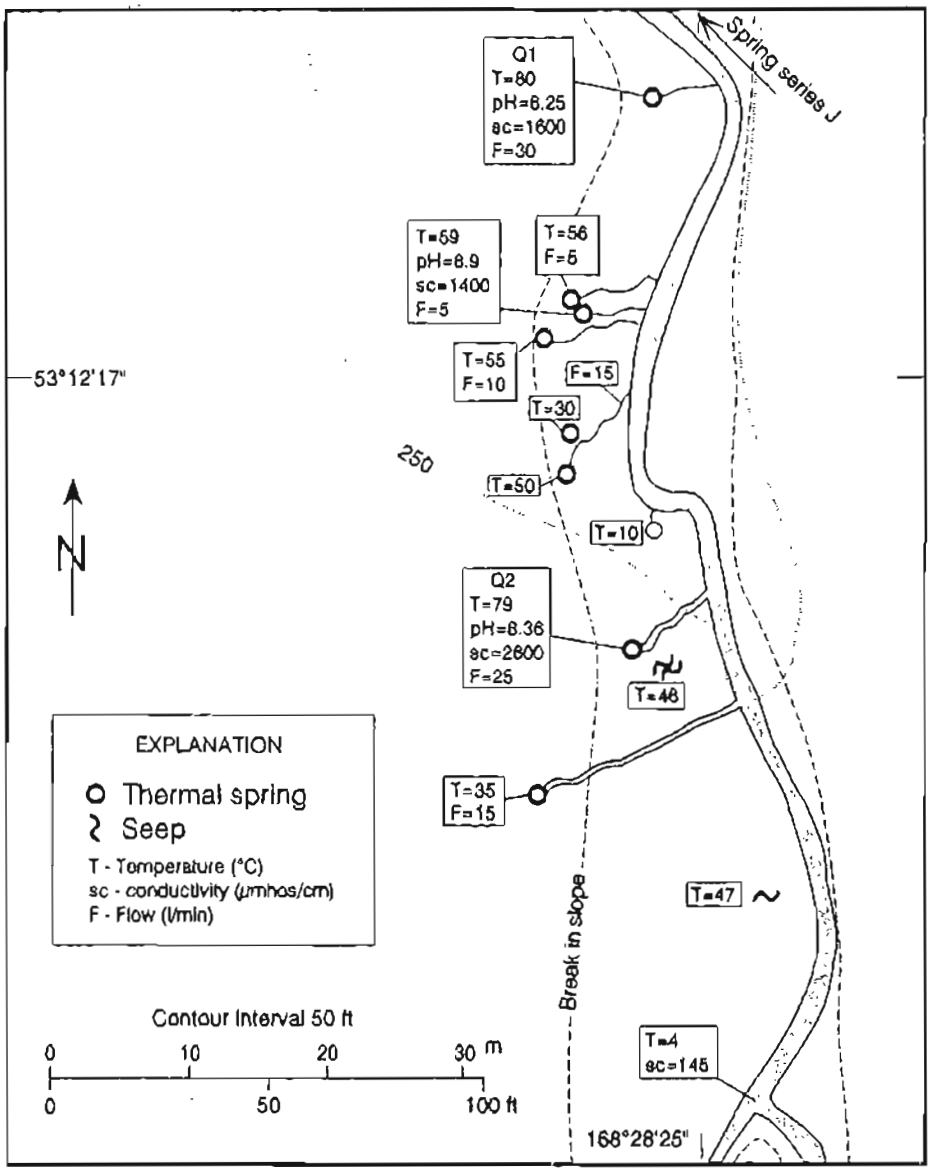

Figure 24. *Map of Geyser Bight spring series Q, central Umnak Island.*

Ca, Mg, and B were analyzed on a direct-coupled plasma system. Silica concentrations were determined by the molybdate blue method. Sulfates were determined by the titrimetric (thorin) method, fluorides by specific ion electrode, and chloride by Mohr titration.

For 1988 thermal-spring waters, HCO_3, NH_3, and H_2S concentrations, temperature, and pH were determined in the field following methods described in Presser and Barnes (1974). Rb and Cs were analyzed at the U.S. Geological Survey (Menlo Park) using an atomic emission spectrometer. Ba and Al were analyzed at the DGGS water laboratory (Fairbanks) on a direct-coupled plasma system (DCP). The MIBK-treated samples were used for the aluminum analysis. Because a laboratory move and equipment changes disrupted the analysis program at DGGS, the remaining constituents were analyzed by the University of Utah Research Institute (UURI) water laboratory (Salt Lake City). At UURI, major, minor, and trace cation concentrations were determined using an inductively coupled argon plasma spectrometer (ICP). Sulfates were determined by the titrimetric (thorin) method, fluorides by specific ion electrode, chloride by Mohr titration, bromide by hypochloride oxidation and titration (UURI), and iodide by titration.

Table 5. *Convective heat discharge, Geyser Bight Geothermal Area, 1988*

Site[a]	Temp °C	Flow[b] l/min	Method[b]	Enthalpy[c] J/gm	Heat discharge kw
G1-A	102.2	5	E	386	30.8
G1-B	99.2	15	E	373	89.6
G1-C*	101.1	30	E	381	182.7
G1-D	80.7	10	E	296	47.9
G1-E	100.3	10	E	378	60.4
G1-F-pool	57.6	1	U	199	3.3
G1-G-pool	67.3	1	U	240	3.9
G1-H	91.8	1	E	342	5.5
G2	100.3	25	E	378	151.0
G3	101.2	20	E	382	122.0
G4	95.6	15	E	358	86.2
G4-s	78.0	1	E	285	4.6
G4.5	83.3	0	E	307	0.0
G5-s	58.0	1	E	201	3.3
G6-A*	94.0	20	E	352	112.9
G6-B	92.8	0	E	347	0.0
G6-Cs	75.0	1	E	272	4.4
G6-Pool	36.1	1	U	109	1.8
G6-s1	97.3	10	E	365	58.5
G6-s2	97.6	5	E	367	29.4
G7-erkblo	18.0	250	E	331	39.5
G7-hi-s	101.0	25	E	381	152.1
G7-lo-s	75.0	25	E	272	110.5
G8-A1-s	65.2	2	E	231	7.6
G8-A2-s	93.3	2	E	349	11.2
G8-A3-s	52.0	2	E	176	5.8
G8-A4-s	89.8	2	E	334	10.8
G8-A5-s	96.3	2	E	361	11.6
G8-A6-s	95.1	2	E	356	11.4
G8-A7-s	91.0	2	E	339	10.9
G8-Gey*	99.9	60	Mc	376	361.0
G9	100.3	36	Mb	378	217.5
G9.5	55.0	5	E	188	15.5
G10	102.4	54	Mb	387	333.3
G10.5-s	52.0	2	E	176	5.8
G11*	86.3	18	Mb	319	92.8
G12	50.8	1	U	171	2.8
			Minimum heat discharge for "G" springs		2,498.3
H1	102.3	400	E	386	2,466.52
H1-s	100.0	5	E	377	30.1
H1.5	99.7	100	E	375	600.4
H2-A*	99.3	50	E	374	298.9
H2-B	100.0	5	E	377	30.1
H2-C	101.6	40	E	383	244.9
H3	47.8	150	E	158	391.1
H4-main*	101.7	400	E	384	2,451.5

[a] Asterisk indicates water-chemistry sample location.

[b] Seeps were given values of 1 l/min for the calculation. Some values refer to group of vents. Mm = measured with meter, Mb = measured by timing bucket filling, E = visual estimates, U = unable to estimate.

[c] Base temperature for calculations is 10 °C.

Table 5. *Convective heat discharge, Geyser Bight Geothermal Area, 1988-Continued*

Site[a]	Temp °C	Flow[b] l/min	Method[b]	Enthalpy[c] J/gm	Heat discharge kw
H4-s1	65.8	10	E	234	38.2
H6-main*	103.6	50	E	392	312.4
H6-s1	86.0	10	E	318	51.3
H6-s2	64.2	10	E	227	37.1
H7*	101.3	135	Mm	382	824.0
H8	98.5	100	E	370	592.9
H9	67.0	200	E	239	779.0
H10-A	97.8			368	0.0
H10-ALL	97.0	150	E	364	875.2
H10-s1	95.6			358	0.0
H10-s2	66.5			237	0.0
H11	96.0	150	E	360	865.7
H11-sa	71.0	10	E	255	41.6
H11.5-s	71.0	10	E	255	41.6
H12	75.0	50	E	272	221.1
H13	75.0	40	E	272	176.9
HW-topL	65.0	25	E	230	94.1
HW-topR	64.0	40	E	226	147.8
HRHS-flat	50.0	250	E	167	689.2
			Minimum heat discharge for "H" springs		12,315.3
J1	80.0	10	E	293	47.5
J2	80.0	2	E	293	9.5
J2-s1	71.0	5	E	255	20.8
J2-s2	55.0	5	E	188	15.5
J2-s3	46.0	2	E	151	5.0
J3-A	70.0	10	E	251	40.9
J3-B	55.0	10	E	188	30.9
J3-C	80.0	20	E	293	94.9
J3-D	60.0	1	E	209	3.4
J4	64.0	20	E	226	73.9
J4-s1,2,3	50.0	2	E	167	5.5
J5*	90	25	E	335	134.8
J6	85.0	25	E	314	126.8
			Minimum heat discharge for "J" springs		609.4
K1	61.0			213	0.0
K-below1+2	55.0	30	Mb	188	92.8
K2	50.0			167	0.0
K2-s1	75.0	1	E	272	4.4
K2-s2	61.0	1	E	213	3.5
K3*	80.0	10	E	293	47.5
K3-seeps	63.0	50	E	222	181.5
K-pools	40.0	10	U	126	20.8
			Minimum heat discharge for "K" springs		350.4

Table 5. *Convective heat discharge, Geyser Bight Geothermal Area, 1988-Continued*

Site[a]	Temp °C	Flow[b] l/min	Method[b]	Enthalpy[c] J/gm	Heat discharge kw
L1	25.0	0	E	63	0.0
L1-a	50.0		U	167	0.0
L1-Pool*	60.0		U	209	0.0
L2	36.0			109	0.0
L3-a*	86.0			318	0.0
L3-b	40.0			126	0.0
L4-a	50.0	20	E	167	55.1
L4-b	78.0	20	E	285	92.3
L4-c	70.0	25	E	251	102.3
L4-d	50.0	20	E	167	55.1
L5	52.0			176	0.0
L-ALL	40.0	250	Mm	126	519.1
			Minimum heat discharge for "L" springs		519.1
Q1*	80.0	30	E	293	142.4
Q1.2-s1	56.0	5	E	193	15.8
Q1.2-s2	59.0	5	E	205	16.8
Q1.2-s3	55.0	10	E	188	30.9
Q1.5-s1	30.0	15	E	84	20.8
Q1.5-s2	50.0	20	E	167	55.1
Q2	79.0	25	E	289	117.1
Q2-s	46.0	1	E	151	2.5
Q2.5	35.0	15	E	105	26.0
Q2++seeps	47.0	5	E	155	12.8
			Minimum heat discharge for "Q" springs		440.3
			Minimum heat discharge for all Geyser Bight springs		**16,732.8**
Increase in enthalpy of creek water as it passes through fumarole fields F1 and F2:					
Crk abv F1	9.2	400	E	0	0.0
Crk blo F1	17.5	450	E	312	35.4
Crk abv F2	16.7	450	E	282	10.4
Crk blo F2	21.2	500	E	473	90.2

Gases were analyzed on dual-column gas chromatographs using argon and helium carrier gases. Chromatographic analyses of gases collected in 1980 were performed at the U.S. Geological Survey (Menlo Park); gases collected in 1981 were analyzed at the Scripps Institution of Oceanography (San Diego).

Stable isotope values of water samples ($^{18}O/^{16}O$ and D/H) were analyzed by the Stable Isotope Laboratory, Southern Methodist University (Dallas). Procedures followed are outlined in Viglino and others (1985). Tritium concentrations were determined by the Tritium Laboratory, University of Miami (Miami). The $^{18}O/^{16}O$ values of sulfate species were analyzed at the U.S. Geological Survey (Menlo Park). Procedures followed are discussed in Nehring and others (1977).

Table 6. *Convective heat discharge by thermal spring flow, Geyser Bight KGRA, 1980 and 1981*

Site	Temp °C	Flow l/min	Enthalpy J/gm	Heat discharge kw
G1	100.0	20	419	134
G2	79.0	5	331	26
G3	100.1	16	419	107
G4	92.4	5	387	31
G6	97.3	20	407	130
G8	100.1	75	419	503
G9	99.3		416	
G10	100.0		419	
G11	81.0		339	
H0	97.3	30	407	195
H1	100.3	300	420	2,016
H2	99.3	100	416	666
H3	45.2	60	189	181
H4	100.3	45	420	302
H5	101.8		427	
H6	99.9	30	419	201
H7	99.8	70	419	469
J1	82.0		343	
J2	77.2	1	322	5
J3	82.5	10	345	55
J4	69.0	5	289	23
J5	92.2	15	386	93
J6	83.9	15	352	84
K	60.5	100	253	405
L	82.3	200	347	1,109
Q	72.5	25	304	121
Minimum heat discharge, all springs.				**6,856**
Heat loss referenced to 10°C.				6,088

Heat loss computed from 1981 stream-flow measurements and increase in chemical constituents using G8 chemistry for hot-water fraction.

	Cl	B	Na	T
Hot water	630	60	487	100
Cold water	6.2	0	5.2	4.8
Mixed	18.8	1.3	14.7	10
Hot water fraction	0.0202	0.0217	0.0197	0.0546

Average of chemically determined fraction	0.0205
Measured stream flow below G, lps	1723
Hot water fraction, lps	35.37
Heat loss referenced to 10°C, MW	13.33

Table 7. *Convective heat discharge by spring flow, Geyser Bight KGRA, 1947*[a]

Site	Temp. °C	Flow l/min	Enthalpy J/gm	Heat discharge kw
G1	101.0	260	423	1,760
G2	88.0	6	369	35
G3	100.5	18	421	121
G4	98.0	36	411	237
G6	95.0	80	398	509
G7	82.0	85	343	466
G8	100.5	170	421	1,145
G9	100.5	6	421	40
G10	99.0	170	415	1,129
G11	77.0	170	322	876
H1	101.5	660	425	4,488
H2	101.0	600	423	4,061
H3	53.0		222	
H4	101.0	340	423	2,301
H5	101.0	85	423	575
H6	100.0	66	419	442
H7	90.0	260	377	1,568
J1	88.0	720	369	4,251
K	64.0	250	268	1,072
L	68.0	170	285	774
			Minimum heat discharge all springs	**25,850**
			Heat loss referenced to 10°C	**23,062**

[a]Byers and Brannock (1949)

GAS CHEMISTRY

Gas flows from steam fields F1 and F2 located at the head of Geyser Bight valley were too diffuse to obtain useable samples in 1980, 1981, and 1988. Weather conditions and lack of time prevented sampling the highly pressurized fumaroles discovered in 1988 at F3.

Gas samples were obtained from thermal spring G6 in 1980 and from an acid spring adjacent to G8 in 1981 (table 8). Both samples consist primarily of nitrogen, carbon dioxide, and oxygen, the latter reflecting air contamination during sample acquisition. The N_2/Ar ratios are nearly that of air, which indicates these constituents are probably primarily atmospheric in origin, from surface air contamination, and from air dissolved in waters that charge the hydrothermal system. Oxidation of H_2S in near-surface groundwaters could account for the apparent depletion of this gas in the G6 sample; a nearby thermal pool has a pH of 3.6. The carbon dioxide is probably of thermal and perhaps also of magmatic origin, as suggested by the helium isotope ratio.

The helium isotope ratio ($^3He/^4He$) of 7.4 times atmospheric ($^3He/^4He$) reflects a probable magmatic influence on the Geyser Bight geothermal system. ^3He is primordial in origin and ^3He enrichments, with respect to atmospheric levels, have been correlated with magmatic activity on a worldwide basis. The excess ^3He is thought to be derived from the mantle (Craig and Lupton, 1981). The 7.4 value is at the upper end of the range for helium isotope ratios for other thermal sites in the Aleutian arc of active volcanism (5.0 to 8.0) (Poreda, 1983) and is nearly the same as the 7.5 average for summit fumaroles in circum-Pacific volcanic arcs (Poreda and Craig, 1989).

Table 8. *Gas chemistry and helium isotope analysis, Geyser Bight Thermal Springs, central Umnak Island*

	G6[a]	G8A[b]
Gas Chemistry, mole %:		
He	0.01	0.01
H_2	0.09	0.26
Ar	0.78	0.64
O_2	0.70	3.90
N_2	85.3	54.0
CH_4	0.04	na
C_2H_6	0.01	na
CO_2	13.45	41.2[c]
H_2S	<0.01	(c)
N_2/Ar	109	84
$^3He/^4He$:		
R/R_a[d]	na	7.4
X[e]	na	70
R_c/R_a[f]	na	7.4

[a]Analysis: W.C. Evans, U.S. Geological Survey, Menlo Park and R.J. Motyka, DGGS.
[b]Analysis: R.J. Poreda and J.A. Welhan, Scripps Institution of Oceanography, La Jolla, and R.J. Motyka, DGGS. Spring G8A is an acid spring adjacent to spring G8.
[c]Analyzed as $CO_2 + H_2S$.
[d]$R/R_A = {}^3He/^4He$ in sample over $^3He/^4He$ in atmosphere.
[e]$X = (He/Ne)_{sample}/(He/Ne)_{air}$.
[f]Measured values of R/R_a corrected for atmospheric contamination by assuming that the neon is of atmospheric origin. $(R_c/R_a) = [(R/R_a)X - 1]/[X - 1]$.
na = not analyzed.

WATER CHEMISTRY

RESULTS

The results of geochemical analyses of the 1988 Geyser Bight thermal spring waters and representative stream waters are shown in tables 9 and 10, respectively. Analyses from previous investigations are also included in these tables. These include data from Byers and Brannock (1949); Ivan Barnes (written commun., U.S. Geological Survey, 1981; Motyka and others, 1981) and previously unpublished data on DGGS stream samples collected in 1981. Comparison of these data show thermal-water compositions did not change significantly from 1946 to 1988. The slight variations in concentrations observed at resampled spring sites (for example, G8) can be attributed to slight differences in dilution ratios or, for boiling springs, the degree of adiabatic boiling. The thermal spring waters are all moderately concentrated Na-Cl waters rich in boron and arsenic.

COMPOSITIONAL TRENDS

For concentrations present in Geyser Bight thermal waters, Cl is considered chemically conservative. Constituent-chloride ratios for the thermal-spring waters are given in table 11. Constituent concentrations are also plotted against chloride in figures 25a-l and figure 26. Na, Li, B, and SO_4 each plot along an approximately linear trend towards a dilute water end member. In contrast, the data for several more reactive constituents (SiO_2, K, Cs, Rb, and F) exhibit two distinct trends; one for down-valley sites (G, J, K, and L), the other for site H. These correlations suggest that the waters are related to a common deep aquifer, but that during ascent to the surface they have partially or totally re-equilibrated to different temperatures and wall rocks in intermediate reservoirs. The observed variations in concentrations that the emergent spring waters display along each of these trends can be explained by dilution or boiling. A logical source of the dilution is meteoric water that infiltrates into the near-surface region beneath the springs. Point A on the constituent-chloride graphs represents a water similar to stream samples unaffected by influx of thermal waters (table 10).

Table 9. *Geochemical analyses of Geyser Bight Hot Spring water samples collected in 1988. Previous analyses shown for comparison. Chemical concentrations in ppm and temperatures in degrees Celsius*

Site	Date	T	pH	SiO_2	Ca	Mg	Na	K	Li	NH_4	Sr	Rb	Cs
DGGS and UURI 1988													
G1	7-14-88	101	9.2	326	16	0.2	482	36	3.1	na	0.07	0.33	0.58
G6	7-14-88	94	7.2	176	20	0.9	269	18	1.8	na	0.09	0.18	0.29
G8	7-10-88	99	7.5	292	19	<0.16	485	35	3.6	1.2	0.14	0.34	0.58
G11	7-12-88	86	7.1	114	32	1.2	220	10	1.4	na	0.26	0.12	0.20
H2	7-22-88	98	7.9	142	28	0.5	311	15	2.1	na	0.27	0.13	0.24
H4	7-20-88	101	7.8	180	36	<0.16	411	20	2.9	1.8	0.31	0.19	0.33
H6	7-16-88	103	7.9	187	33	<0.16	407	19	2.9	1.4	0.29	0.20	0.33
H7	7-16-88	102	8.4	134	29	2.5	230	17	1.3	na	0.22	0.15	0.23
J1	7-24-88	80	8.2	264	20	<0.16	464	33	3.2	na	0.15	0.33	0.57
J5	7-24-88	90	8.3	254	22	<0.16	465	34	3.1	na	0.13	0.34	0.50
K3	7-26-88	80	7.2	134	29	2.5	230	17	1.3	na	0.22	0.14	0.29
L1	7-09-88	60	6.5	119	32	1.9	223	16	1.2	na	0.33	0.14	0.28
L3	7-08-88	86	6.6	159	41	0.8	330	23	1.8	1.8	0.54	0.20	0.35
Q	7-25-88	78	8.2	140	32	2.0	259	12	1.6	na	0.13	0.13	0.29
DGGS 1980													
G6	7-26-80	97	7.5	178	22	1.2	248	17	1.8	na	0.07	na	na
G8	7-26-80	100	8.0	270	19	0.2	487	30	3.9	na	0.10	na	na
H1	7-25-80	100	7.3	170	33	0.3	355	16	2.8	na	0.23	na	na
H6	7-25-80	99	7.3	190	36	0.1	442	19	3.4	na	0.21	na	na
J1	7-26-80	82	7.6	272	19	0.0	447	31	3.5	na	0.08	na	na
K1	7-25-80	62	7.8	148	25	2.8	179	13	1.2	1.0	0.13	na	na
L1	7-25-80	85	6.9	160	39	1.4	280	20	1.8	1.0	0.24	na	na
Barnes, 1975													
Gx	6-14-75	85	8.2	250	14	0.2	420	26	2.4	na	na	na	na
G8	6-14-75	102	8.3	255	20	0.1	480	32	3.2	na	na	na	na
J1	6-14-75	93	7.9	245	22	0.1	460	31	2.7	na	na	na	na
J4	6-14-75	65	7.7	224	22	0.1	460	33	2.6	na	na	na	na
Byers and Brannock, 1946													
G1	8-17-46	100	7.5	303	15	0.1	441	33	3.0	na	na	na	na
H1	8-17-46	101	6.9	150	40	0.2	350	18	2.0	na	na	na	na

T, pH, HCO_3, H_2S, NH_4 = DGGS field measurements. Al and Ba analyzed at DGGS, Fairbanks. Rb and Cs analyzed at U.S. Geological Survey, Menlo Park. All other constituents analyzed at University of Utah Research Institute, Salt Lake City.

na = not analyzed.

Table 9. *Geochemical analyses of Geyser Bight Hot Spring water samples collected in 1988. Previous analyses shown for comparison. Chemical concentrations in ppm and temperatures in degrees Celsius-Continued*

Site	Al	Fe	As	Ba	B	HCO_3	SO_4	Cl	F	Br	I	H_2S	TDS	Balance %
DGGS and UURI 1988														
G1	na	<0.02	6.6	0.005	53	66	180	623	2.0	1.0	1.0	na	1764	2.7
G6	na	0.07	3.3	0.007	30	41	110	362	0.9	1.5	0.8	na	1015	1.8
G8	0.047	<0.02	6.4	0.004	56	62	174	657	2.1	2.4	1.1	0.4	1766	0.6
G11	na	0.05	2.6	0.012	24	75	93	288	0.9	1.0	0.6	na	826	2.3
H2	na	<0.02	4.7	0.009	40	35	124	412	1.0	1.3	0.9	na	1100	4.3
H4	na	<0.02	6.6	0.009	53	51	162	560	1.5	2.0	1.0	0.7	1464	2.5
H6	0.103	<0.02	6.5	0.008	51	52	149	556	1.4	1.9	1.2	0.6	1444	2.5
H7	na	<0.02	5.1	0.008	40	52	90	294	0.9	1.0	0.5	na	872	3.0
J1	na	<0.02	6.1	0.003	49	52	189	589	2.1	2.6	1.0	na	1650	4.4
J5	na	<0.02	6.5	0.003	52	39	206	598	2.0	1.9	0.9	na	1665	3.2
K3	na	<0.02	3.2	0.039	25	105	90	294	0.9	1.0	0.5	na	882	3.0
L1	na	0.30	3.2	0.032	26	90	79	295	1.1	0.9	0.6	na	846	4.7
L3	0.050	0.40	4.7	0.035	40	125	118	426	1.5	1.5	0.7	1.2	1214	4.3
Q	na	<0.02	3.3	0.019	29	72	118	343	1.2	1.2	0.6	na	979	1.1
DGGS 1980														
G6	na	0.05	na	na	15	na	96	339	0.9	1.1	0.7	na	922	-
G8	na	0.05	na	na	60	72	170	630	2.3	2.2	1.1	na	1712	3.7
H1	na	0.03	na	na	51	na	131	492	1.3	1.7	1.1	0.3	1256	-
H6	na	0.04	na	na	58	na	154	591	1.6	1.9	1.2	na	1499	-
J1	na	0.05	na	na	50	55	168	591	2.4	2.1	1.0	na	1615	2.2
K1	na	0.07	na	na	18	133	63	225	0.9	1.2	0.5	na	747	-0.7
L1	na	0.08	na	na	30	130	90	370	1.6	1.1	0.7	0.5	1062	3.7
Barnes, 1975														
G?	0.025	na	na	na	44	61	150	540	2.1	na	na	na	1478	2.7
G8?	na	na	na	na	36	52	170	640	1.2	na	na	na	1663	2.8
J1	0.018	na	na	na	49	46	180	610	2.2	na	na	na	1625	2.0
J4	0.012	na	na	na	48	44	180	610	2.2	na	na	na	1603	2.4
Byers and Brannock, 1946														
G1	<0.5	<0.1	0.1	na	28	66	160	569	1.9	na	na	na	1586	3.1
H1	<0.5	<0.1	3.8	na	27	49	130	482	1.2	na	na	na	1228	4.6

Table 10. *Geochemical analysis of stream waters in the Geyser Creek drainage. All analyses in ppm unless otherwise noted*

Site	SiO_2	Ca	Mg	Na	K	Li	Sr	B	HCO_3	SO_4	Cl	F
1981												
abv H	23	2.3	0.9	5.2	1.3	<0.01	0.01	<0.1	na	0.4	6.2	0.1
blo G	20	2.9	0.9	15	1.2	0.07	0.01	1.3	na	5.3	18	0.1
1988												
trib KL	18	1.8	0.8	5.4	0.8	0.01	0.02	0.1	11	2.4	6.3	0.05
blo KL	17	5.7	0.9	14	1.2	0.08	0.01	2.9	na	11	20	0.1
blo G	23	3.9	1.0	25	2.0	0.16	0.01	5.3	13	11	33	0.1
blo H	32	4.6	1.0	32	3.4	0.24	0.02	7.1	16	13	44	0.1
abv H	25	2.4	1.0	7.3	1.5	0.02	0.01	0.3	na	7.0	24	0.1
blo J	14	2.1	0.8	7.6	0.8	0.03	0.01	0.5	na	4.4	13	0.1
abv Q	12	1.8	0.8	5.1	0.7	0.01	0.01	0.2	na	2.4	7.6	0.04

Distinct compositional mixing trends toward local cold stream waters are evident in plots of Ca, Mg, and Na and HCO_3, SO_4, and Cl (figs. 27a, b). The inverse correlation observed between Mg and Cl (fig. 25e) is also indicative of dilution of thermal waters. Because Mg is usually removed from high-temperature thermal waters through hydrothermal reactions, the presence of Mg in thermal waters is commonly a sign of cold-water mixing.

The constituent-chloride plots for Ca and HCO_3 are more scattered, although they too appear inversely correlated with Cl (figs. 25d, f). Spring waters at or above the boiling point have significantly less HCO_3 than lower temperature springs, probably due to the partitioning of dissolved CO_2 into the steam phase. The higher pH exhibited by the boiling springs is probably also due to the loss of CO_2 and other acid gases to the volatile phase that separates from the boiling water. Acid-sulphate springs that emanate near Spring G8 corroborate to this conclusion. Ca and HCO_3 in the boiling spring waters could also have been removed by precipitation of calcite because these waters are all near saturation with respect to calcite.

The Rb/Cl and Cs/Cl ratios for sites H and Q are lower than those for down-valley sites (figs. 25h, i) but the Rb/Cs ratios are similar (table 11), ranging from 0.45 to 0.68. Cs can be removed from thermal waters at temperatures less than about 200°C by analcime and other zeolites (Goguel, 1983; Keith and others, 1983). Thus, the difference in Cs/Cl ratios suggests that the site H thermal-spring waters are derived from a lower temperature environment than site G, J, K, and L waters..

Cs concentrations and Cs/Cl ratios for Geyser Bight thermal waters are similar to those found for thermal waters from Upper and Lower Geyser Basins at Yellowstone National Park (Keith and others, 1983). Keith and others (1983) suggested that the Cs/Cl ratio may be useful in determining the host rock of the hydrothermal system. The Cs/Cl ratios for the Geyser Bight thermal waters are similar to data Keith and others (1983) selected as representing equilibration within rhyolitic rock. Rhyolite is rare in the Aleutians. Based on Geyser Creek valley geology (sheet 1), rhyolitic reservoir rocks are not expected at Geyser Bight. The presence of a linear zone of 135 ka rhyolite domes about 4 km southwest of site H and 1.5 km southwest of fumarole F3, however, indicates that conditions appropriate for rhyolite generation existed in the recent past. Such conditions could exist today, although there is no evidence of a rhyolitic component in the youngest lavas erupted from Mt. Recheshnoi (see p. 28).

ARSENIC AND BORON

As and B in Geyser Bight thermal waters deserve specific attention because concentrations of these constituents and particularly their ratios to Cl appear anomalously high when compared to other geothermal areas. Concentrations of both constituents increase linearly with Cl at Geyser Bight (figs. 25g, j).

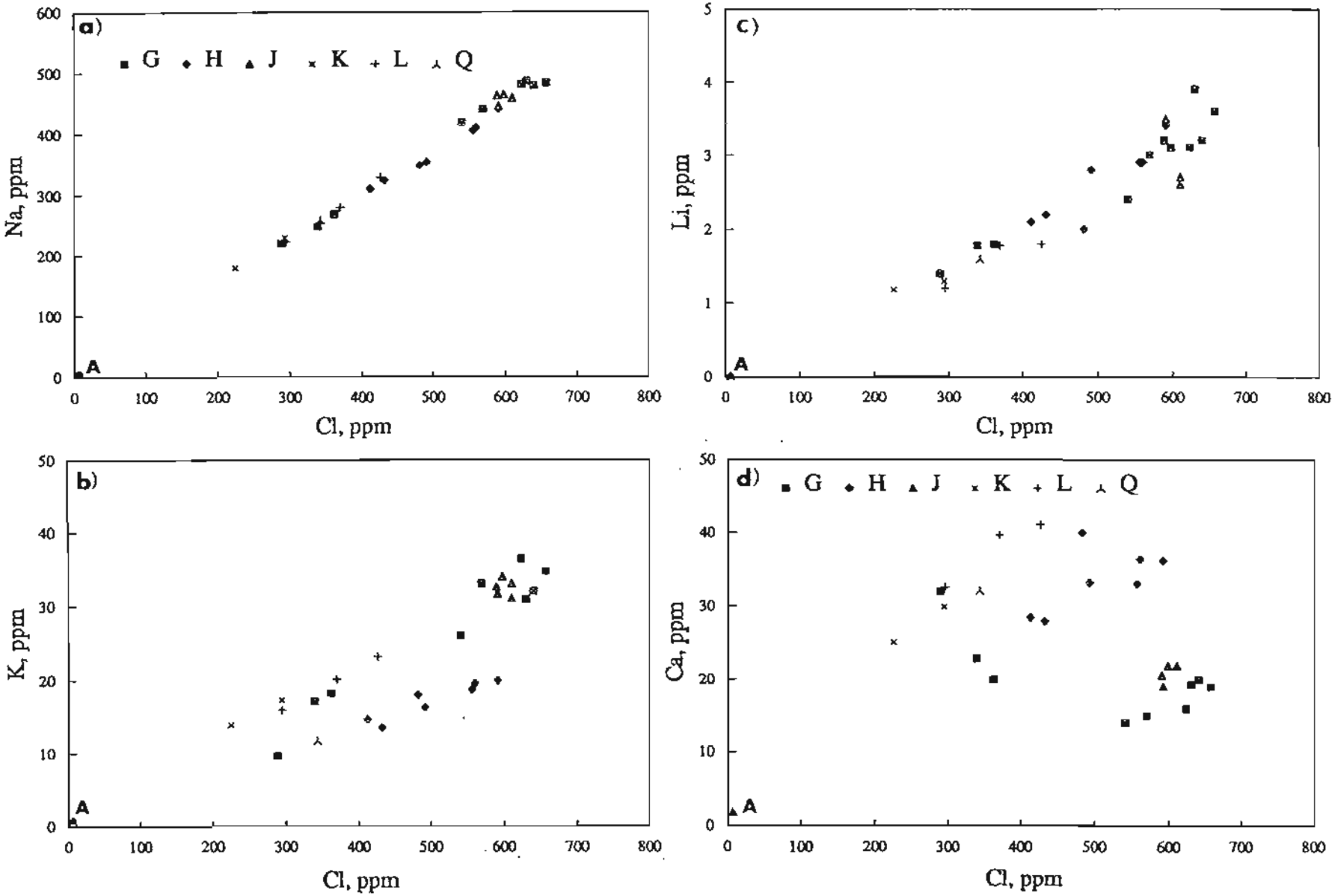

Figure 25a, b, c, d. *Constituent concentrations vs. chloride: (a) sodium, (b) potassium, (c) lithium, and (d) calcium.*

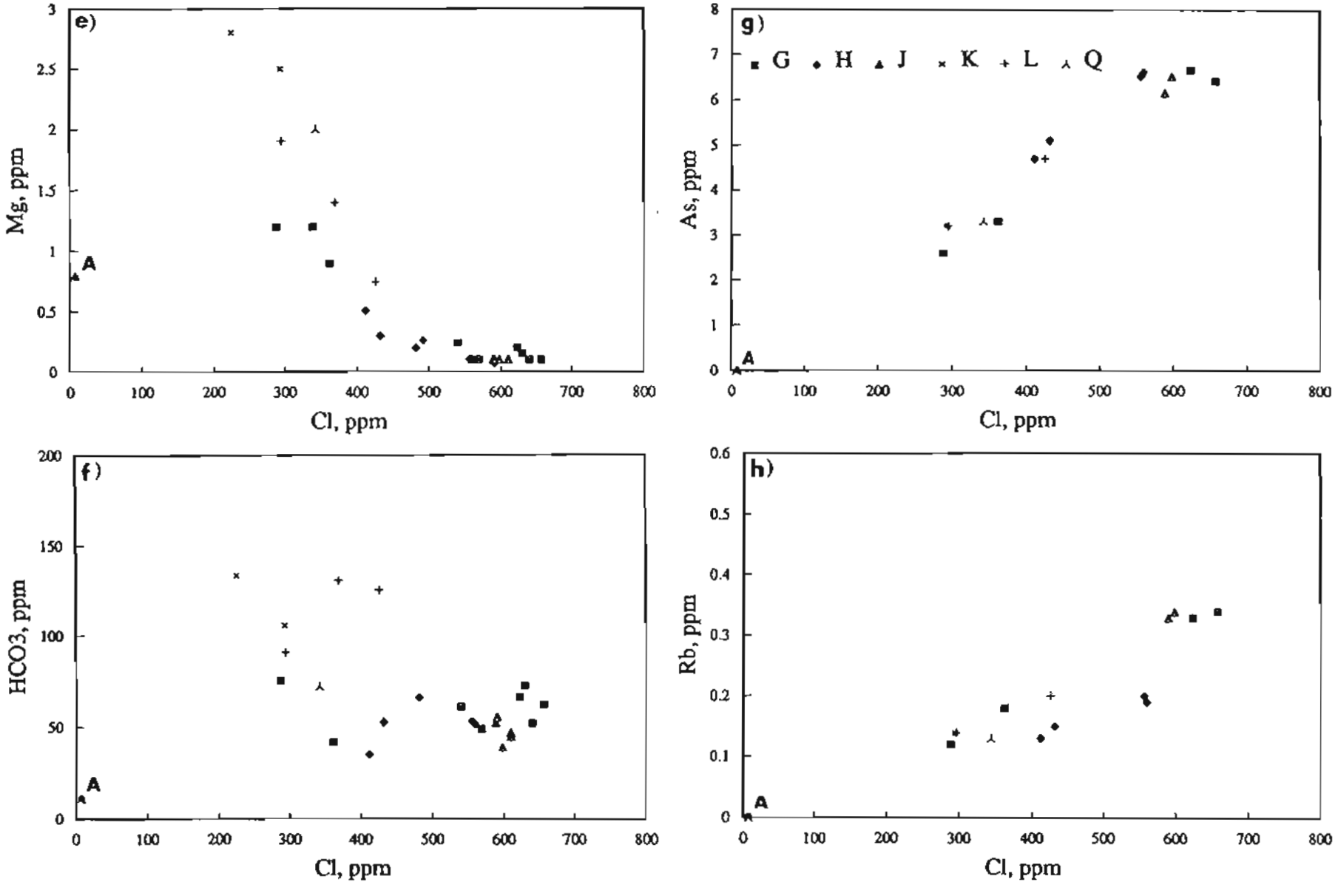

Figure 25e, f, g, h. *Constituent concentrations vs. chloride: (e) magnesium, (f) bicarbonate, (g) arsenic, and (h) rubidium.*

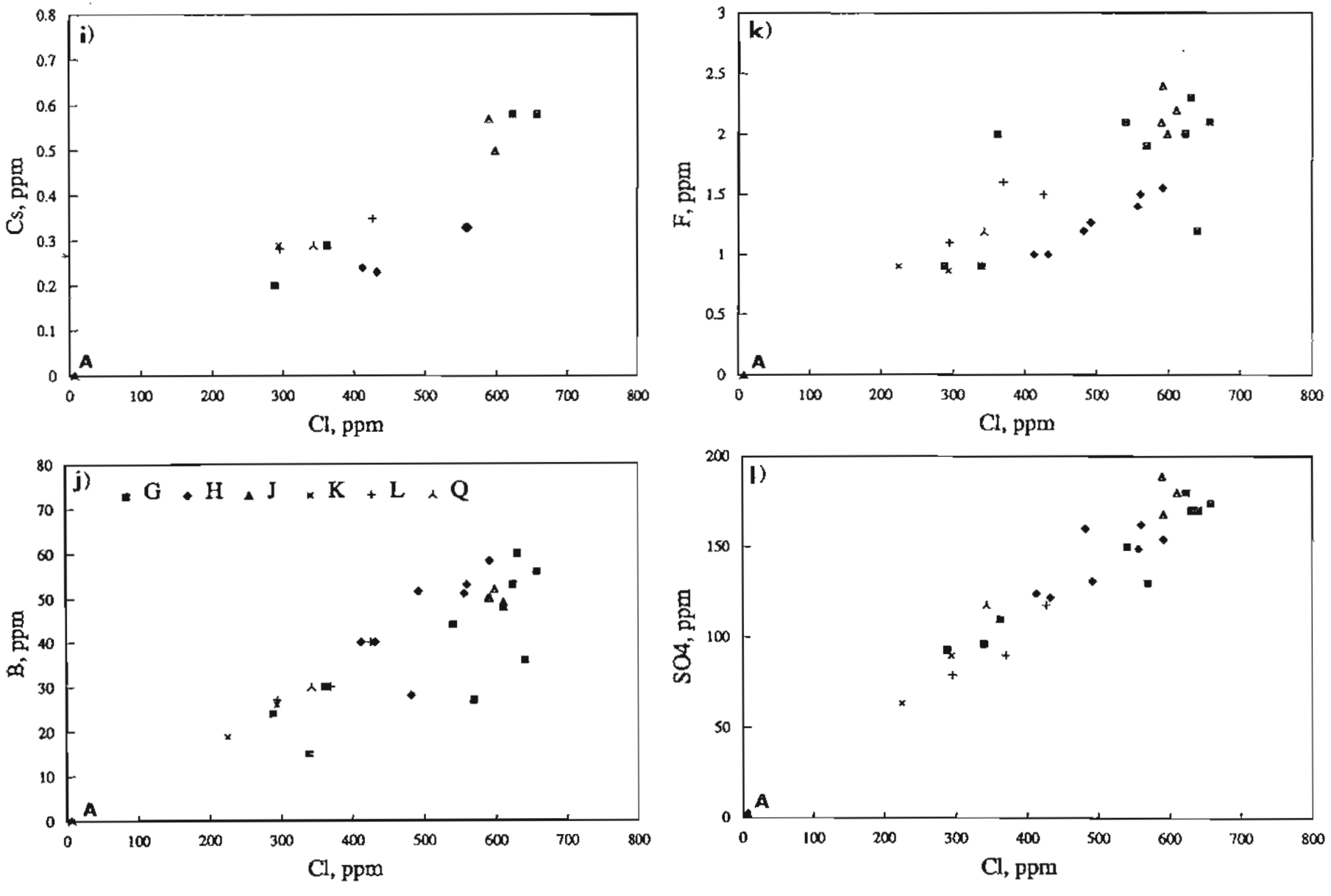

Figure 25i, j, k, l. *Constituent concentrations vs. chloride: (i) cesium, (j) boron, (k) fluorine, and (l) sulfate.*

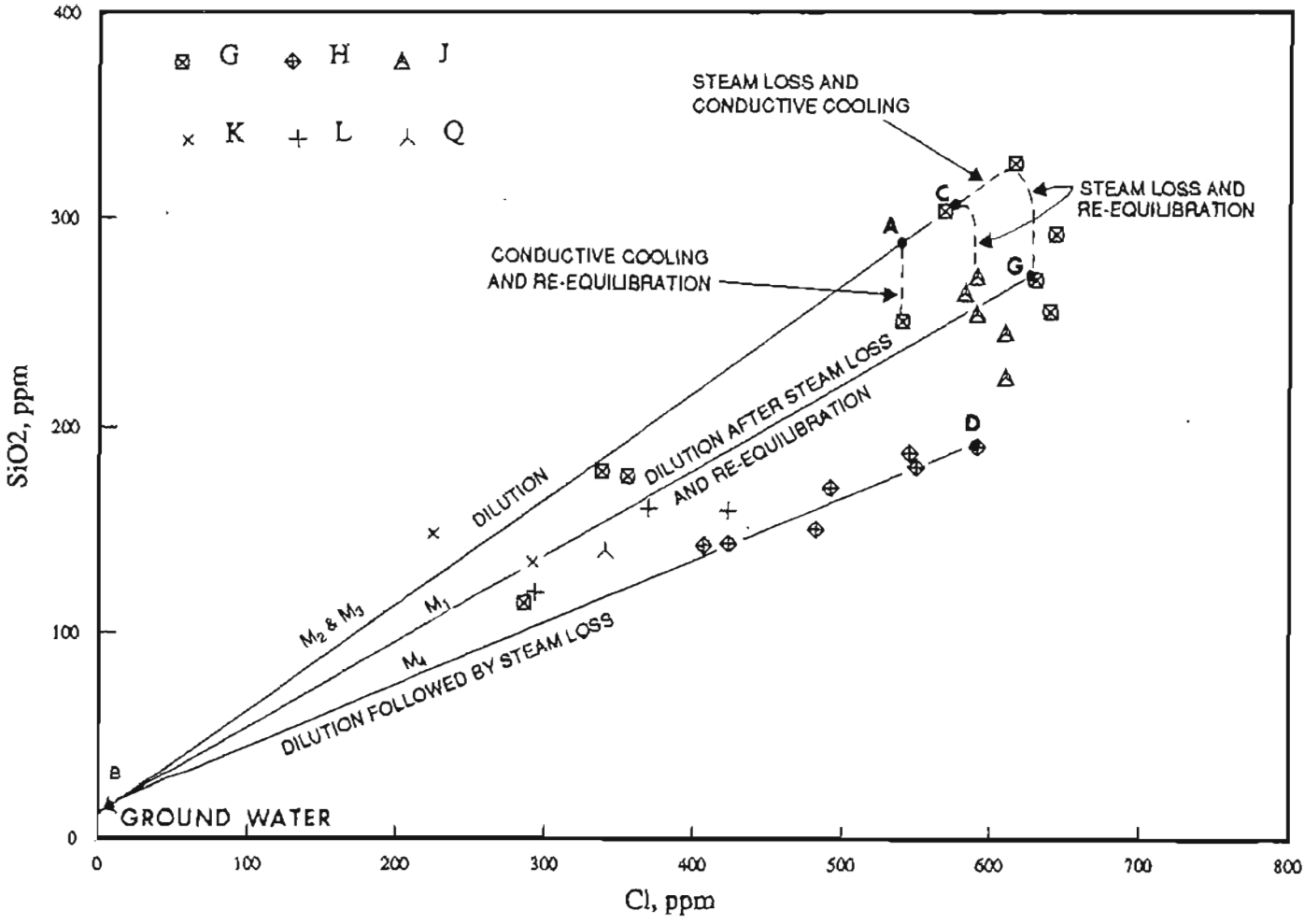

Figure 26. *Silica vs. chloride for thermal-spring waters. The dilution, conduction, steam-loss, and re-equilibration paths are discussed in the text under choloride-enthalpy analysis (p. 76).*

Although concentration of As in the Geyser Bight thermal-spring waters (6.6 ppm) is similar to that found in geothermal well waters at the Makushin geothermal area on neighboring Unalaska Island (10 ppm) (Motyka and others, 1988), the As/Cl ratio at Geyser Bight is three times greater than at Makushin. Few of the volcanically hosted hydrothermal systems for which data are available have As concentrations as high as at Geyser Bight or Makushin (compare Stauffer and Thompson, 1984). With one exception, the As/Cl ratio for the Geyser Bight waters (0.01) is greater than that reported for other geothermal systems. For example, the As/Cl ratio for Yellowstone thermal waters ranges from 0.003 to 0.005 (Stauffer and Thompson, 1984), while thermal springs at Lassen have As/Cl ratios of 0.005, except one spring that has a As/Cl ratio of 0.01 (Thompson and others, 1985). A principal source of As in geothermal waters appears to be leaching of reservoir rocks. Arsenic occurs in minor to trace amounts in most rocks and averages about 0.5 ppm in the Geyser Bight pluton. Stauffer and Thompson (1984) concluded that at least 30 to 50 per cent of the As in the Yellowstone hot spring waters was derived by rock leaching. However, rock-water interaction appears insufficient to entirely explain elevated As concentrations found at Yellowstone, Lassen, and some other volcanically hosted hydrothermal systems (Stauffer and Thompson, 1984; Thompson and others, 1985). Although a magmatic source for As in geothermal systems remains unproven, it seems a likely candidate for explaining elevated As concentrations in these cases and perhaps for Geyser Bight.

Boron concentrations at Geyser Bight are also similar to the Makushin geothermal area (60 ppm). However, the B/Cl ratio is substantially higher, over an order of magnitude greater at Geyser Bight than at Makushin (0.8 vs. 0.02). Although B concentrations in geothermal waters are quite variable, ranging up to 1,000 ppm for the Ngawha system in New Zealand, the B concentrations and B/Cl ratios observed at Geyser Bight are similar to

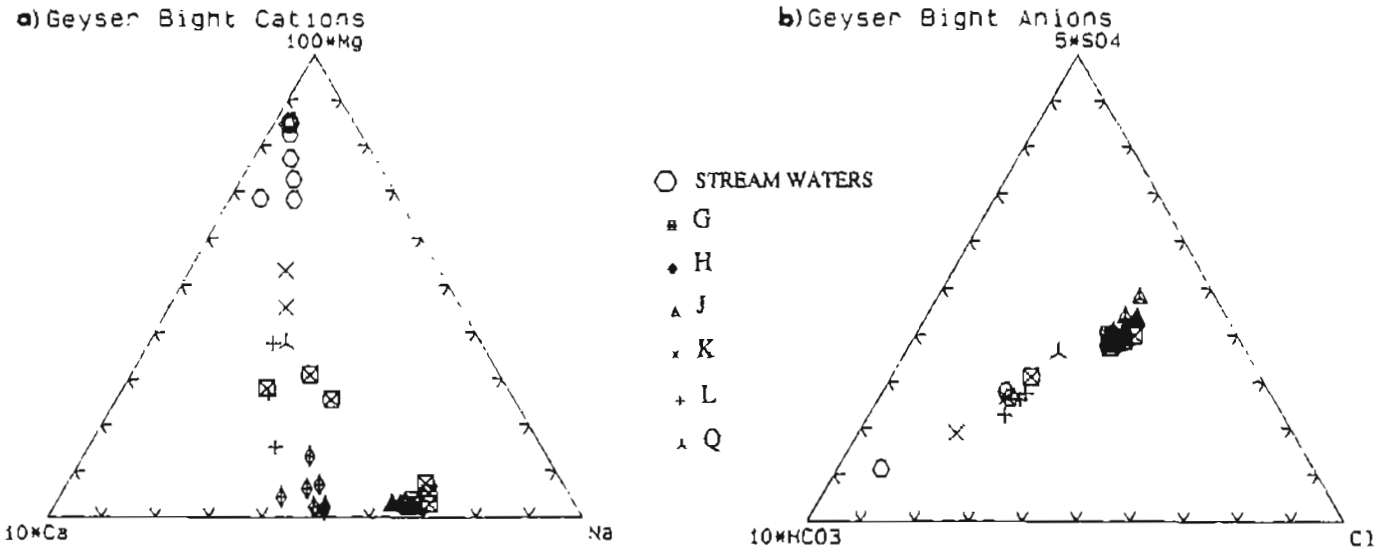

Figure 27a, b. *Cation (a) and anion (b) trilateral diagrams of Geyser Bight thermal springs and stream waters illustrating mixing trends between meteoric and thermal waters.*

or higher than those found at most other geothermal systems. Elevated concentrations of B in some systems have been attributed to leaching of sedimentary formations (Stauffer and Thompson, 1984; Thompson, 1985). Although Byers (1959) reported albitized shales and sandstones in the vicinity of Geyser Bight, detailed geologic mapping did not uncover any unequivocally sedimentary units in the Geyser Bight area. Boron concentration in the Geyser Bight pluton, the presumed reservoir rock, is only 7.5 ppm. In comparison, shales have an average concentration of 100 ppm (Krauskopf, 1979). Shales and sandstones exposed elsewhere on Umnak Island may still underlie the area, but are not exposed. If so, hydrothermal fluids that circulate through such rocks could have dissolved B and account for the elevated concentrations found in the thermal-spring waters. Alternatively, the excess B may have been derived directly from a degassing magmatic heat source. B has been shown to be selectively adsorbed on clay particles during circulation through both near-shore and deep-sea pelagic sediments (Palmer and others, 1985). Boron, along with other volatile elements, would have been expelled from any subducted pelagic sediments and incorporated into magma rising from the region above the subducted slab into the shallow crustal regions.

STABLE ISOTOPES

Results of stable isotope analyses of Geyser Bight meteoric and thermal waters are given in table 12 and plotted in figures 28a and b. Two meteoric water lines are included: the first is the meteoric water line of Craig (1961), which is based on analyses of worldwide precipitation; the second is the Aleutian-Adak meteoric water line (A-AMWL) (Motyka and others, in prep.). The latter was derived from a combination of stable isotope values for 57 Adak weather station precipitation samples [data obtained from the International Atomic Energy Agency, Vienna (IAEAV)] and for 52 stream and precipitation samples obtained from various Aleutian Islands. Craig's meteoric water line is slightly steeper in slope than the A-AMWL, and the two lines intersect at $\delta D = -73$ per mil and $\delta^{18}O = -10.3$ per mil.

The Umnak Island meteoric water samples (which were included in deriving the A-AMWL) fall into two distinct groups; the 1980-81 samples plot to the left of the meteoric water lines while the 1988 samples plot to the right (fig. 28a). These differences cannot be attributed to systematic error in analyses because results for control samples were well within the analytical error limit of previously reported results. In addition, $\delta^{18}O$ results for the most chemically concentrated of the 1988 thermal spring samples are similar to previously reported results for the same springs. The Aleutian Islands are subject to weather fronts that originate from both the North Pacific Ocean and the Bering Sea. The differences in stable isotope values for these stream waters may be due to differences in prevailing meteorological conditions prior to and during the respective sampling periods.

Table 11. *Ratios of major and minor constituents to Cl and Rb/Cs ratios*

Site	SiO_2	Ca/0.1	Na	K/0.1	Li/0.01	Rb/0.001	Cs/0.001	As/0.01	B/0.1	HCO_3	SO_4	F/0.01	Br/0.01	I/0.01	Rb/Cs
DGGS and UURI 1988															
G1	0.52	0.26	0.77	0.58	0.50	0.53	0.93	1.07	0.85	0.11	0.29	0.32	0.16	0.16	0.57
G6	0.49	0.55	0.74	0.50	0.50	0.50	0.80	0.91	0.83	0.12	0.30	0.23	0.41	0.22	0.62
G8	0.44	0.29	0.74	0.53	0.55	0.52	0.88	0.97	0.85	0.09	0.26	0.32	0.37	0.17	0.59
G11	0.40	1.11	0.76	0.34	0.49	0.42	0.69	0.90	0.83	0.26	0.32	0.31	0.35	0.21	0.60
H2	0.34	0.69	0.75	0.36	0.51	0.32	0.58	1.14	0.97	6.00	0.30	0.24	0.32	0.22	0.54
H4	0.32	0.65	0.73	0.35	0.52	0.34	0.59	1.18	0.95	0.09	0.29	0.27	0.36	0.18	0.58
H6	0.34	0.59	0.73	0.34	0.52	0.36	0.59	1.17	0.92	0.10	0.27	0.25	0.34	0.22	0.61
H7	0.46	1.02	0.78	0.59	0.44	0.51	0.78	1.73	1.36	0.18	0.31	0.29	0.34	0.17	0.65
J1	0.45	0.35	0.79	0.55	0.54	0.56	0.97	1.04	0.84	0.09	0.32	0.36	0.44	0.17	0.58
J5	0.42	0.37	0.78	0.57	0.52	0.57	0.84	1.09	0.87	0.07	0.34	0.33	0.32	0.15	0.68
K3	0.46	1.02	0.78	0.59	0.44	0.48	0.99	1.09	0.87	0.36	0.31	0.29	0.34	0.17	0.48
L1	0.40	1.11	0.76	0.54	0.41	0.47	0.95	1.08	0.91	0.31	0.27	0.37	0.31	0.20	0.50
L3	0.37	0.97	0.77	0.54	0.42	0.47	0.82	1.10	0.94	0.29	0.28	0.35	0.35	0.16	0.57
Q	0.41	0.94	0.76	0.34	0.47	0.38	0.85	0.96	0.87	0.21	0.34	0.35	0.35	0.17	0.45
DGGS 1980															
G6	0.53	0.68	0.73	0.50	0.53	-	-	-	0.44	0.00	0.28	0.27	0.32	0.21	-
G8	0.43	0.31	0.77	0.49	0.62	-	-	-	0.95	0.12	0.27	0.37	0.35	0.17	-
H1	0.35	0.67	0.72	0.33	0.57	-	-	-	1.05	0.00	0.27	0.26	0.34	0.22	-
H6	0.32	0.61	0.75	0.34	0.58	-	-	-	0.99	0.00	0.26	0.26	0.32	0.20	-
J1	0.46	0.32	0.76	0.54	0.59	-	-	-	0.85	0.09	0.28	0.41	0.36	0.17	-
K1	0.66	1.12	0.80	0.62	0.52	-	-	-	0.84	0.59	0.28	0.40	0.54	0.22	-
L1	0.43	1.07	0.76	0.54	0.48	-	-	-	0.81	0.35	0.24	0.43	0.29	0.19	-
Barnes, 1975															
Gx	0.46	0.26	0.78	0.48	0.44	-	-	-	0.81	0.11	0.28	0.39	-	-	-
G8	0.40	0.31	0.75	0.50	0.50	-	-	-	0.56	0.08	0.27	0.19	-	-	-
J1	0.40	0.36	0.75	0.51	0.44	-	-	-	0.80	0.08	0.30	0.36	-	-	-
J4	0.37	0.36	0.75	0.54	0.43	-	-	-	0.79	0.07	0.30	0.36	-	-	-
Byers and Brannock, 1946															
G1	0.53	0.26	0.78	0.58	0.53	-	-	0.01	0.49	0.12	0.28	0.33	-	-	-
H1	0.31	0.83	0.73	0.37	0.41	-	-	0.79	0.56	0.10	0.27	0.25	-	-	-

Table 12. *Stable isotope compositions of Umnak Island thermal springs, streams, and meteoric waters, per mil*

Thermal spring waters			Streams and meteoric waters		
Site	$\delta^{18}O$	δD	Site	$\delta^{18}O$	δD
1988			**1988**		
G1	-7.7	-67	H+	-9.6	-71
G6	-8.3	-66	H-	-9.4	-74
G8	-8.5	-68	G-	-9.6	-71
G8A	-1.3	-56	J-	-10.0	-77
G11	-8.8	-69	Q+	-9.9	-74
H2	-8.9	-71	KL-	-10.0	-74
H4	-8.7	-71	Kl-side	-9.6	-70
H6	-8.7	-72	RB-H	-11.4	-86
H7	-9.4	-71	RB-M	-10.3	-78
J1	-7.6	-67	RB-L	-9.7	-70
J5	-7.9	-68	CS-H6	-9.9	-71
K3	-9.3	-71	**1981**		
L1	-8.9	-72	above H	-10.6	-72
L3	-9.4	-72	**1980**		
Q	-9.0	-72	rain	-5.5	-36
1980			snow	-10.6	-71
G6	-9.0	-66	Creek mouth	-11.0	-73
G8	-8.4	-67	H1 stream	-10.3	-69
H1	-8.2	-70	J1 cold spr	-10.8	-71
H6	na	-67	HSC, near E	-9.7	-68
J1	-7.9	-63	Partov	-8.9	-59
K1	-9.3	-70			
L1	-9.3	-68			
1975					
Gx	-8.2	-68			
G8	-8.1	na			
J1	-8.0	-67			
J4	-7.1	-67			

Stream waters generally follow the well-known altitude effect associated with precipitation (see, for example, Gat, 1980), with streams at higher elevations correlating with lighter isotopic values. Examples of this effect are samples RB-H, RB-M, and RB-L, which were collected on the same day at elevations of 650 ft, 500 ft, and 150 ft, respectively (table 12).

The isotope values for all Geyser Bight thermal-spring waters plot to the right of the meteoric water lines, and the different spring groups have distinct isotopic signatures (fig. 28). Deuterium values for sites H, K, L, and Q are similar to or slightly heavier than the calculated average for local stream waters, while δD for G and J springs are all slightly heavier than the average stream water. In contrast to δD, $\delta^{18}O$ values for all thermal springs are positively shifted with respect to local stream waters, with the degree of shift correlating with Cl concentration. The greatest shift occurs for sites G and J, which are 2 to 2.5 per mil heavier than the calculated average for local stream waters.

Near-boiling, low Cl acid springs occur at site G and have much heavier isotopic values then the surrounding high-chloride springs (table 12). These acid springs, which exhibit little flow, are probably surface and shallow ground waters that are heated by condensing steam and acid gases derived from the waters feeding the nearby high-Cl, near-neutral thermal springs. Their isotopic values are probably a result of continuous evaporative

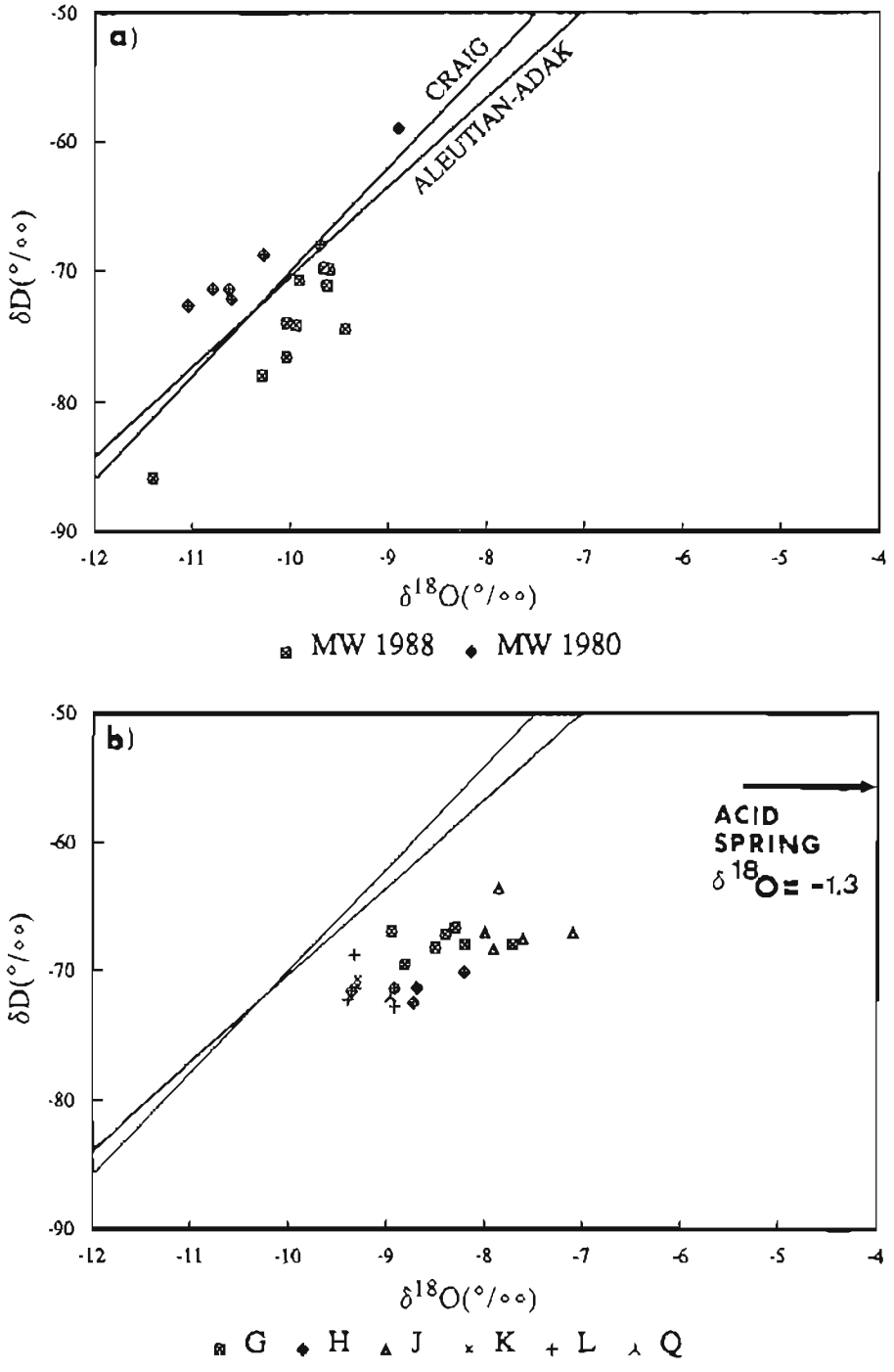

Figure 28a, b. *Stable isotope results for (a) meteoric waters, and (b) Geyser Bight thermal waters. The Aleutian-Adak and Craig (1961) meteoric water lines are shown for comparison.*

fractionation of the lighter isotopes into the vapor phase. The comparatively heavier δD values for Spring G6 suggest that these thermal waters may have a small component derived from such an acid spring or that they have mixed with a heavier meteoric water. The 1980 δD value for J1 is also anomalously high compared to the other springs in the G and J groups. J1 is a large, open, hot pool, with a low rate of flow, that may be subject to evaporative concentration of heavier isotopes.

Truesdell and others (1977) showed how the original isotopic composition of boiling thermal spring waters can be calculated after allowing for fractionation processes that affect the compositions. However, a deep water composition (as determined from a well fluid) is required as a starting point for the treatment of the data, and no such analysis is available for Geyser Bight. By using isotope values for site G waters as an end point, a range of starting point values can nevertheless be estimated. Changes in δD and $\delta^{18}O$ in the residual liquid as a water boils are a function of beginning and ending temperature and the degree to which the steam remains in contact with the liquid. Using data from Truesdell and others (1977), figure 29a illustrates the change in composition a thermal water would undergo as it ascends from a reservoir to emerge boiling at the surface with a δD value and Cl concentration similar to site G thermal-spring waters. The paths correspond to two extreme cases: (a) SS, single-stage steam separation, and (b) C, continuous steam separation. The beginning point temperatures used in the analysis correspond to geothermometer estimates of reservoir temperatures discussed later. The estimated range of δD reservoir values lies within the range of values for local stream waters. Similar correlations between deuterium of geothermal waters and local meteoric waters have led many investigators to conclude that geothermal systems are mainly recharged by local precipitation (see Truesdell and Hulston, 1980, for review) and such is probably the case for the Geyser Bight geothermal area. A similar analysis for site H resulted in slightly lighter δD reservoir values compared to G, which suggests that the zone of recharge for the reservoir feeding the H system lies at a higher elevation than that for the G/J reservoir.

Applying similar techniques to $\delta^{18}O$ vs. Cl gives "reservoir" values of $\delta^{18}O$ that are 0.6 to 1.0 per mil lighter than spring G8 and H4. The isotope boiling paths roughly parallel the meteoric water lines so that the apparent ^{18}O shift with respect to these lines remains at 2 to 2.5 per mil. Similar shifts in the ^{18}O content of geothermal waters to more positive values with respect to local meteoric waters have been observed in most high-temperature geothermal systems. These positive shifts have been attributed to ^{18}O exchange between the deeply circulating meteoric waters and reservoir wallrocks with the degree of shift depending on temperature and rock/water ratio (Truesdell and Hulston, 1980). Comparable shifts in δD do not take place because reservoir rocks contain little deuterium.

Nearly all H springs and many G springs are vigorously boiling at the surface. In addition, these and the other springs may also have been diluted. Using techniques described by Truesdell and others (1977), the effects of mixing and boiling can be analyzed. Figure 29b illustrates the case for site H spring waters. Here, M_1 is a mixing line between a hypothetical meteoric water with a temperature of 10°C, Cl concentration of 10 ppm, and δD value of -70 per mil and an ascending thermal water with T = 165°C, Cl = 490 ppm, and δD = -74 per mil. SS and C show compositions of waters that ascend to the surface without mixing and emerge as boiling spring waters for the cases of single-stage and continuous steam separation, respectively. SS^m and C^m show the surface compositions of the residual liquid phase of waters that mix at depth along M^1 and then ascend to the surface for the cases of single-stage and continuous steam separation, respectively. This model adequately accounts for the δD and Cl compositions of spring Q and H springs sampled in 1988. Both 1980 H samples are heavier in δD than the 1988 samples, which suggests that the diluting water may have had a different composition in 1980.

A similar analysis performed for G, J, K and L spring waters is illustrated in figure 29c. The value chosen for the reservoir water (δD = -72 per mil, Cl = 520 ppm) lies between the single-stage and continuous steam separation values determined for the case of a 200°C reservoir (fig. 29a). M_1 is a mixing line between this deep thermal water and a hypothetical cold water (δD = -71 per mil, Cl = 10 ppm). M_2 illustrates a mixing line between the cold water and shallow thermal waters whose composition is similar to site G boiling spring waters.

This model suggests that the compositions of site G boiling spring waters are adequately explained as the result of a steam separation process intermediate between single-stage and continuous without mixing with cold waters. Other springs in the area are below boiling. The isotopic values for some of these spring waters appear to be the result of mixing fractionated thermal waters, similar to site G boiling water, with meteoric waters along M_2 rather than by mixing meteoric waters with the deep thermal water along M_1, followed by boiling to the surface (SS_m and C_m). Data points for other down-valley, lower-temperature, and comparatively more dilute springs cannot be explained by this model and appear to have formed by mixing with a greater variety of meteoric waters.

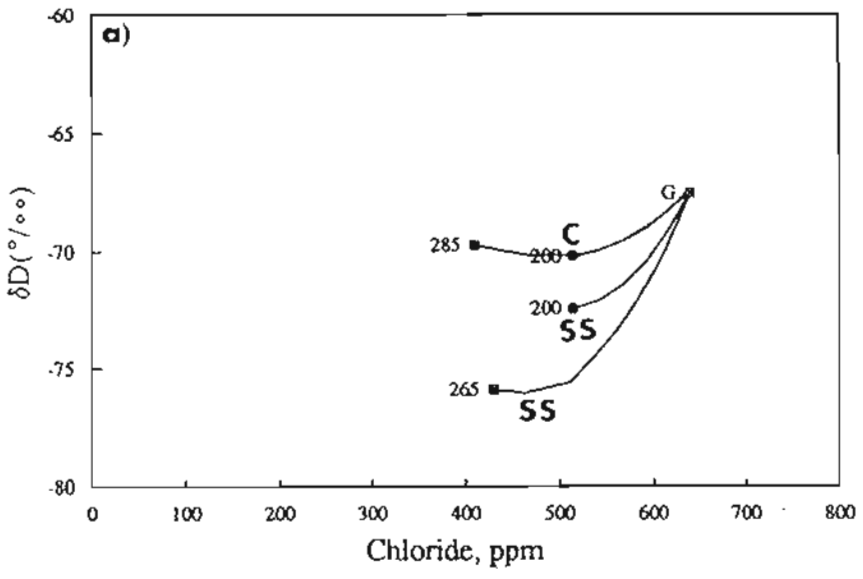

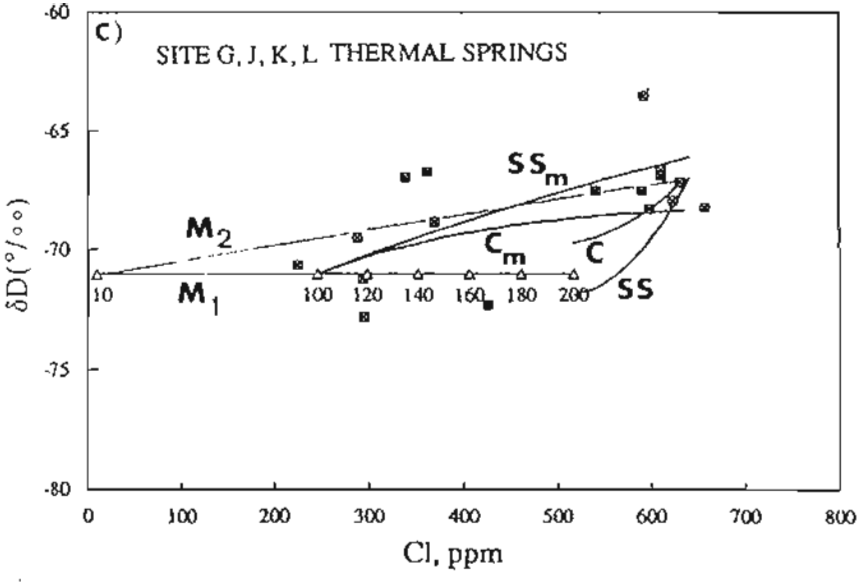

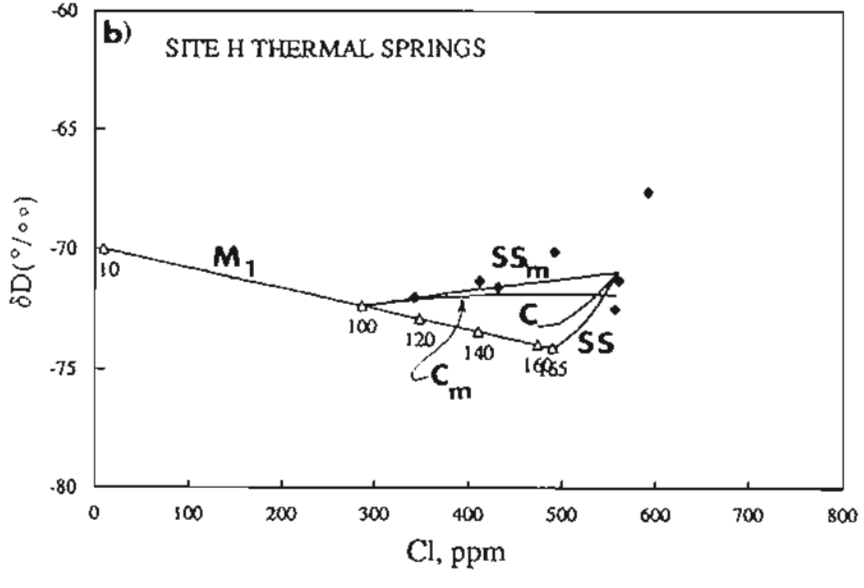

Figure 29a, b, c. *Possible compositional changes in thermal waters that ascend from reservoirs: (a) at 285°, 265°, and 200°C and emerge boiling at the surface at spring G; (b) at 165°C and mix with 10°C meteoric water to produce site H spring waters; and (c) at 200°C and mix with 10°C meteoric water to produce spring waters at sites G, J, K, and L. Triangles mark end-point and mixed water compositions at various temperatures. SS and C indicate paths for single-stage and continuous steam separation, respectively. Lines SS_m and C_m show surface compositions of a mixed water following single-stage and continuous steam separation, respectively.* *See page 65 for further discussion.*

TRITIUM

Results of tritium analyses of two Geyser Bight thermal-spring waters and two streams are given in table 13. Reviews of tritium in atmospheric waters and in groundwaters are found in Gat (1980) and Fontes (1980), respectively. Tritium occurs in atmospheric waters as a result of both natural and manmade processes. It is produced naturally by the interaction of cosmic radiation with the upper atmosphere. Enormous amounts of manmade tritium were released into the atmosphere during the period of thermonuclear testing from 1952 to 1962. Although pre-1952 data are sparse, natural tritium levels in precipitation appear to range from about 4 to 25 tritium units (TU), depending on location (Gat, 1980), with an average of about 10 TU in temperate zone, continental meteoric waters (Panichi and Gonfiantini, 1978). Average tritium concentrations in precipitation fluctuated widely following thermonuclear tests, reaching peak levels of over 2,200 TU in the northern hemisphere in the late spring of 1963 (Gat, 1980). Reported tritium concentration in precipitation at Adak Island for June 1963 averaged 3,900 TU (data from IAEAV).

Table 13. *Results of tritium analyses, Geyser Bight waters. Tritium concentrations are in tritium units (TU). Analyses performed by Tritium Laboratory, University of Miami, Florida*

Sample	TU	Std Dev
Hot Springs:		
88-H6	2.4	0.1
88-H6[a]	2.9	0.1
88-G8	0.0	0.1
Cold Streams:		
88-E Geyser Cr H+	9.6	0.3
88-Side Cr KL-	6.3	0.2

[a]Repeat analysis.

Since 1963, atmospheric concentrations of tritium have steadily declined through radioactive decay and precipitation of tritiated tropospheric waters, and average concentrations are beginning to approach pre-1952 levels. Tritium concentrations in precipitation undergo seasonal variations that are linked to exchanges between the stratosphere and the troposphere (Gat, 1980). Maximum concentrations occur in late spring followed by a minimum in late fall. As an example, in Anchorage in 1980 (the most recent year for which data are available), the weighted annual average tritium concentration dropped to 29 TU, with a seasonal variation that ranged from a winter minimum of 16 TU to a late-spring maximum of 51 TU.

Because of its relatively short half-life (12.3 yr), tritium is a good indicator of meteoric waters of relatively young age and has therefore been extensively used to estimate age and mixing of waters in groundwater and geothermal systems (see Fontes, 1980, and Panichi and Gonfiantini, 1978 for reviews). At Geyser Bight, tritium concentrations in G8 thermal-spring waters are below detection (< 0.1 TU), which indicates that the meteoric waters recharging the site G geothermal reservoir system must be at least 70 yr old. In comparison, thermal-spring waters from H6 have a tritium concentration of 2.4 to 2.9 TU, one-quarter to one-half that of local stream water. Because of the surprisingly high concentration of tritium in H6 waters, a repeat analysis was performed with nearly identical results.

Interpretation of the elevated tritium concentration in the H6 waters remains ambiguous. The H6 tritium concentration could reflect mixing of meteoric waters of very recent age, but analyses of water chemistry and stable isotope data do not support a 25 to 50 percent admixture of near-surface meteoric waters in the H6 thermal spring waters. An alternate possibility is that recharge of the site H geothermal reservoir system is considerably more rapid than at site G. A 1950 water with an initial tritium concentration of 10 TU would have decayed to

about 2.5 TU by 1988. Another possibility is that small amounts of meteoric waters associated with periods of thermonuclear testing are intercepting and slightly diluting ascending thermal waters at deep levels. Northern hemisphere precipitation in 1954, with a peak tritium concentration of about 900 TU (Gat, 1980), would have decayed to concentrations of about 130 TU in 1988.

GEOTHERMOMETRY

SILICA

Results of applying the silica geothermometer (Fournier and Potter, 1982) to Geyser Bight hot-spring waters are given in table 14. Silica concentrations are plotted against vent enthalpy in figure 30, along with the quartz solubility curve. For pressures normally encountered in geothermal systems, silica concentrations in geothermal waters are a function of temperature, pH, and the controlling silica mineral phase. For the probable temperatures and host rocks for the Geyser Bight reservoirs (> 150°C; quartz monzonite to granodiorite), quartz is the mostly likely phase controlling the dissolved silica concentration (Fournier, 1981).

Table 14. *Silica and cation geothermometry applied to Geyser Bight hot-spring waters. Temperatures in degrees Celsius*

		Quartz[a]		Cation		
Site	T, spring	Conductive	Adiabatic	Na-K[b]	Na-K[c]	Na-K-Ca[b]
1988						
G1	101	216	197	194	211	186
G6	94	171	161	186	203	168
G8	100	207	190	190	207	182
G11	86	145	139	156	174	140
H2	98	158	150	160	179	150
H4	102	173	162	160	179	152
H6	104	175	164	158	177	152
H7	103	158	150	152	171	145
J1	80	200	184	188	206	179
J5	90	197	182	192	208	181
K3	80	154	147	194	211	167
L1	60	147	141	190	207	164
L3	86	165	156	189	206	167
Q	78	157	149	157	176	144
1980						
G6	97	172	162	187	204	166
G8	100	201	185	181	198	175
H1	100	169	159	158	177	149
H6	100	176	165	157	176	151
J1	82	202	186	189	206	180
K1	62	160	152	196	213	166
L1	86	165	156	190	207	166
1975						
G?	85	196	181	179	197	174
G8	102	197	182	185	202	177
J1	93	194	180	185	203	176
J4	65	188	175	190	207	180
1946						
G1	100	210	192	193	210	185
H1	101	161	153	166	184	153

[a]Fournier and Potter (1982).
[b]Na-K: Fournier equation; Na-K-Ca: Fournier and Truesdell equation (Fournier, 1981).
[c]Giggenbach (1988).

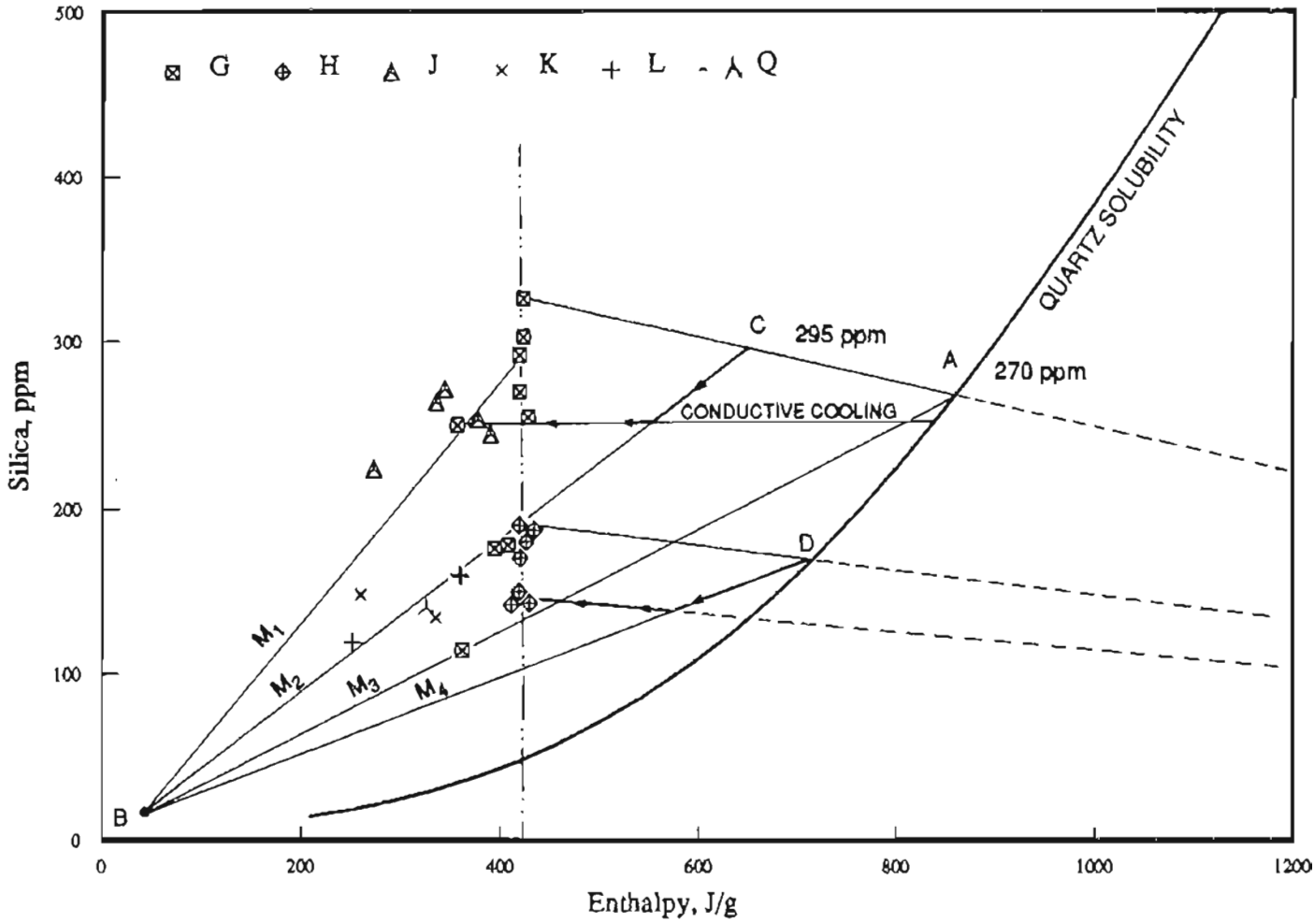

Figure 30. *Silica concentrations vs. vent enthalpy. Interception of dashed rays with quartz solubility curve at points A and D represents enthalpy and silica concentrations of parent waters for G and H springs, respectively. M_1, M_2, M_3, and M_4 represent hypothetical mixing lines between a cold meteoric water (b) and various thermal waters (A, C, D, and G) and are discussed in the section on chloride-enthalpy analysis (p. 76).*

For vigorously boiling springs, the quartz adiabatic geothermometer was applied. The effect of adiabatic cooling is illustrated in figure 30. Following the method of Fournier and Potter (1982), rays originating from a point representing separated steam at 1 atm pressure with an enthalpy of 2676 J/g and less than 1 ppm silica are drawn to points representing boiling springs G1 and H6. Intersection of these lines with the quartz solubility curve (A and D, respectively) marks the enthalpy and silica concentration of the parent water for the case of adiabatic cooling and single-stage steam separation at the surface. As this water ascends and cools adiabatically , boiling concentrates silica in the residual liquid phase. The case of continuous steam separation would provide slightly higher temperature estimates.

Fournier and Potter's (1982) quartz geothermometers are based on neutral or near-neutral solutions. For a pH greater than 7.5, the solubility of quartz increases with increasing pH and is most pronounced for temperatures between 100° and 250°C (Fournier, 1981). However, pH values of solutions in high-temperature geothermal reservoirs are likely to be below 7.5 because of the buffering of hydrogen ions by silicate hydrolysis reactions. The high pH values for some Geyser Bight hot-spring waters probably result from the loss of CO_2 and H_2S as the water boils after leaving the high-temperature reservoir. Following the recommendation of Fournier (1981) for this situation, the silica concentration of the hot-spring water is assumed to reflect near-neutral pH reservoir conditions; no correction was applied to the observed silica concentration.

The silica geothermometer is based on absolute concentration, and subsurface dilution of ascending thermal water by cooler low-silica water can result in underestimating reservoir temperature. Dilution probably accounts for the lower temperatures predicted by the quartz geothermometer for non-boiling springs at sites G, K, L, and Q. Solutions initially above 200°C can also become supersaturated with respect to amorphous silica, and precipitation can take place as the waters ascend and cool adiabatically. The loss of dissolved silica in such a hot-spring water would also cause the quartz geothermometer to underestimate reservoir temperature. Site G boiling spring waters and site J waters have similar concentrations of Cl and Na, indicative of little or no dilution, but have varying SiO_2 concentrations, evidence that silica was lost from these waters by precipitation or re-equilibration (fig. 25a, m). In contrast, hot-spring waters of group H show marked linearity between both SiO_2 and Cl and Na and Cl (figs. 25a, 26). Here, dilution rather than precipitation appears to have affected the silica concentrations of some of the H site boiling hot-spring waters.

Using the results of the most concentrated spring waters, the minimum reservoir temperatures predicted by the quartz geothermometer are 200°C for groups G and J, and 165°C for H.

CATION

Three cation geothermometers were applied to the Geyser Bight hot-spring waters (table 14). Because these geothermometers are based on ratios of constituents rather than on absolute concentrations, they are less susceptible to dilution. Temperatures predicted by the Na-K geothermometer of Fournier (1981) are in excellent agreement with temperatures predicted by the quartz geothermometer for spring waters with the highest silica concentrations. The Na-K-Ca geothermometer (Fournier and Truesdell, 1973) gives lower temperatures than the Fournier Na-K geothermometer, with the difference ranging up to 20°C. In contrast, the Na-K geothermometer of Giggenbach (1988) predicts temperatures 15° to 20°C higher than the Fournier Na-K geothermometer.

The Na-K-Ca geothermometer was empirically derived specifically to deal with calcium-rich waters, particularly low-temperature thermal waters, because application of the Na-K geothermometer to such waters gave anomalously high calculated temperatures (Fournier and Truesdell, 1973). Calcium concentrations are generally low in all Geyser Bight hot-spring waters, and calcium enrichment in Geyser Bight hot-spring waters appears to correlate with spring waters that are below boiling and considered to be of mixed origin. This correlation suggests the Ca enrichment may in part be associated with the dilution process. In addition, for the boiling springs, calcite was also found to be near saturation, which suggests that $CaCO_3$ may have precipitated from these waters during their ascent. Such loss of Ca would affect the reliability of the Na-K-Ca geothermometer. For thermal waters thought to be derived from high-temperature environments, the Na-K method generally gives excellent results (Fournier, 1981) and is preferable for Geyser Bight. Using Fournier's Na-K geothermometer, reservoir temperatures of 190° to 194°C are estimated for site G and J thermal waters and 160° to 165°C for site H thermal waters. In contrast, the Na-K-Ca geothermometer gives 175° to 186°C for sites G and J and 150° to 152°C for site H.

The Na-K geothermometers of Fournier (1981) and Giggenbach (1988) are based on analytical data for a wide range of deep well discharges. The steeper temperature dependence of the Giggenbach Na-K geothermometer is due to his selection of data points that represent only maximum Na/K ratios at a given temperature (Giggenbach, 1988). The latter approach assumes that maximum Na/K ratios are more representative of full equilibration.

SULFATE - WATER OXYGEN ISOTOPE

The results of applying the sulfate-water oxygen isotope geothermometer to the Geyser Bight hot springs are given in table 15. The data include results for a sample obtained by Ivan Barnes (U.S. Geological Surveys written commun., 1975) three samples we obtained in 1980, and two samples we collected in 1988.

The data for spring G8 are the easiest to interpret because the lack of tritium in Spring G8 waters rules out mixing of young meteoric waters. Good correspondence exists between isotopic values for samples obtained in 1975 and 1980. Spring G8 is a boiling-point geyser, and the presence of warm ground and acid springs nearby indicate that steam separation from the spring conduit is intermediate between single-stage and continuous.

Table 15. *Sulfate-water isotope geothermometer applied to Geyser Bight hot spring waters. Temperatures in degrees Celsius*

Site	T, spring	$\delta^{18}O$-SO_4	$\delta^{18}O$-H_2O	T1	T2	T3
1988:						
H4	102	-2.3	-8.7	248	221	228
L3	86	-3.5	-9.4	262	225	235
1980:						
H1	100	-2.0	-8.2	254	225	232
J1	82	-4.1	-7.9	333	265	287
G8	100	-4.2	-8.4	315	263	279
1975:						
G8	102	-4.1	-8.1	322	264	282

Geothermometer temperatures computed using formulas and tables from McKenzie and Truesdell (1977): T1 = conductive cooling, T2 = single stage steam removal, T3 = continuous steam removal.

All $\delta^{18}O$-SO_4 and $\delta^{18}O$-H_2O of spring G8 (1975) analyzed by N.L. Nehring and C.J. Janik, U.S. Geological Survey, Menlo Park. Remaining $\delta^{18}O$-H_2O analyzed by Stable Isotope Laboratory, Southern Methodist University. $\delta^{18}O$ in per mil WRT SMOW.

Following the recommendation of McKenzie and Truesdell (1977), the appropriate range for the reservoir temperature is 263° to 282°C.

Spring J1 is a large, open, hot pool whose water is geochemically very similar to G8 water. Compared to G8, J1 has the same $\delta^{18}O$ value for dissolved sulfate, but is slightly heavier in $\delta^{18}O$ for H_2O. As discussed previously, the slightly heavier isotopic composition could be attributed to evaporative concentration. Because J1 is below the boiling point, the conductive cooling temperature, T1, would ordinarily be chosen as the SO_4-H_2O geothermometer estimate. However, this temperature for J1 seems excessively high when compared to that found for G8. As at G8, warm marshy ground near the J springs suggests that steam may be separating from the spring conduit at depth. There is the intriguing possibility that J1 is a geyser with a relatively long period. Chloride concentration of J1 is slightly lower than G8, which suggests that a small amount of cold water may be diluting the thermal water and quenching residual boiling below the pool. If so, the range 265° to 287°C, given by T2 and T3, is more applicable. These latter temperatures are in much better agreement with G8 results.

Spring L3 is below the boiling point and has a chloride concentration substantially below that of G8. As discussed previously, based on similarities of constituent/chloride ratios, L3 is probably a diluted version of G-type water. Examination of Na vs. Cl (fig. 25a) suggests mixing of about 35 percent cold meteoric water with G8-type water to produce L3 water. No boiling springs, acid or otherwise, occur near L3, and it is likely that boiling of the ascending deep thermal water is completely quenched by near-surface mixing of cold meteoric water.

Dilution complicates interpretation of the L3 SO_4-H_2O geothermometer because the near-surface mixing of meteoric water obscures the calculation of the $\delta^{18}O$ value of the deep thermal water. Surface stream waters sampled near spring groups K and L in 1988 had $\delta^{18}O$ values of -9.6 and -10 per mil, while the average for all stream-water samples was -10.2 per mil. These values are 1.5 to 2 per mil lighter than $\delta^{18}O$-H_2O values for the most concentrated spring waters at Geyser Bight. Dilution of deep thermal water with meteoric water would then result in mixed water with a lighter $\delta^{18}O$ value than the thermal water. The T1 conductive SO_4-H_2O

geothermometer for the L3 spring water $\delta^{18}O$ value therefore provides only a minimum estimate for the deep thermal-water temperature. This estimate of 262°C compares well with the lower range of G8 and J1 estimates.

Results of isotopic analysis of the two H springs samples are consistent with each other (table 15). Compared to G and J spring waters, the $\delta^{18}O$ values for dissolved sulfate are about 2 per mil heavier, although the $\delta^{18}O$ values for these H spring waters are similar. The difference in isotope values for dissolved sulfate is probably not attributable to formation of sulfate by oxidation of H_2S at low temperatures. No odor of H_2S was detected at site H, and hot-spring waters analyzed from site H have nearly identical SO_4/Cl ratios (fig. 25k), which indicates that oxidation of H_2S is probably unimportant (McKenzie and Truesdell, 1977). We suggest two possibilities to explain the differences in $\delta^{18}O$ values for dissolved sulfate: 1) there are two deep reservoirs with different temperatures; or 2) $\delta^{18}O$-SO_4 partially re-equilibrates while the waters reside in lower temperature reservoirs at intermediate depth.

Tritium analyses indicated the presence of young meteoric water in the H spring system, but the data were insufficient to determine the amount of mixing or whether mixing was responsible for the high tritium value. As with spring L3, any addition of near-surface meteoric water to ascending thermal water would tend to produce a spring water with $\delta^{18}O$ values lighter than the thermal water. The temperatures predicted by the SO_4-H_2O geothermometer for the H springs are therefore minimum estimates. Because both H springs sampled are at boiling, the applicable temperature range is 221° to 232°C.

ASSESSMENT OF GEOTHERMOMETERS

Accuracy of chemical and isotopic geothermometers depends on a number of conditions: availability of constituents used in the geothermometer, full equilibration between the thermal water and the constituents; no re-equilibration, precipitation, or additional reaction with wallrock upon ascent; and no mixing with other waters. All or none of these conditions may actually be met in real systems. In reviewing the Geyser Bight geothermometers, we find that the temperatures predicted by two traditionally used geothermometers, that is, the quartz geothermometer and the Na-K cation of Fournier, are in excellent agreement with each other for the Geyser Bight hot-spring waters that have the highest concentrations of dissolved solids, for example, G1, G8, J1, H6, and H4, and probably represent minimum estimates of temperatures for subsurface aquifers. For springs that issue below boiling point at sites G, J, K, and L, the Fournier Na-K temperature exceeds the quartz conductive geothermometer by several to tens of degrees Celsius. Because the quartz geothermometer is more susceptible to dilution, this discordance probably reflects near-surface mixing of cold meteoric waters with thermal waters (Fournier and Truesdell, 1974). Mixing at H is not as clearly indicated by comparison of Na-K and quartz geothermometers. Results for the most concentrated springs H6 and H4 show that the Na-K temperature is identical or slightly lower than the quartz adiabatic temperature. For the more dilute springs suspected to be of mixed origin (H1, H2, and H7), the Na-K temperature is similar to or slightly higher than the quartz temperature.

For the pH and temperature range of most deep geothermal waters, the rates of the sulfate oxygen isotope exchange reaction are very slow compared to silica solubility and cation exchange reactions (Fournier, 1981; Truesdell and Hulston, 1980). Once equilibrium is attained in the deep reservoir, there is little re-equilibration of the oxygen isotopes of sulfate as the water cools during movement to the surface, unless that movement is very slow. Therefore, temperatures predicted by the SO_4-H_2O oxygen isotope geothermometers, which are substantially higher than the cation and silica temperatures, may reflect temperatures in deep reservoirs at Geyser Bight.

Assuming that this is the case at Geyser Bight, geothermometry suggests that thermal waters initially reside in deep reservoirs with a minimum temperature of 265°C. Thermal water from these deep reservoirs ascends to reservoirs at intermediate depths where cations and silica re-equilibrate to temperatures of 200°C for waters emerging at sites G and J and other down-valley sites and to temperatures of 165°C for waters emerging at site H and perhaps site Q. Residence time in these intermediate reservoirs must be on the order of several months or more to achieve new cation equilibrium. Residence and travel time for site H waters may have been sufficiently long for partial re-equilibration of the sulfate oxygen isotopes.

CHEMICAL EQUILIBRIA

Proper evaluation of chemical equilibrium in subsurface aquifers requires information on dissolved constituents, gas partial pressures (CO_2, H_2S), aquifer pH, and wallrock characteristics. Such information, which is normally obtained from a well, is lacking for Geyser Bight, and aquifer conditions must be inferred from available surface thermal-spring chemistry. Aquifer chemical composition can be estimated by adjusting for the concentration of constituents caused by boiling, but lack of information on the volatile phases and on the possibility that calcite has precipitated hinder accurate calculation of aquifer pH and aquifer Ca concentration, parameters that are critical in evaluating mineral stabilities. Nevertheless, with reasonable assumptions, some reservoir fluid-mineral equilibria can be estimated.

An activity diagram showing the principal phases in the system Na_2O-K_2O-Al_2O_3-H_2O at 200°C is shown in figure 31. Stability fields for albite, potassium feldspar (K-feldspar), and muscovite (K-mica) at 150°C are also shown for comparison. Log activities for Geyser Bight waters calculated using 1988 thermal-spring chemistry show that the most concentrated waters from sites G and J are in equilibrium with both albite and potassium feldspar. The more dilute springs plot on or near the extension of the albite-potassium feldspar equilibrium line into the field of muscovite stability. In contrast, site H thermal-spring waters plot closer to the 150°C equilibrium line. Points G8-B and H6-B, which illustrate the effects of adjusting concentrations but not pH for steam losses, are only slightly displaced on the albite-potassium feldspar equilibrium line. The effect of decreasing pH to more realistically reflect probable aquifer conditions is to displace points G8-B and H6-B further toward muscovite stability. Calculated pH at the albite-potassium feldspar-muscovite 200°C triple point is 7.2.

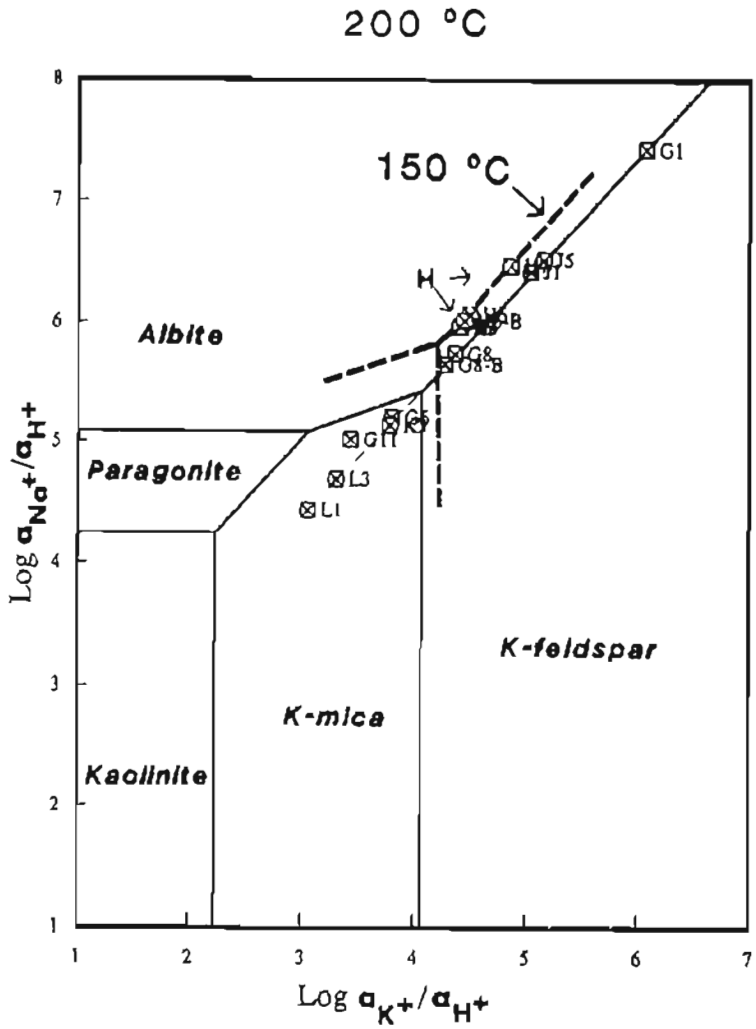

Figure 31. *Activity diagram of the Na_2O-K_2O-Al_2O-H_2O system at 200°C showing principal mineral phases with 150°C overlay.*

It is readily apparent in the trilateral plot of Na-K-√Mg shown in figure 32a that thermal waters at site H vs. the down-valley sites have equilibrated at different temperatures. This diagram and its application to geothermal systems are described by Giggenbach (1988). The "full-equilibrium" curve in figure 32a represents compositions of waters in full equilibrium with the mineral system albite-potassium feldspar-muscovite-clinochlore-silica at the temperatures indicated. The boundary between partially equilibrated and immature waters shown in figure 32a is somewhat arbitrary and serves only as a rough guideline (Giggenbach, 1988). The isotherms correspond to the equilibrium equations

$$L_{kn} = \log (C_K/C_{Na}) = 1.75 - (1390/T) \quad (1)$$

for the pair K-Na and

$$L_{km} = \log (C_{2K}/C_{Mg}) = 14.0 - (4410/T) \quad (2)$$

for the pair K-Mg, where C is in mg/kg and T in °K as derived by Giggenbach (1988).

Magnesium concentrations in thermal waters are highly temperature dependent, with hotter temperatures favoring depletion of Mg from the water through hydrothermal reactions. For more mature thermal waters, Mg is commonly present in only trace quantities. The effect of increasing or decreasing Mg is to move the points down or up respectively, parallel to the K-Na isotherms.

In figure 32a the spring waters from group H plot on or near the 180°C isotherm, while those from groups G, J, L and K lie on or between the 200° and 210°C isotherms. The K-Mg system adjusts to cooling temperature more rapidly than the K-Na system, and spring waters that plot below the "immature water" line probably reflect the dissolution of Mg in the shallow environment as the waters cool conductively or, more likely, cool by mixing with colder ground waters.

Giggenbach (1988) also devised a CO_2 "geobarometer" based on K and Ca concentrations:

$$L_{kc} = \log (C_{2K+}/C_{Ca++}) = \log f(CO_2) + 3.0 \quad (3)$$

Equation (2) is used to correlate CO_2 fugacities with their likely equilibration reference temperatures because K and Mg are more likely to equilibrate at similar rates and under similar conditions as the K-Ca-geobarometer. Giggenbach's graphical representation of this geobarometer based on end-member mineral phases assumed to control CO_2 fugacities in geothermal systems is reproduced in figure 32b with data points for Geyser Bight geothermal area thermal springs superimposed. Based on data from explored systems, Giggenbach (1988) concluded that the geobarometer is only reliable for data points close to the full equilibrium line; those that plot above this line probably come from a rock-dominated, CO_2-deficient environment. Using this criteria, site G waters appear the most suitable for application of this geobarometer. Assuming equilibrium with calcite, the graphically predicted $f(CO_2)$ is about 0.1 bar for G1 and G8 waters. The $f(CO_2)$ corresponding to equilibrium with calcite at the predicted Na-K and quartz geothermometer temperature of 200°C suggested by the equilibrium curve is about 1.0 bar.

Assuming these values for $f(CO_2)$ and assuming that calcite is at saturation at the predicted geothermometer reservoir temperature of 200°C, an estimate of reservoir pH can be made by using the reaction (Henley and others, 1984):

$$CaCO_3 + 2H^+ = Ca^{++} + H_2O + CO_2 \quad (4)$$

The calculated pH range of 6.1 to 6.6 compares well with pH values found in wells at explored geothermal systems; for example, the Makushin geothermal system on neighboring Unalaska Island has a reservoir pH of about 6.1 (Motyka and others, 1988). Figures 33a and b are SiO_2-Ca activity diagrams at 200°C for various zeolites and clays with Makushin water plotted for comparison. The range for Geyser Bight water was plotted using the reservoir pH estimated from site G water and spring G8 Ca concentration adjusted for boiling. The low end of the pH range suggests that the reservoir fluid is in equilibrium with prehnite, laumontite, and kaolinite.

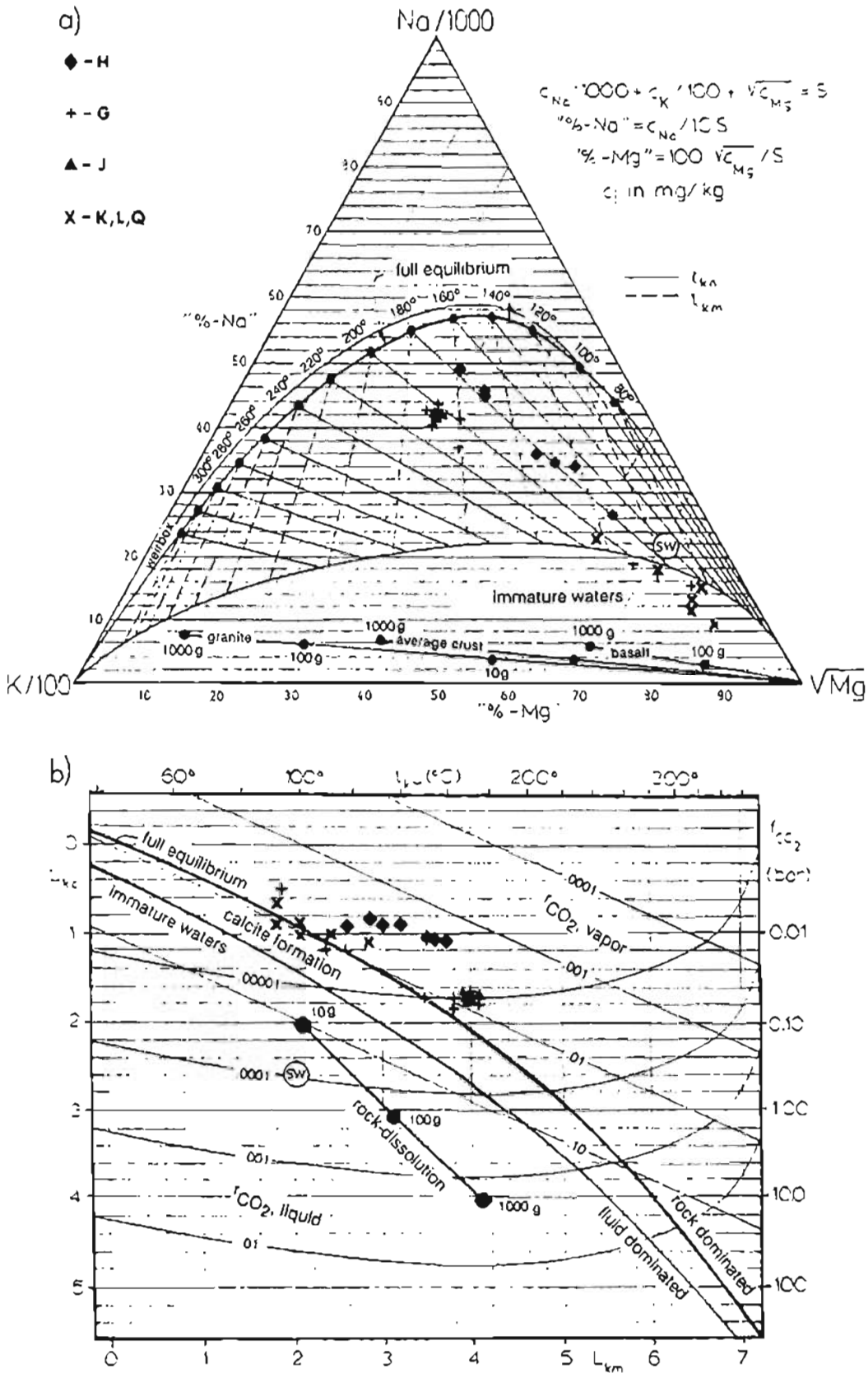

Figure 32. *(a) Giggenbach's (1988) Na-K-√Mg trilateral diagram for evaluating Na-K and K-Mg equilibration temperatures; (b) Giggenbach's (1988) graphical CO_2 geobarometer.*

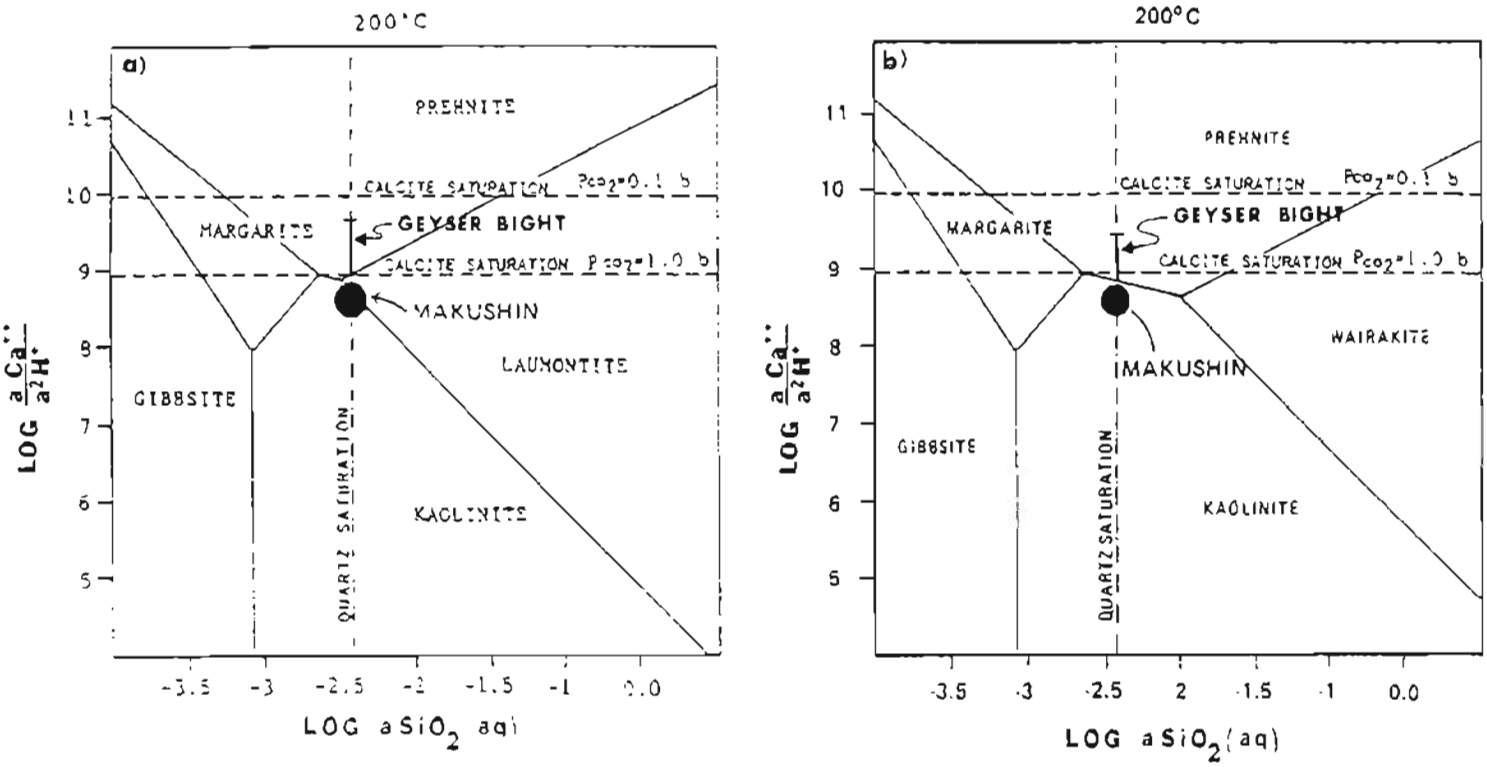

Figure 33a, b. *Silica-calcium activity diagrams at 200°C for various zeolites. Makushin test well results shown for comparison.*

MODEL OF HYDROTHERMAL SYSTEM

CHLORIDE-ENTHALPY ANALYSIS

Thermal water that ascends from a deep reservoir may cool by boiling, by conduction of heat to surrounding rock, by dilution with colder waters, or by a combination of these processes, depending on the depth of the reservoir, channel geometry, pathway, rate of flow, coefficient of thermal diffusion through surrounding rock, and initial temperature (Fournier, 1979). During ascent, its chemical and isotopic composition can be affected by water-rock reactions, re-equilibration, precipitation, mixing, and boiling. The emergent hot-spring waters can, and commonly do, have compositions and enthalpies significantly different from the original parent thermal water. Despite these complexities, chemical compositions of hot-spring waters can still be useful for deriving information on underground conditions. Cl-enthalpy and SiO_2-chloride diagrams, when used in conjunction with other evidence, are particularly useful for tracing the origins of spring waters compositions and for determining underground temperatures, salinities, and boiling and mixing relationships. Figure 34 shows Cl concentrations of sampled Geyser Bight hot-spring waters plotted as a function of enthalpy at the measured vent temperature. In our analyses, we seek consistency between these diagrams and 1) geochemical and isotopic compositions; 2) SiO_2-enthalpy relationships; 3) geothermometry ; 4) chemical equilibria; and 5) rates of spring discharge.

Truesdell and others (1977) calculated the maximum rates of mass flow for conductive cooling without boiling and the minimum rates of mass flow for adiabatic cooling with negligible conductive cooling for water moving vertically from different initial depths. Waters were assumed to start at 200°C and emerge at 100°C. Conduits were assumed to be small-diameter cylinders. The results of these calculations, some of which are shown in table 16, are particularly useful for our assessment of the Geyser Bight hydrothermal system because geothermometry and chemical equilibria indicate that many boiling and near-boiling spring waters originated from an aquifer or aquifers at 200°C. Although the reservoir depths at Geyser Bight are unknown, given the degree of thermal activity observed at the surface, it is reasonable to assume that the reservoir depths are unlikely to be much greater than 1 km. As a comparison, the depth to the hot-water reservoir at the Makushin geothermal area on neighboring Unalaska Island, as determined by drilling, is about 0.6 km.

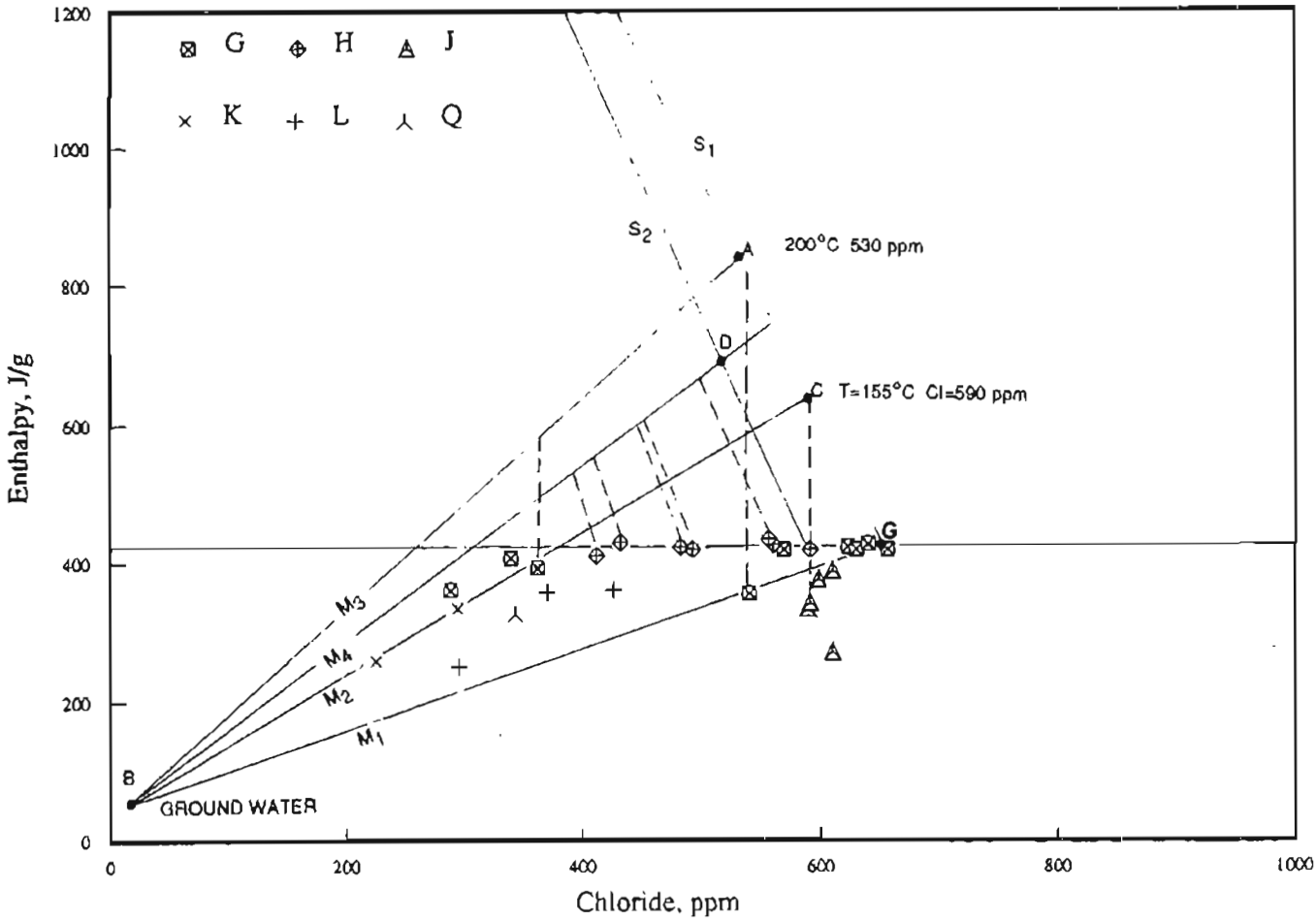

Figure 34. *Chloride concentrations of thermal waters vs. vent enthalpy. Lines S1 and S2 show enthalpy and chloride concentrations of the residual water phase as a thermal water cools adiabatically upon ascent to the surface. M_1, M_2, M_3, and M_4 represent hypothetical mixing lines between a cold meteoric water (B) and various thermal waters (A, C, D, and G) as discussed on page 78. Dashed lines represent hypothetical cooling by conduction and boiling (see page 78 for further discussion).*

Table 16. *Maximum mass-flow rates in a conduit of circular cross-section for waters to cool by conduction without boiling and minimum mass-flow rates for waters to cool adiabatically with negligible conductive cooling. All waters are assumed to come from a reservoir at 200°C and emerge at 100°C. Data from Truesdell and others (1977)*

Depth (km)	Conductive cooling (kg/min)	Adiabatic cooling (kg/min)
0.5	13	117
1.0	26	234
1.5	40	355

Sites G, J, K, and L

We first analyze the origin of spring systems located in the upper part of the Geyser Creek valley floor. As discussed previously, based on constituent ratios, these springs appear to be geochemically related. As the starting point we use spring G8. G8 has the highest concentration of Cl and dissolved solids of the entire suite of

samples, and its chemistry is therefore likely to be closest to the deep thermal water. Lack of tritium eliminates mixing of cold meteoric waters as a factor in interpreting the concentrations and enthalpy of the 1988 G8 spring waters. Our assessment of quartz and cation geothermometers indicated site G thermal waters were derived from an aquifer with an estimated minimum temperature of 200°C. Flow rate of the G8 spring was estimated to be 150 lpm in 1988. Compared to table 16, conductive cooling of the G8 thermal water is unlikely to be a significant factor for depths <0.75 km. This leaves boiling as the sole process by which these waters have cooled. The boiling curve S_1 in figure 34 represents the evaporative concentration of chloride in the thermal water as a function of enthalpy as it adiabatically cools and emerges as spring G8('88). Point A on this curve corresponds to the Cl concentration and enthalpy at the estimated reservoir temperature of 200°C.

Spring Gx and the springs sampled at site J issue at below boiling (80° to 90°C), are comparatively rich in Cl and SiO2, and have relatively low Mg. The location and flow rate of spring Gx sampled by the U.S. Geological Survey in 1975 (Ivan Barnes, written commun.) are not known. Flow rates of site J springs (< 30 lpm) indicate these springs could have cooled by conduction. Perpendicular projection of a line from Gx, simulating conductive cooling, intersects the G8 ('88) boiling curve at an enthalpy equivalent to 195°C, which is consistent with the predicted reservoir temperature and the silica-enthalpy diagram (fig. 13). Perpendicular projections from the J springs intersect the G8 boiling curve at enthalpies well below point A, which suggests J waters would have first boiled to point C, then conductively cooled to the surface. Alternatively, the site J and Gx spring waters could have formed by near-surface dilution of G8 water with groundwater along the path M_1, followed in some cases by conductive cooling. The latter explanation appears more consistent with silica-enthalpy and deuterium-chloride relationships. Conductive cooling should have produced waters with deuterium values similar to deep thermal waters. Instead, figure 29c shows these waters have δD values similar to site G boiling spring waters. Mixing rather than conductive cooling is favored by analysis of the SiO_2 vs. enthalpy diagram for site J springs (fig. 30) and is also consistent with our interpretation of the SO_4-H_2O oxygen isotope results for spring J1.

The remaining spring waters at these sites and further down-valley are below boiling. Concentrations of most constituents in these waters are substantially lower than spring G8 water (table 9). One exception is Mg (0.9 to 2.8 ppm), where the increase in Mg correlates with decreasing chloride (fig. 25e). The temperatures predicted by the Na/K geothermometer for these springs are also significantly higher than the quartz conductive geothermometers. The combination of these factors is strong evidence that these springs are a mixture of ascending thermal waters and shallow groundwaters. Two mixing lines, M_2 and M_3, are illustrated on the Cl-enthalpy and SiO_2-enthalpy diagrams to account for these springs (figs. 34, 30). Cl and SiO_2 concentrations of 10 ppm and 15 ppm, respectively, and a temperature of 10°C, were chosen for the cold water end member, point B, in these mixing models. These values are similar to cold stream waters that enter Geyser Creek valley unaffected by input of thermal waters (table 10). M_2 extends to point C on the G boiling curve (enthalpy = 650 J/g), a hypothetical thermal water end-member that coincides with the perpendicular projection from J1 on the chloride-enthalpy diagram; M_3 extends to point A. The corresponding chloride and silica concentrations and temperatures for the hypothetical thermal water end members are 590 ppm, 290 ppm, 155°C, respectively, for point C, and 530 ppm, 260 ppm, and 200°C, respectively for point A.

Many dilute hot springs lie on or near M_2 on both the Cl and SiO_2 -enthalpy diagrams, which suggests that their compositions and temperatures are fixed mainly by mixing. However, these springs have relatively low rates of flow, and conduction may have also played a part in cooling the ascending waters. Springs that plot below line M_2 may have cooled additionally by conduction or by mixing with a different end member.

M_3 illustrates mixing between the assumed 200°C reservoir water and groundwater. Spring waters formed by mixing along this line had to cool appreciably by conduction to produce the dilute springs. Both M_2 and M_3 mixing relationships appear to be generally consistent with stable isotope values (fig. 29c); some springs correlate with a deep, thermal-water end member and others with a shallow, fractionated thermal water. The variation in δD for the dilute springs suggests they were formed by mixing with groundwaters that had different δD values.

The preceding paths for formation of the G, J, K, and L thermal springs are illustrated on the SiO_2-Cl diagram (fig. 26). A deep water originating at point A cools adiabatically and by conduction to produce spring G1 waters. Continued steam loss and re-equilibration of SiO_2 leads to formation of G8. Site J and Gx springs

form by conductive cooling from the point A steam-loss line or by near-surface dilution of G8 waters, or both. SiO_2 had to re-equilibrate to varying degrees following dilution and conductive cooling to account for the remaining dilute springs.

Site H

Application of chloride-enthalpy analysis to site H springs results in a comparatively simple boiling and mixing model (fig. 34). Our geothermometry showed that site H spring waters were derived from a reservoir with a minimum temperature of 165°C. As with the down-valley sites, sulfate-water oxygen isotope geothermometry predicts even higher temperatures at deeper levels (225°C). The most concentrated spring of our sample suite is 1980 H6; its values for Cl and SiO_2 were used to derive the composition of the parent thermal water for site H springs. Although H6 (1980) has a relatively low rate of flow (50 lpm), conductive cooling is probably not an important factor given the much lower initial temperature in contrast to the values used to generate table 16. The boiling curve S_2 in figure 34 represents the evaporative concentration of chloride in the thermal water as a function of enthalpy as it adiabatically cools and emerges as spring H6 (1980). Point D on this curve corresponds to the chloride concentration (520 ppm) and enthalpy at the estimated reservoir temperature of 165°C. The point that correspondes to the "deep" reservoir is also shown on this curve.

All remaining springs sampled at site H can be explained as forming through a combination of mixing of point "D" type thermal water with groundwater B (line M_4), followed by adiabatic cooling. Na/K temperatures for these spring waters are nearly uniform, which indicates they originated from a common reservoir. All sampled springs were at or near boiling point and had relatively high rates of flow, factors that eliminate conduction as a major cause for cooling these waters. H6 and H4 had nearly identical compositions in 1988 and appear to be slightly dilute versions of H6 as it was in 1980. The presence of measurable Mg in H2 and H7 spring waters also indicates these springs have a cold-water component and must have cooled at least in part by mixing. This mixing-boiling model for the formation of site H springs is consistent with both the SiO_2-Cl and SiO_2-enthalpy diagrams (figs. 30, 26) and with the δD-chloride considerations for the 1988 samples (fig. 29b).

THERMAL WATER RELATIONSHIPS AND RESERVOIRS

The preceding analysis offers a contrast in the cooling style of ascending thermal waters. At site H, dilution appears to occur at deeper levels followed by boiling as the mixed water rises to the surface. At the down-valley sites, some steam loss appears to occur at deeper levels before mixing, with dilution primarily occurring in the near-surface region.

The proximity of Site H to the down-valley sites and the linear correlation of the more conservative chemical constituents with Cl suggest these spring waters are related at depth. Tritium analysis showed that H6 (1988) has a component of modern water, but ambiguities in interpreting tritium make it difficult to estimate the amount. In figure 34, type "D" waters could have formed from type "A" waters by boiling along S_1, then mixing along path M_4, or by first mixing along path M_3, followed by boiling along S_2. In either case, residence in the "D" reservoir must have been long enough for potassium, silica, and other more reactive constituents to re-equilibrate to new temperature and wallrock conditions. Travel and residence time for the thermal waters may also have been long enough for the SO_4-oxygen isotope ratios to begin re-equilibrating to lower temperature conditions.

Figure 35 presents a conceptual model of the reservoir system at the Geyser Bight geothermal area as suggested by the preceding analysis. In it, we show a "deep" reservoir (R1) housed in a fractured quartz diorite to quartz monzonite pluton with a temperature of 265°C underlying the geothermal area that is recharged by deeply circulating meteoric water. Chloride concentrations in this reservoir would be about 450 ppm. Waters ascend from this deep reservoir to a reservoir at an intermediate depth (R_2), where they re-equilibrate to a temperature of 200°C. Some water from this intermediate reservoir further migrates into a more shallow reservoir (R_3), where it mixes with meteoric groundwaters and re-equilibrates to a temperature of about 165°. Alternatively, waters may ascend directly from R_1 to R_3 and mix with deeply infiltrating meteoric waters. Following re-equilibration, waters from R_3 continue to ascend, further mix with meteoric groundwaters, and boil to the surface to emerge as springs and geysers at site H.

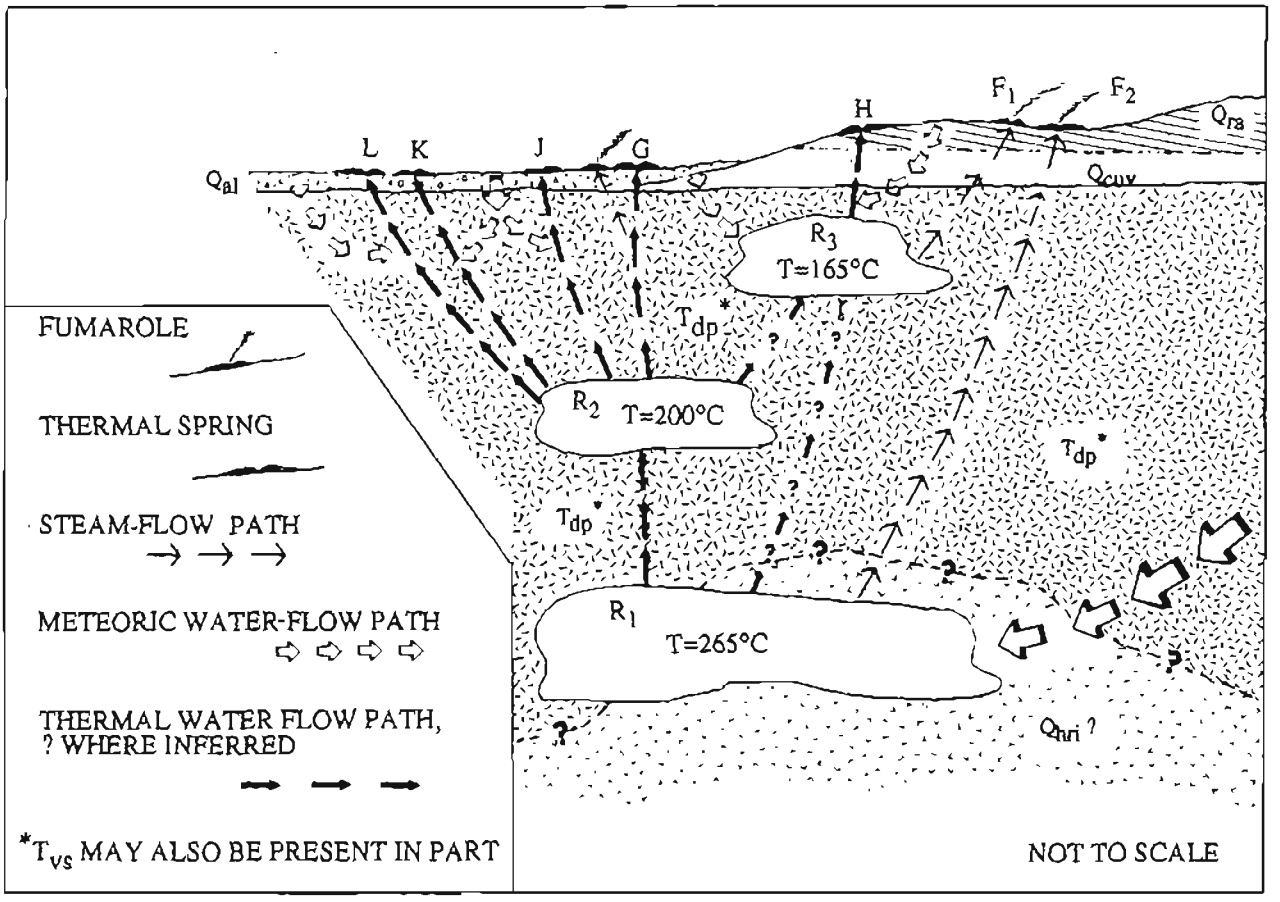

Figure 35. *Conceptual model of reservoir system at the Geyser Bight KGRA. Rock units are defined on sheet 1 and on pages 9-12.*

At R_2, following re-equilibration, some waters ascend directly to the surface and emerge as boiling springs and geysers (for example, G8). Part of the ascending thermal water branches off, mixes with a small amount of groundwater near the surface (which quenches boiling), and then cools conductively to form J springs. A third fraction cools primarily by mixing with cold groundwaters in the near-surface region to emerge as dilute warm springs throughout the valley. As the deep thermal water ascends and boils, some or all steam may separate in the subsurface to heat marshy areas and perched groundwater tables and produce acid springs. Steam may also separate at deeper levels and migrate directly along fractures to produce the fumaroles above the valley floor.

The chemistry of Q spring waters appears to have attributes of both H type (similar K/Cl) and G/J type (similar Rb/Cl and Cs/Cl) thermal waters. Q spring waters may be derived from a reservoir intermediate between the other two or perhaps are a mixture of waters from both reservoirs.

SUMMARY AND CONCLUSIONS

The Geyser Bight geothermal area is a zone of hot springs and fumaroles located on the flank of Mt. Recheshnoi, a large calcalkaline stratocone on central Umnak Island (fig. 1). Geologic basement consists of volcanic and marine volcanogenic rocks of probable Oligocene age (McLean and Hein, 1984). These rocks are only gently deformed and lightly metamorphosed. One or more quartz-diorite to quartz-monzonite stocks have intruded the basement in the Geyser Bight area. K-Ar dating of one sample at 9.5 Ma establishes a much younger plutonic event than is represented by the Oligocene stocks described by McLean and Hein (1984) from southwestern Umnak. Our mapping shows that plutonic rock occurs much further up Geyser Creek valley than previously mapped by Byers (1959), which increases the probability that plutonic rock hosts the geothermal reservoir system.

The valley walls are composed of volcanic material, primarily lava flows, which were erupted first from several unnamed vents to the northeast, and then from Mt. Recheshnoi, to the southwest (fig. 2). Since about 500 ka, the primary source of lava has been Mt. Recheshnoi. The most recent flows are mid-Holocene andesite from flank vents on the upper slopes of Mt. Recheshnoi.

Two flank volcanic units are of special interest. These are the Russian Bay valley rhyolite and the quartz-bearing andesite above Hot Springs Bay. These units document the presence of small volumes of silicic melt in the volcanic system and are notable in their rarity. There are only four other reported rhyolite localities among late Quaternary volcanoes on the Alaska Peninsula and Aleutian Islands. Dacite is more common throughout the Aleutians.

The Russian Bay rhyolite is not likely to come from a large, well-established, upper crustal rhyolitic chamber. It is probably the result of heating and partial melting (or "sweating") of the upper crust by repeated passage of more mafic magma. Such a process may also be responsible for the observed magmatic evolutionary trends at Mt. Recheshnoi, which become generally more mafic with time. This trend may reflect progressive heating of the crust, which would produce decreased thermal contrast between magma and crust, and thus decreased cooling and fractional crystallization of the magma (Myers and others, 1985; Myers and Marsh, 1987).

Geyser Bight has one of the most extensive areas of thermal activity known in Alaska, and includes numerous boiling springs, steam vents, and three regions of fumarolic activity. One fumarole, discovered in 1988, is superheated with a temperature in excess of 125°C. Geyser Bight is the only area in Alaska with documented geysers. In 1988, at least five springs were observed to geyser. Vent geometries suggest that some other springs are also geysers whose eruptive cycles have not been observed, or have been geysers and are now inactive.

Thermal-spring activity appears to have declined significantly since 1947. Using data from Byers and Brannock (1949), we estimate that convective heat discharged by spring flow was 25 MW in 1947 vs. 16.7 MW in 1988. The decline in spring activity may be due to the choking of spring vents by silica, calcite, and other hydrothermal minerals. Declining activity probably does not reflect reservoirs cooling because water chemistry and geothermometry results are essentially unchanged between 1947 and 1988.

Most thermal-spring activity occurs at the head of Geyser Creek valley. Chemical and isotopic data acquired in this study provide strong evidence that the thermal-spring waters are derived from two intermediate-depth reservoirs with minimum temperatures (as estimated by geothermometry) of 200° and 165°C, respectively. These reservoirs in turn appear to be related to an underlying parent reservoir with a minimum estimated temperature of 265°C. The $^{3}He/^{4}He$ ratio of 7.4 found in gases that emanate from the thermal springs provides evidence for a magmatic influence on the hydrothermal system. The 7.4 value is nearly the same as the average value for summit fumaroles in circum-Pacific volcanic arcs.

The most likely reservoir rock is the highly fractured quartz monzonite-to-diorite pluton that is exposed in lower Geyser Creek valley. Reservoir recharge is likely through deeply infiltrating meteoric waters that have isotopic compositions similar to surface stream waters. Tritium concentrations indicate thermal waters that feed spring G8 are over 70 yr old. Thermal waters that feed spring H6 are either younger or have been diluted by near-surface meteoric waters. Examination of chemical equilibria suggests that the waters in the reservoir that feed sites G and J are in equilibrium with the mineral assemblage albite + K feldspar + muscovite + clinochlore + quartz ± prehnite ± laumontite ± kaolinite ± analcime.

The site G boiling spring waters have low to moderate concentrations of Cl (650 ppm) and total dissolved solids (1760 ppm), but are rich in B (60 ppm) and As (6 ppm) compared to most other geothermal systems. Variations in spring-water chemistries can be explained through boiling and steam loss, and/or mixing of ascending thermal water-derived from one or the other of the intermediate reservoirs-with infiltrating meteoric waters. The As/Cl ratios in Geyser Bight thermal-spring waters are among the highest reported for geothermal areas. The source of B and As is unknown, but may be in part of magmatic origin.

Using the areal extent of thermal activity at the surface as a reference, the U.S. Geological Survey estimated the area of the subsurface reservoir to be 6.3 km^2 (Mariner and others, 1978). This estimate can be considered a minimum, given our discovery of a superheated fumarole field on the lower east flank of Mt. Recheshnoi. The presence of this field suggests the reservoir(s) may extend another 4 km to the southwest of Geyser Creek valley. Using the assumptions regarding thickness of unexplored reservoirs (1.7 km) and methods established by the U.S. Geological Survey (Brook and others, 1978) for estimating geothermal reserves, we estimate that for a reservoir temperature of 200°C and an assumed depth to mid-reservoir of 1 km, the reservoir contains approximately 5.4×10^{18} J of thermal energy. This energy base is sufficient to produce up to 132 MW of electrical power for 30 yr. The corresponding estimates for a reservoir temperature of 265°C and a depth to mid-reservoir of 3 km are 7.3×10^{18} J of thermal energy and up to 225 MW of extractable electrical power for 30 yr.

We believe that the probability of finding a high-temperature, hot-water reservoir at Geyser Bight is excellent. We recommend that follow-up work include a program of geophysical exploration and exploratory drilling to determine depth and extent of reservoirs. The accessibility of the resource from the sea (5 km) and the nearly certain probability of intercepting a hot water reservoir with temperatures of at least 200°C make Geyser Bight one of the most promising areas for geothermal resource development in the Aleutians. Because of its remoteness from population centers, the site would be best developed for energy intensive industries that could locate and operate in the Aleutian Chain.

ACKNOWLEDGMENTS

The Geyser Bight study was funded by the U.S. Department of Energy (grants DE-FG07-88IDI2742 and DE-FG07-88IDI2744); the State of Alaska, Department of Natural Resources; and the University of Alaska-Fairbanks, Geophysical Institute.

We acknowledge J.M. Thompson, C.J. Janik, and W.C. Evans of the U.S. Geological Survey, Menlo Park, for their help and cooperation in performing chemical and isotopic analyses of thermal waters and gases, and thank M.J. Reed, U.S. Department of Energy, and J.N. Moore, University of Utah Research Institute, for their help in acquiring analyses of the thermal water samples collected in 1988. We thank H.P. Ross, J.N. Moore and M.C. Adams for technical and scientific reviews. We are grateful to Eugene Pavia for his major contribution to the very difficult logistical operations required by this project and for his skilled assistance with the geologic mapping. Robin Cottrell provided technical assistance with the K-Ar measurements. David Kuentz performed the X-ray fluorescence analyses at the University of California, Santa Cruz. We thank Scott Kerr for his able seamanship and Scott Kerr and Peat Galaktionoff for their warm hospitality in Nikolski.

Any opinions, findings, conclusions, or recommendations expressed herein are those of the authors and does not necessarily reflect the views of the U.S. Department of Energy.

REFERENCES CITED

Baker, D.R., and Eggler, D.H., 1987, Compositions of anhydrous and hydrous melts coexisting with plagioclase, augite, and olivine or low-Ca pyroxene from 1 atm to 8 kbar: application to the Aleutian volcanic center of Atka: American Mineralogist, v. 72, p. 12-28.

Barnes, Ivan, unpublished report.

Black, R.F., 1975, Late-quaternary geomorphic processes: effects on the ancient Aleuts of Umnak Island in the Aleutians: Arctic, v. 28, p. 159-169.

Brook, C.A., Mariner, R.H., Mabey, D.R., Swanson, J.R., Guffanti, Marianne, and Muffler, L.J.P., 1978, Hydrothermal convection systems with reservoir temperatures greater than or equal to 90°C, *in* Assessment of geothermal resources of the United States - 1978: U.S. Geological Survey Circular 790, p. 18-85.

Byers, F.M., Jr., 1959, Geology of Umnak and Bogoslof Islands, Alaska: U.S. Geological Survey Bulletin 1028-L, 369 p.

Byers, F.M., Jr., 1961, Petrology of three volcanic suites, Umnak and Bogoslof Islands, Aleutian Islands, Alaska: Geological Society of America Bulletin, v. 72, p. 93-128.

Byers, F.M., Jr., and Brannock W.W., 1949, Volcanic activity on Umnak and Great Sitkin Islands, 1946-1948. American Geophysical Union Transactions, v.30, no.5, p. 719-734.

Coe R.S., Globerman, B.R., Plumley, P.W., Thrupp, G.A., 1985, Paleomagnetic results from Alaska and their tectonic implications, *in* Howell, D.G., ed., Tectonostratigraphic terranes of the circum-Pacific region: Houston Texas, Circum-Pacific Council for Energy and Mineral Resources, p. 85-108.

Craig, H.A., 1961, Isotopic variations in meteoric waters: Science, v. 133, p. 1702.

Craig, H.A., and Lupton, J.E., 1981, Helium-3 and mantle volatiles in the ocean and oceanic crust, *in* The oceanic lithosphere, v. 7, The sea: New York, John Wiley and Sons, p. 391-428.

Dall, William H., 1870, Alaska and its resources: Boston, Lee and Shepard, 627 p.

Eichelberger, J.C., 1975, Origin of andesite and dacite: evidence of mixing at Glass Mountain in California and at other circum-Pacific volcanoes: Geological Society of America Bulletin, v. 86, p. 1381-1391.

Fontes, J.C., 1980, Environmental isotopes in groundwater hydrology, *in* Fritz, P. and Fontes, J.C., eds., Handbook of environmental isotope geochemistry: New York, Elsevier Scientific Publishing Company, p. 75-134.

Fournier, R.O., 1979, Geochemical and hydrological considerations and the use of enthalpy-chloride diagrams in the prediction of underground conditions in hot-spring systems: Journal of Volcanology and Geothermal Research, v.5, p. 1-16.

_____1981, Application of water chemistry to geothermal exploration and reservoir engineering, *in* Ryback, L. and Muffler, L.P.J., eds., Geothermal systems: principles and case histories: New York, John Wiley and Sons, p. 109-144.

Fournier, R.O., and Potter, R.W. II., 1982, A revised and expanded silica (quartz) geothermometer: Geothermal Resources Council Bulletin, v. 11, p. 3-12.

Fournier, R.O., and Truesdell, A.H., 1973, An empirical Na-K-Ca geothermometer for natural waters: Geochimica et Cosmochimica Acta, v. 37, p. 1255-1275.

Fournier, R.O., and Truesdell, A.H., 1974, Geochemical indicators of subsurface temperature, II. Estimation of temperature and fraction of hot water mixed with cold water: U.S. Geological Survey Journal of Research, v. 2, p. 263-270.

Gat, J.R., 1980, The isotopes of hydrogen and oxygen in precipitation, *in* Fritz, P. and Fontes, J.C., eds., Handbook of environmental isotope geochemistry: New York, Elsevier Scientific Publishing Company, p. 75-144.

Geist E.L., Childs, J.R., and Scholl, D.W., 1988, The origin of summit basins of the Aleutian ridge: implications for block rotation of an arc massif: Tectonics, v. 7, p. 327-341.

Giggenbach, W.F., 1988, Geothermal solute equilibria: derivation of Na-K-Mg-Ca geoindicators: Geochimica et Cosmochimica Acta, v. 52, p. 2749-2765.

Gill, J.B., 1981, Orogenic andesites and plate tectonics: New York, Springer-Verlag, 390 p.

Goguel, R.L., 1983, The rare alkalies in hydrothermal alteration as Wairaki and Broadlands geothermal fields, New Zealand: Geochimica et Cosmochimica Acta, v. 47, p. 429-437.

Grewingk, C., 1850, Beitrag zur Kenntniss der orographischen Besschaffenheit der Nordwest-Kuste Amerikas mit den anliegenden Inseln, *abstracted from* Verhandlungen der Russich-Kaiserlichen Mineralogishen Gesellschalt zur St. Petersburg, Jahrgan 1848 ung 1849, p. 76-342.

Grove, T.L., and Bryan, W.B., 1983, Fractionation of pyroxene phyric MORB at low pressure: an experimental study: Contributions to Mineralogy and Petrology, v. 84, p. 293-309.

Grove, T.L., Gerlach, D.C., and Sando, T.W., 1982, Origin of calc-alkaline series lavas at Medicine Lake Volcano by fractionation, assimilation, and mixing: Contributions to Mineralogy and Petrology, v. 80, p. 160-182.

Henley, R.W., Truesdell, A.H., and Barton, Jr., P.B., 1984, Fluid-mineral equilibria in hydrothermal systems: Reviews in Economic Geology, v. 1, 267 p.

Jacob, K.H., Nakamura, K., and Davies, J.N., 1977, Trench-volcano gap along the Alaska-Aleutian arc: facts and speculations on the role of terrigenous sediments, *in* Talwani, M. and Pitman W.C., eds., Island arcs, deep sea trenches, and back-arc basins: Washington, D.C., American Geophysical Union, p. 243-258.

Kay, S.M., and Kay, R.W., 1985, Aleutian tholeiitic and calc-alkaline magma series I: the mafic phenocrysts: Contributions to Mineralogy and Petrology, v. 90, p. 276-290.

Kay, S.M., Kay, R.W., and Citron, G.P., 1982, Tectonic controls on tholeiitic and calc-alkaline magmatism in the Aleutian arc: Journal of Geophysical Research, v. 87, p. 4051-4072.

Keith, T.E.C., Thompson, J.M., and Mays, R.E., 1983, Selective concentration of cesium in analcime during hydrothermal alteration, Yellowstone National Park, Wyoming: Geochimica et Cosmochimica Acta, v. 47, p. 795-804.

Krause, K.J., 1986, Transmission powerline and road corridor geotechnical study for the proposed Makushin geothermal field power facility on Unalaska Island, *in* Engineering geology technical feasibility study makushin geothermal power project Unalaska, Alaska: Alaska Division of Geological and Geophysical Surveys Public-data File 86-60, p. C1-C17.

Krauskopf, K.B., 1979, Introduction to Geochemistry, (2d ed.): New York, McGraw-Hill, 617 p.

Mariner, R.H., Brook, C.A., Swanson, J.R., and Mabey, D.R., 1978, Selected data for hydrothermal convection systems in the United States with reservoir temperatures greater than or equal to 90°C: U.S. Geological Survey Open-file Report 78-858, 475 p.

McKenzie, W.F., and Truesdell, A.H., 1977, Geothermal reservoir temperatures estimated from the oxygen isotope compositions of dissolved sulfate and water from hot springs and shallow drillholes: Geothermics, v. 5, p. 51-61.

McLean, Hugh, and Hein, J.R., 1984, Paleocene geology and chronology of southwestern Umnak Island, Aleutian Islands, Alaska: Canadian Journal of Earth Sciences, v.21, p. 171-180.

Miyashiro, A., 1974, Volcanic rock series in island arcs and continental margins: American Journal of Science, v. 274, p. 321-355.

Motyka, R.J., Liss, S.A., and Nye, C.J., Geothermal resources of the Aleutian arc: in preparation.

Motyka, R. J., Moorman, M. A., and Liss, S. A., 1981, Assessment of thermal spring sites, Aleutian Arc, Atka Island to Becharof Lake--preliminary results and evaluation: Alaska Division of Geological and Geophysical Surveys Open-file Report 144, 173 p.

Motyka, R.J., Queen, L.D., Janik, C.J., Sheppard, D.S., Poreda, R.J., and Liss, S.A., 1988, Fluid geochemistry and fluid mineral equilibria in test wells and thermal gradient holes at the Makushin geothermal area, Unalaska Island, Alaska: Alaska Division of Geological and Geophysical Surveys, Report of Investigations 88-14, 90 p.

Muffler, L.J.P., 1979, Assessment of geothermal resources of the United States-1978: U.S. Geological Survey Circular 790, 163 p.

Myers, J.D., and Marsh, B.D., 1987, Aleutian lead isotopic data: additional evidence for the evolution of lithospheric plumbing systems: Geochemica et Cosmochemica Acta 51, p. 1833-1842.

Myers, J.D., Marsh, B.D., and Sinha, A.K., 1985, Strontium isotopic and selected trace element variations between two Aleutian volcanic centers (Adak and Atka): implications for the development of arc volcanic plumbing systems: Contributions to Mineralogy and Petrology, v. 91, p. 221-234.

Nakamura, K., Jacob, K.H., and Davies, J.N., 1977, Volcanoes as possible indicators of tectonic stress orientation - Aleutians and Alaska: Pure and Applied Geophysics, v. 115, p. 87-112.

Nakamura, K., Plafker, George, Jacob, K.H., and Davies, J.N., 1980, A tectonic stress trajectory map of Alaska using information from volcanoes and faults: Bulletin of the Earthquake Research Institute, v.55, p. 89-100.

Nehring, N.L., Bowen, P.A., and Truesdell, A.H., 1977, Techniques for the conversion to carbon dioxide of oxygen from dissolved sulfate in thermal waters: Geothermics, v. 5, p. 63-66.

Nye, C.J., and Turner, D.T., 19___, ____: Fairbanks, University of Alaska, unpublished data.

Nye, C.J., and Turner, D.L., 1990, Petrology, geochemistry, and age of the Spurr volcanic complex, eastern Aleutian arc: Bulletin of Volcanology, v. 52, p. 205-226.

Palmer, M.R., Spivack, A.J. and Edmond, J.M., 1985, Absorption of boron on marine sediments: EOS, v. 66, p. 916.

Panichi, C.R., and Gonfiantini, R., 1978, Environmental isotopes in geothermal studies: Geothermics, v. 6, p. 143-161.

Panuska B.C., and Stone, D.B., 1985, Latitudinal motion of the Wrangellia and Alexander terranes and the southern Alaska Superterrane, *in* Howell, D.G., ed., Tectonostratigraphic terranes of the circum-Pacific region: Houston Texas, Circum-Pacific Council for Energy and Mineral Resources, v. 6, p. 109-120.

Poreda R.J., 1983, Helium, neon, water and carbon in volcanic rocks and gases: San Diego, University of California, Ph.D. thesis, 215 p.

Poreda, R.J. and Craig, H.A., 1989, Helium isotope ratios in circum-Pacific volcanic arcs: Nature, v. 338, p. 473-478.

Presser, T.S. and Barnes, Ivan, 1974, Special techniques for determining chemical properties of geothermal waters: U.S. Geological Survey Water Resources Investigation Report 22-74, 11 p.

Scholl, D.W., Vallier, T.L., and Stevenson, A.J., 1987, Geologic evolution and petroleum geology of the Aleutian ridge, *in* Scholl, D.W., Grantz, Arthur, and Vedder, J.G., eds., Geology and resource potential of the continental margin of western North America and adjacent ocean basins - Beaufort Sea to Baja California: Houston Texas, Circum-Pacific Council for Energy and Mineral Resources Earth Science Series, v 6, p. 123-155.

Skougstad, M.W., Fishman, M.J., Friedman, M.J., Erdmann, D.E. and Duncan, S.S., 1979, Methods for determination of inorganic substances in water and fluvial sediments: U.S. Geological Survey Techniques of Water-Resource Investigations, bk. 5, chap. A1, 626 p.

Smith, D.R., and Leeman, W.P., 1987, Petrogenesis of Mount St. Helens dacitic magmas: Journal of Geophysical Research, v. 92, p. 10,313-10,334.

Spencer, S.G., Long, G.A., and Chapman-Riggsbee, W., 1982, An analysis of geothermal resource development on Unalaska Island, Alaska: Geothermal Resources Council Transactions, v. 6., p. 393-396.

Stauffer, R.E., and Thompson, J.M., 1984, Arsenic and antimony in geothermal waters of Yellowstone National Park, Wyoming, USA: Geochimica et Cosmochimica Acta, v. 48, p. 2,547-2,562.

Stone, D.B., 1988, Bering Sea - Aleutian Arc, Alaska, *in* Nairn, A.E.M., and others, eds., The ocean basins and margins, v. 7b: Plenum Publishing, p. 1-84.

Thompson, J.M., 1985, Chemistry of thermal and nonthermal springs in the vicinity of Lassen Volcanic National Park: Journal of Volcanology and Geothermal Research, v. 25, p. 81-104.

Thompson, J.M., Keith, T.E.C., and Consul, J.J., 1985, Water chemistry and mineralogy of Morgan and Growler Hot Springs, Lassen KGRA, California: Geothermal Resources Council Transactions, v. 9, pT. I, p. 357-362.

Truesdell, A.H. and Hulston, J.R., 1980, Isotopic evidence on environments of geothermal systems, *in* Fritz, P., and Fontes, J.C., eds., Handbook of environmental isotope geochemistry: New York, Elsevier Scientific Publishing Company, p. 179-226.

Truesdell, A.H., Nathenson, Manuel, and Rye, R.O., 1977, The effects of subsurface boiling and dilution on the isotopic compositions of Yellowstone thermal waters: Journal of Geophysical Research, v. 82, p. 3,694-3,704.

Viglino, J.A., Harmon, R.S., Borthwick, James, Nehring, N.L., Motyka, R.J., White, L.D. and Johnson D.A., 1985, Stable-isotope evidence for a magmatic component in fumarole condensates from Augustine Volcano, Cook Inlet, Alaska, USA: Chemical Geology, v. 49, p. 141-157.

Walker, David, Shibata, T., and DeLong, S.E., 1979, Abyssal tholeiites from the Oceanographer Fracture Zone II - phase equilibria and mixing: Contributions to Mineralogy and Petrology, v. 70, p. 111-125.

Waring, G.A., 1917, Mineral springs of Alaska: U.S. Geological Survey Water-Supply Paper 418, 114 p.

White, D.E., 1967, Some principles of geyser activity, mainly from Steamboat Springs, Nevada: American Journal of Science, v. 265, p. 641-684.

Worner, Gerhard, Harmon, R.S., Davidson, Jon, Moorbath, S., Turner, D.L., McMillan, Nancy, Nye, C.J., Lopez-Escobar, Leo, and Moreno, Hugo, 1988, The Nevados de Payachata volcanic group (18°S/69°W, N. Chile): I. Geological, geochemical and isotopic observations: Bulletin of Volcanology, v. 50, p. 287-303.